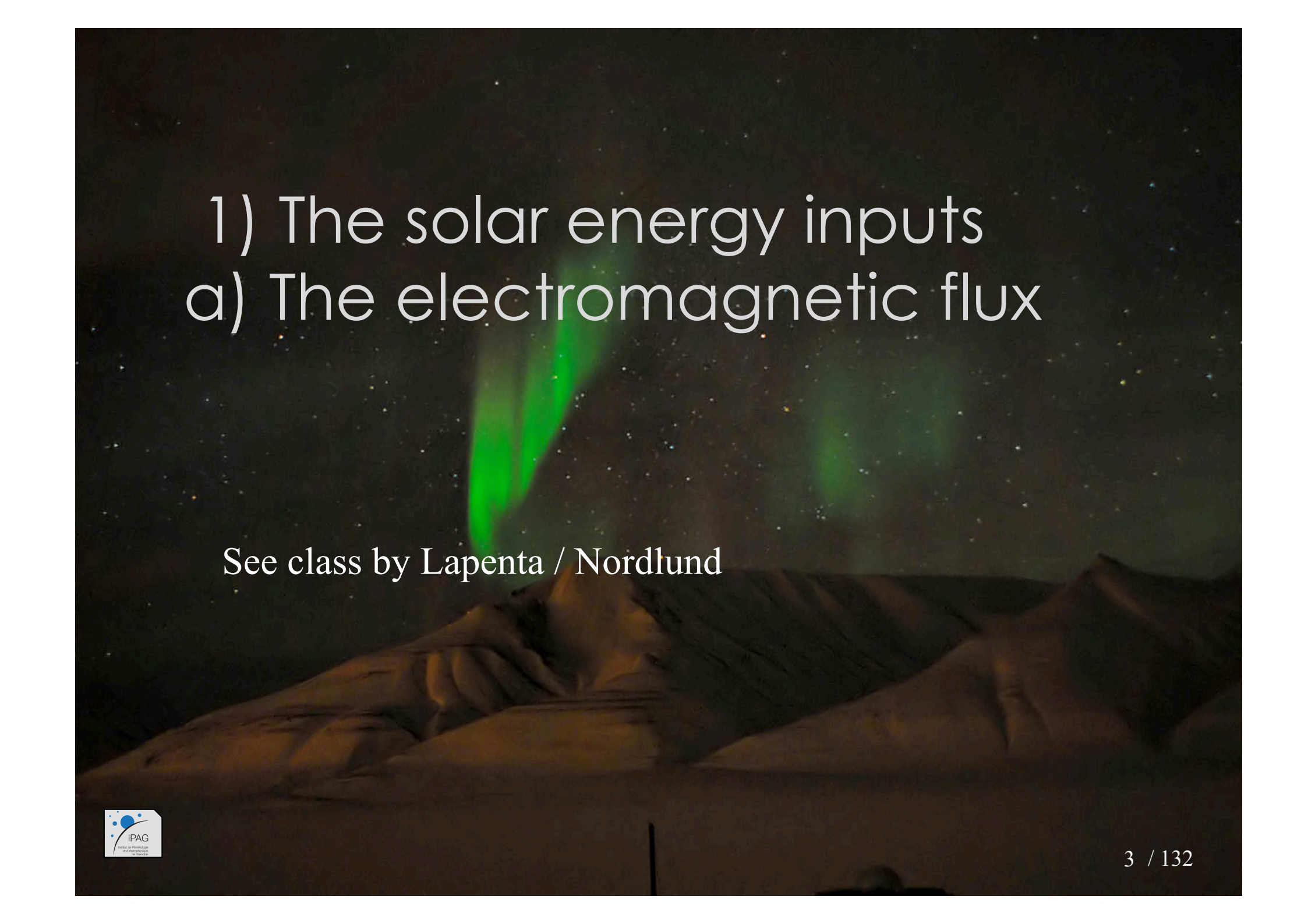


Basic processes for Space Weather

Jean Lilensten

Space weather is the physical and phenomenological state of natural space environments. The associated discipline aims, through observation, monitoring, analysis and modelling, at understanding and predicting the state of the sun, the interplanetary and planetary environments, and the solar and non-solar driven perturbations that affect them; and also at forecasting and nowcasting the possible impacts on biological and technological systems



1) The solar energy inputs
a) The electromagnetic flux

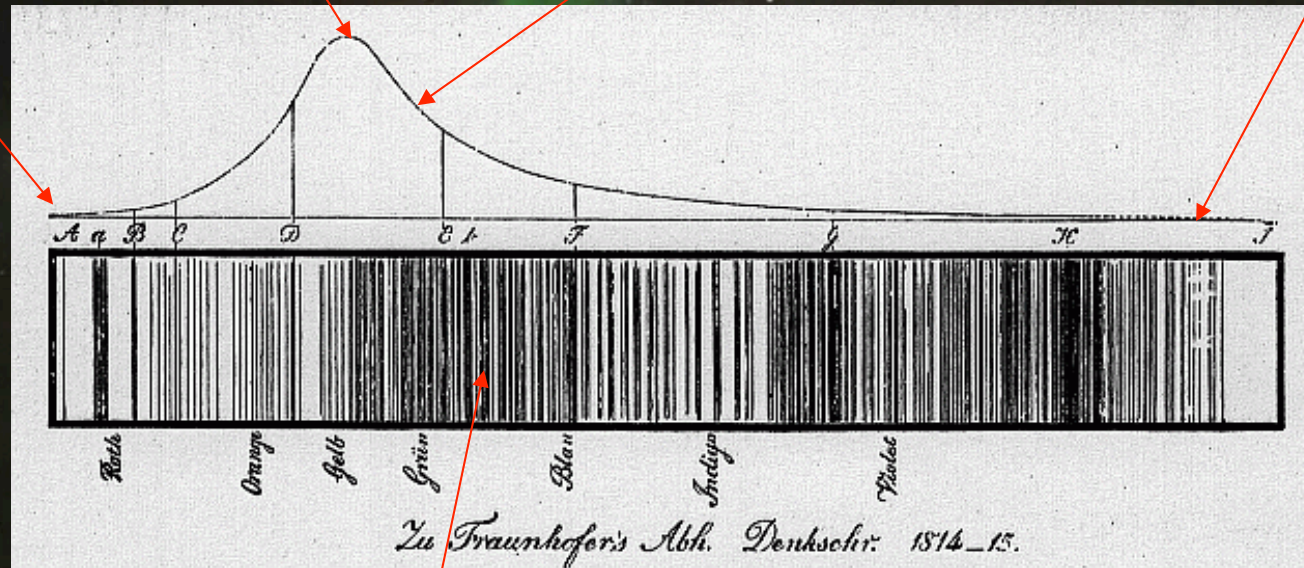
See class by Lapenta / Nordlund

Nothing

460 nm

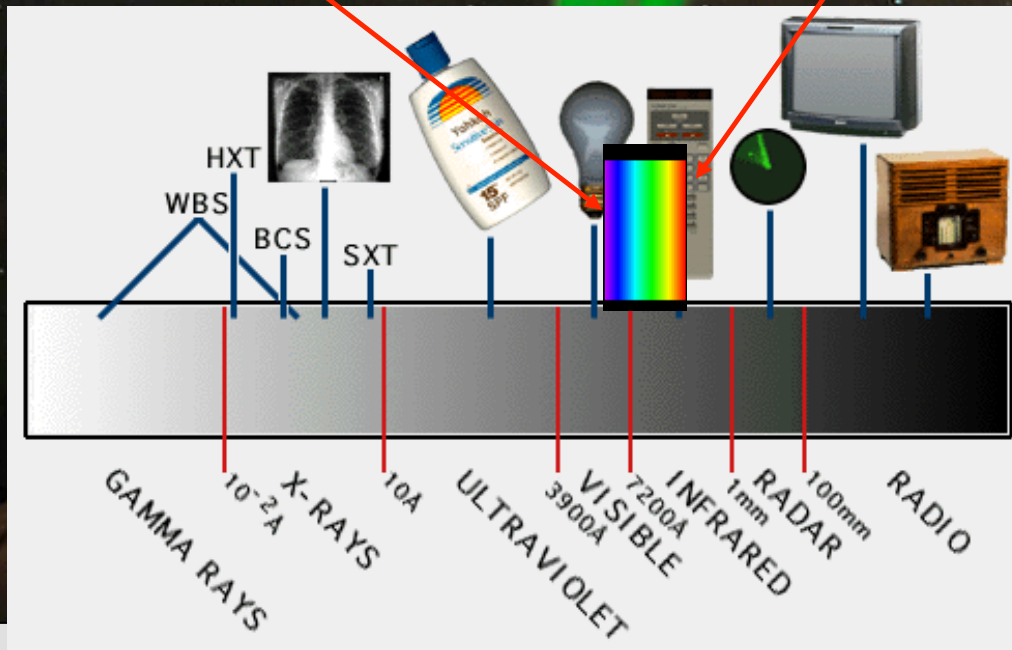
Plank's law

Nothing
as well



Fraunhofer absorption lines

From the Sun, most of what was essentially known until recently its visible light



However, the invisible is quite interesting too...

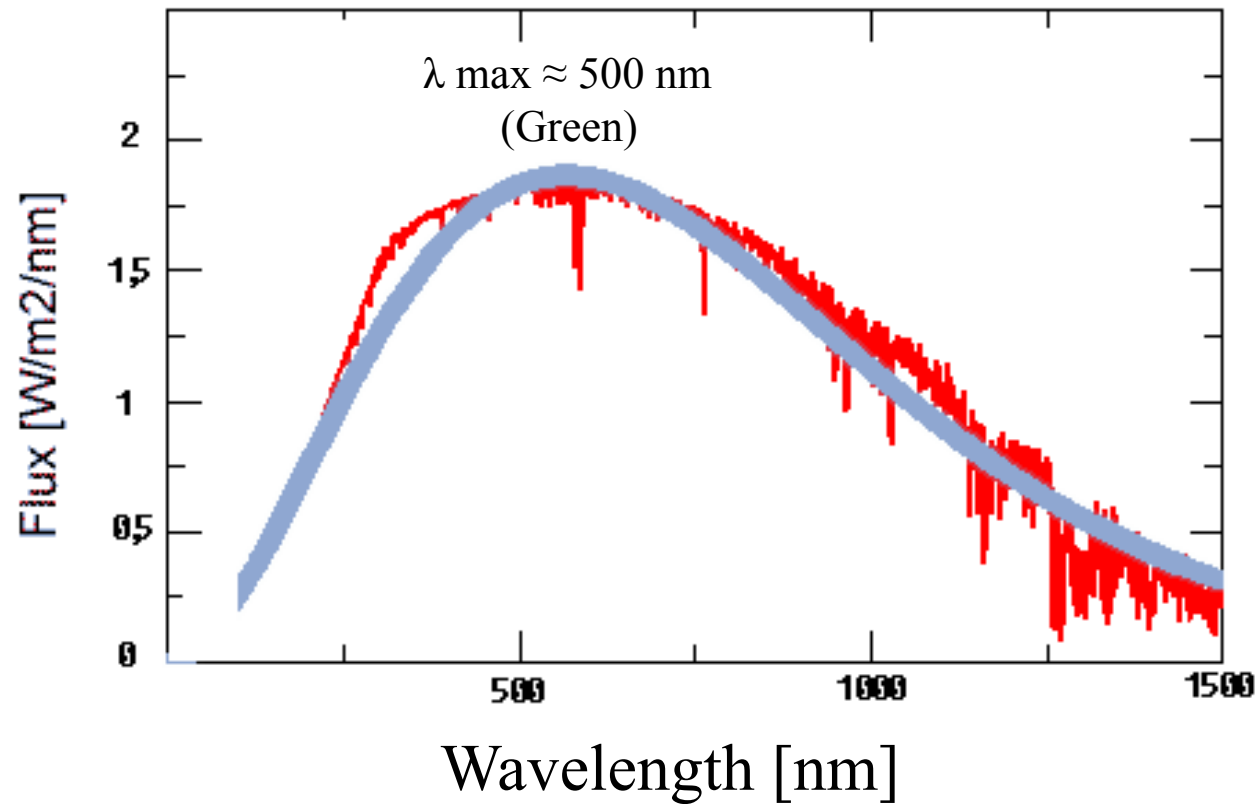
To continue : let's take some hints of what is a low energy, or a high energy in space weather...

Definition of the UV, EUV and X ranges (ISO)

Irradiance	Sub domain	$\Delta\lambda$	Energy (eV) $\left(\frac{hc}{\lambda}\right)$	Associated temperature (K) $(E=\frac{1}{2} kT)$
Radio		> 1.5 cm	< 8×10^{-5}	< 0.2
Micro-wave		1 mm to 1.5 cm	8×10^{-5} to 1.25×10^{-3}	0.2 to 3
Micro-wave	W	3.3 mm	3.75×10^{-4}	1
Micro-wave	V	5 mm	2.5×10^{-4}	0.6
Micro-wave	Q	7.5 mm	1.65×10^{-4}	0.5
Micro-wave	Ka	10 mm	1.25×10^{-4}	0.4
Micro-wave	K	13.6 mm	9×10^{-5}	0.2

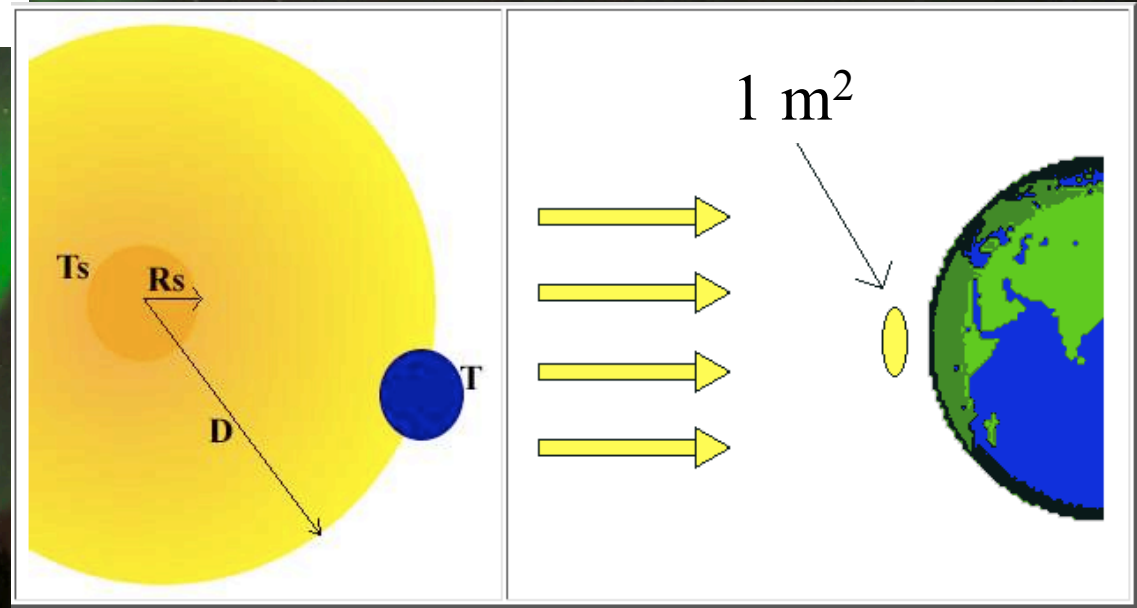
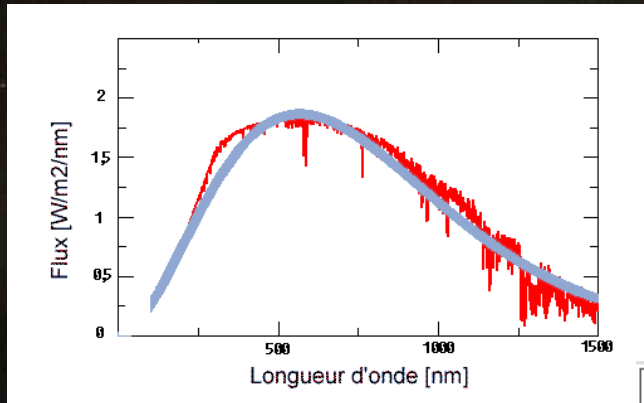
Irradiance	Sub domain	$\Delta\lambda$	Energy (eV) $\left(\frac{hc}{\lambda}\right)$	Associated temperature (K) $(E=\frac{1}{2} kT)$
Infrared⁽¹⁾		700 nm to 350.000 nm	10^{-3} to 1,8	2.7 to 4700
infrared	Nea r	700 nm to 5000 nm	0.25 to 1.8	630 to 4700
infrared	Mid (⁽²⁾)	5000 nm to 25.000 nm	0.05 to 0.25	130 to 630
infrared	Far ⁽²⁾)	> 25.000 nm	< 0.05	< 130
Visible		400 nm to 700 nm	1,8 to 3	4600 to 7700

Irradiance	Sub domain	$\Delta\lambda$	Energy (eV) $\left(\frac{hc}{\lambda}\right)$	Associated temperature (K) $\left(E=\frac{1}{2} kT\right)$
Ultraviolet		30 nm to 400 nm	3 to 41	7700 to 10^6
Ultraviolet	A ⁽³⁾	315 nm to 400 nm	3 to 4	7700 to 10^5
Ultraviolet	B ⁽³⁾	280 nm to 315 nm	4 to 4.5	10^5
Ultraviolet	C ⁽³⁾	100 nm to 280 nm	4.5 to 12.5	10^5 to $3 \cdot 10^5$
Ultraviolet	Near ⁽⁴⁾	200 nm to 400 nm	3 to 6	70.000 to 140.000
Ultraviolet	Far ⁽⁵⁾	120 nm to 200 nm	6 to 10	140.000 to 230.000
Ultraviolet	Ex-treme ⁽⁵⁾	30 nm to 120 nm	10 to 41	230.000 to 10^6
X-rays⁽⁵⁾		0,005 nm to 30 nm	41 to $2,5 \times 10^5$	10^6 to $6 \cdot 10^9$
X-rays	XU V or Soft ⁽⁵⁾	1 nm to 30 nm	41 to 125	10^6 to $3 \cdot 10^6$
X-rays	Hard	0,005 nm to 1 nm	125 to $2,5 \times 10^5$	$3 \cdot 10^6$ to $6 \cdot 10^9$
γ		< 0,005 nm	> $2,5 \times 10^5$	> $6 \cdot 10^9$

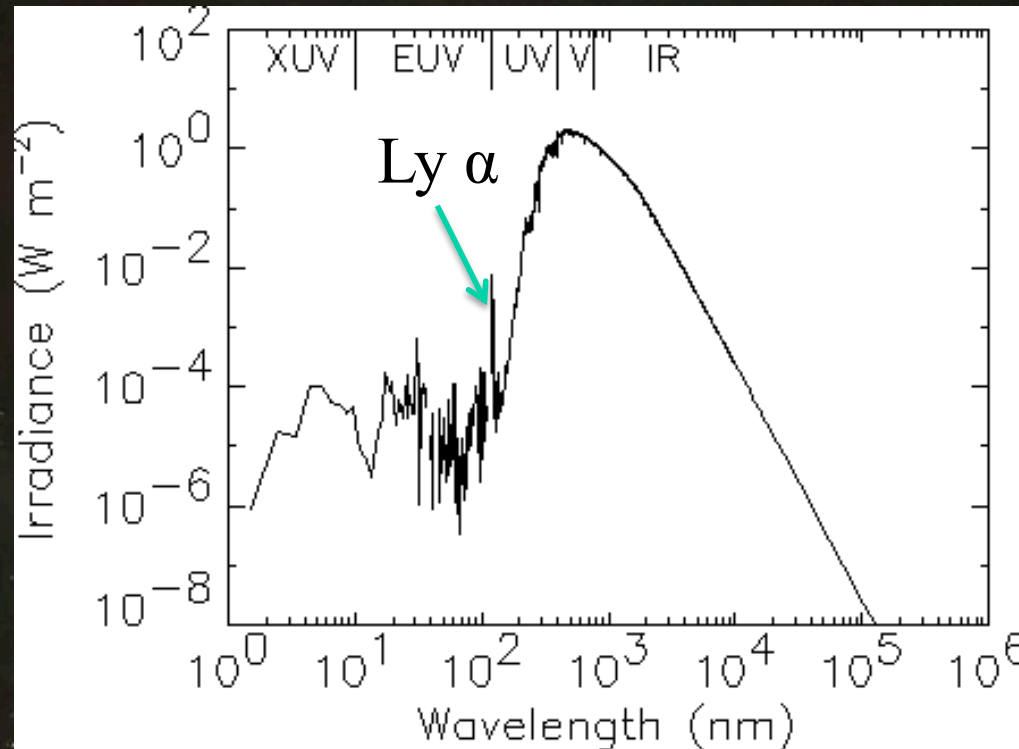


Emittance = Integrated flux over wavelengths
Total Power / surface (W.m⁻²)

The physics of the blackbody allows computing the energy received at Earth, called (unfortunately) the « solar constant »).
Let's do it.



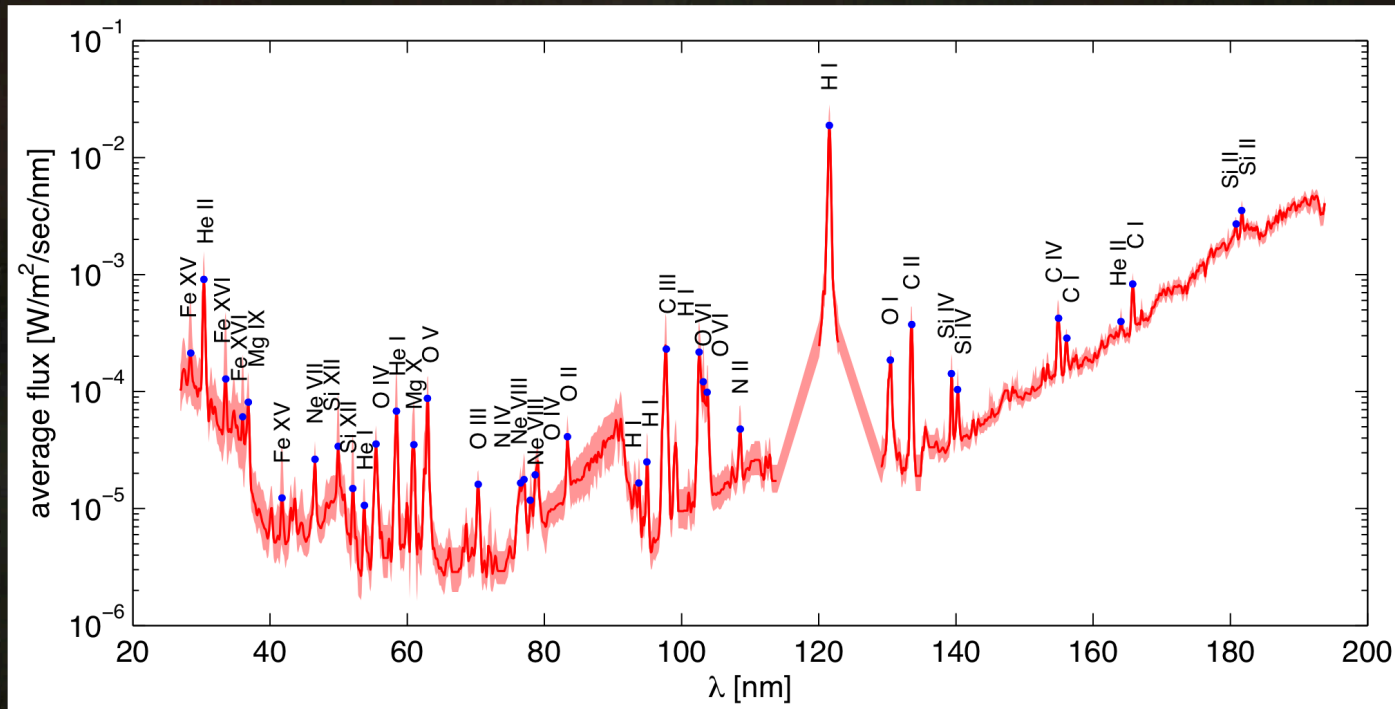
The solar « constant »: The agreed value is
 $\rightarrow E = 1362 \text{ W.m}^{-2}$



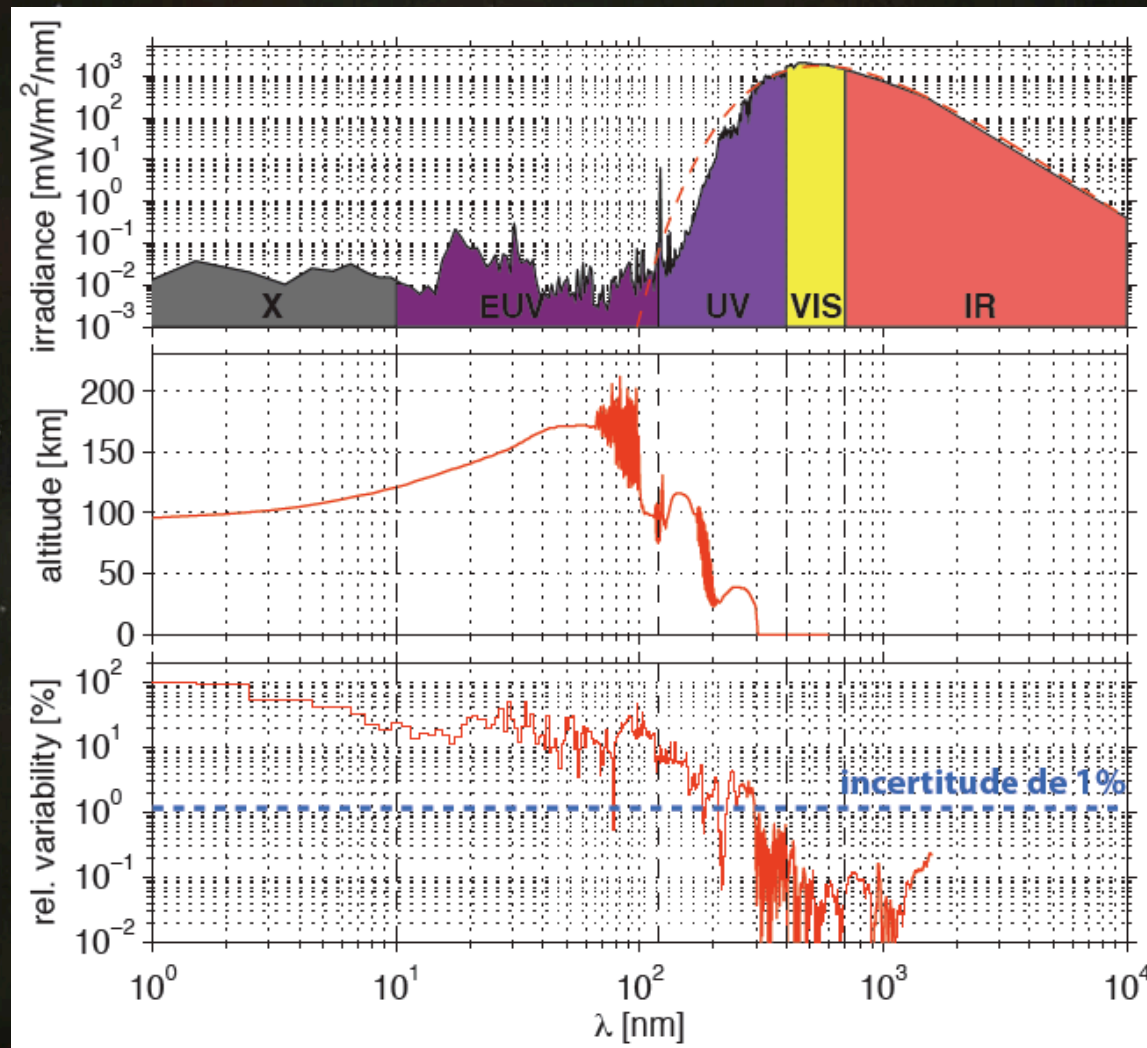
However, even if it only represents a weak part in energy, the energetic spectrum (UV / EUV / XUV) is important

Recall : total $E_m = 6,4 \cdot 10^7 \text{ W.m}^{-2}$

Energetic wavelengths emittance: 10^5 W.m^{-2} (1/600)

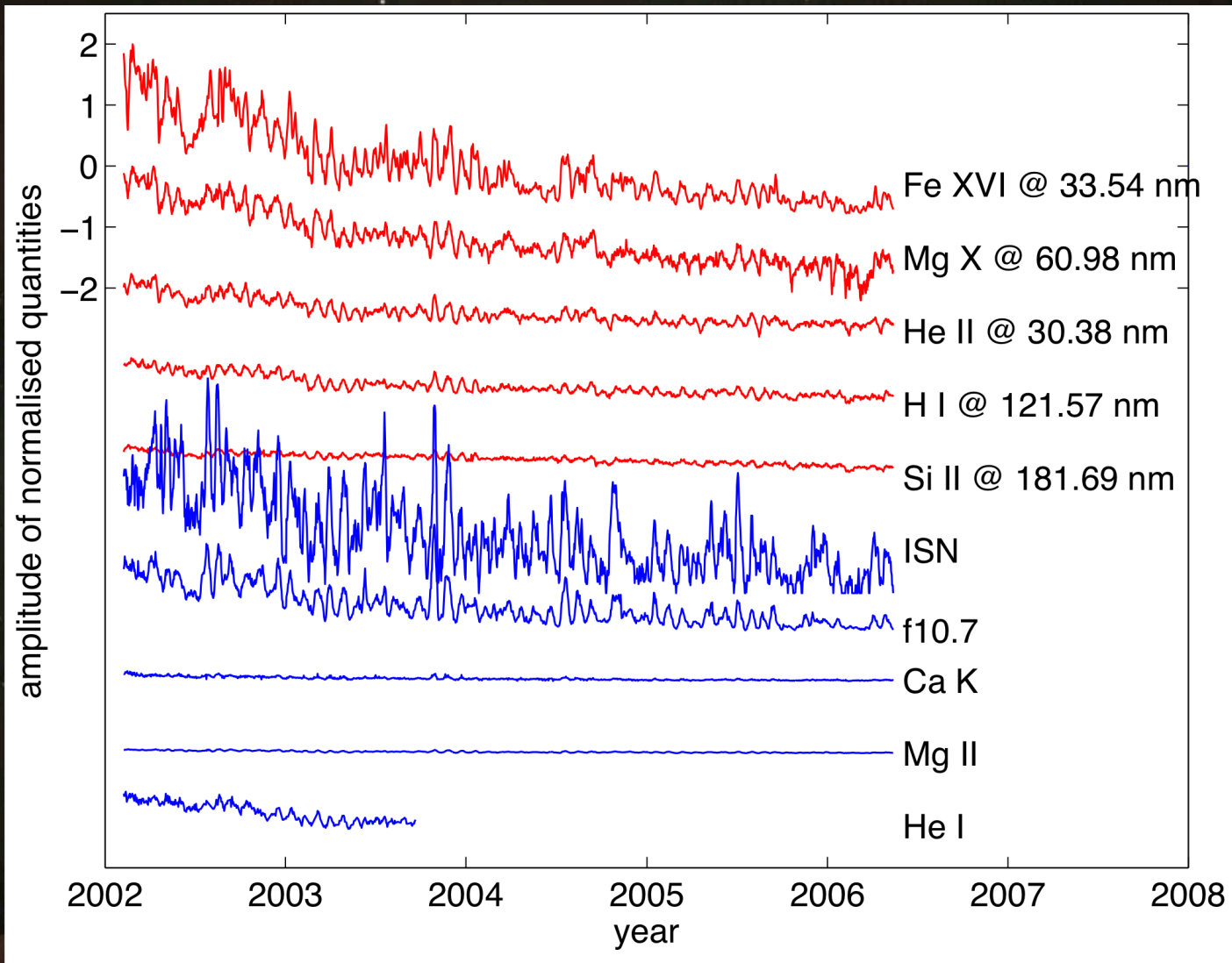


It is made of the superposition of a continuum and emission lines

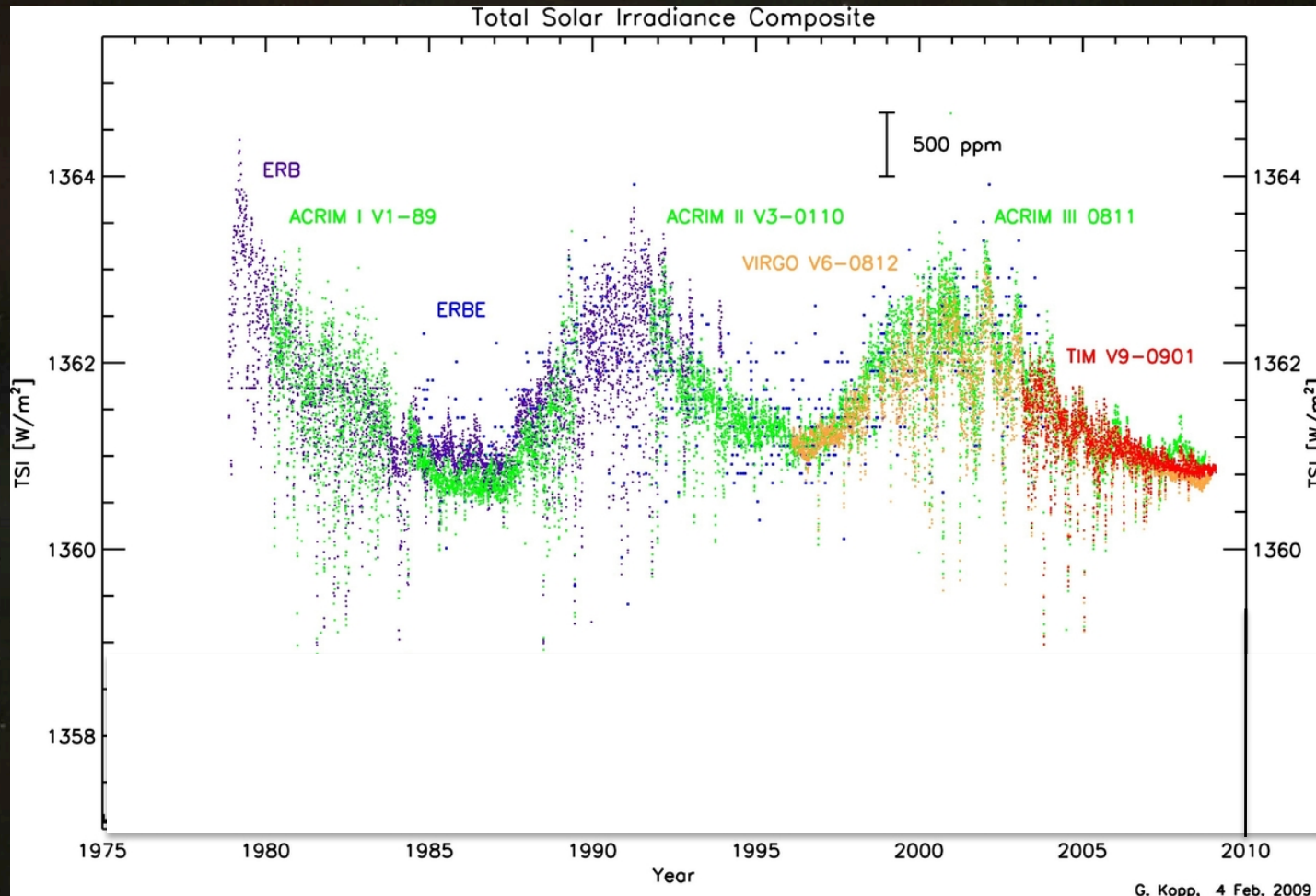


It is very variable

Its variation is one way to define
the Schwabe cycle.



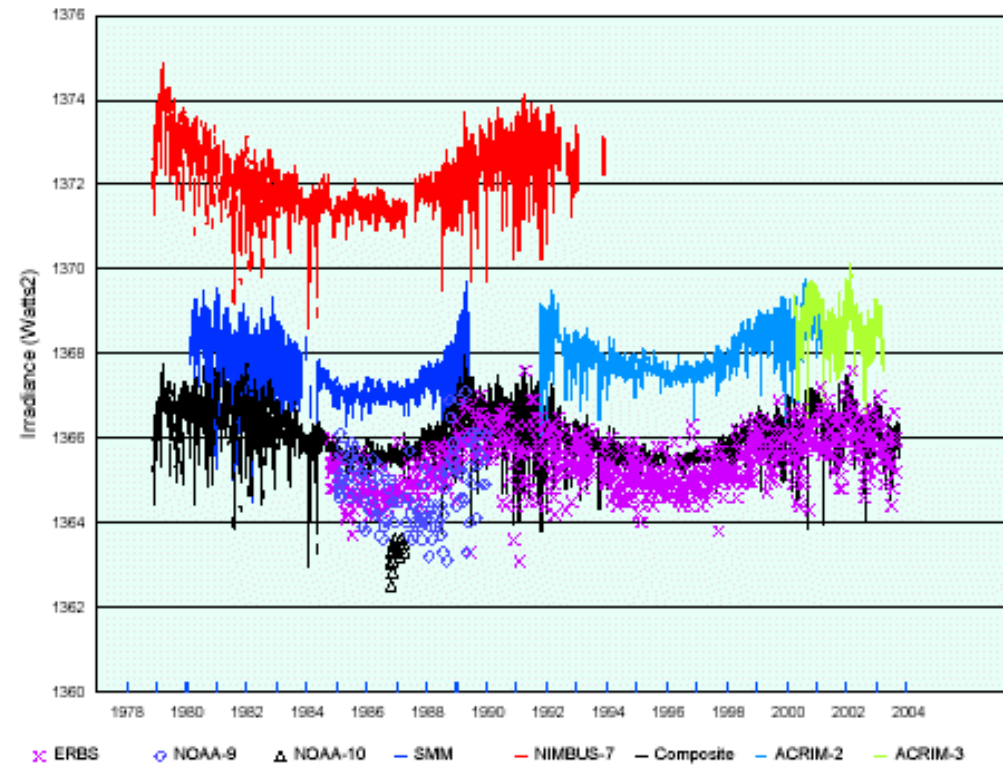
The wavelenghts do not vary the same way
although they more or less all follow the Schwabe
cycle



G. Kopp, 4 Feb. 2009

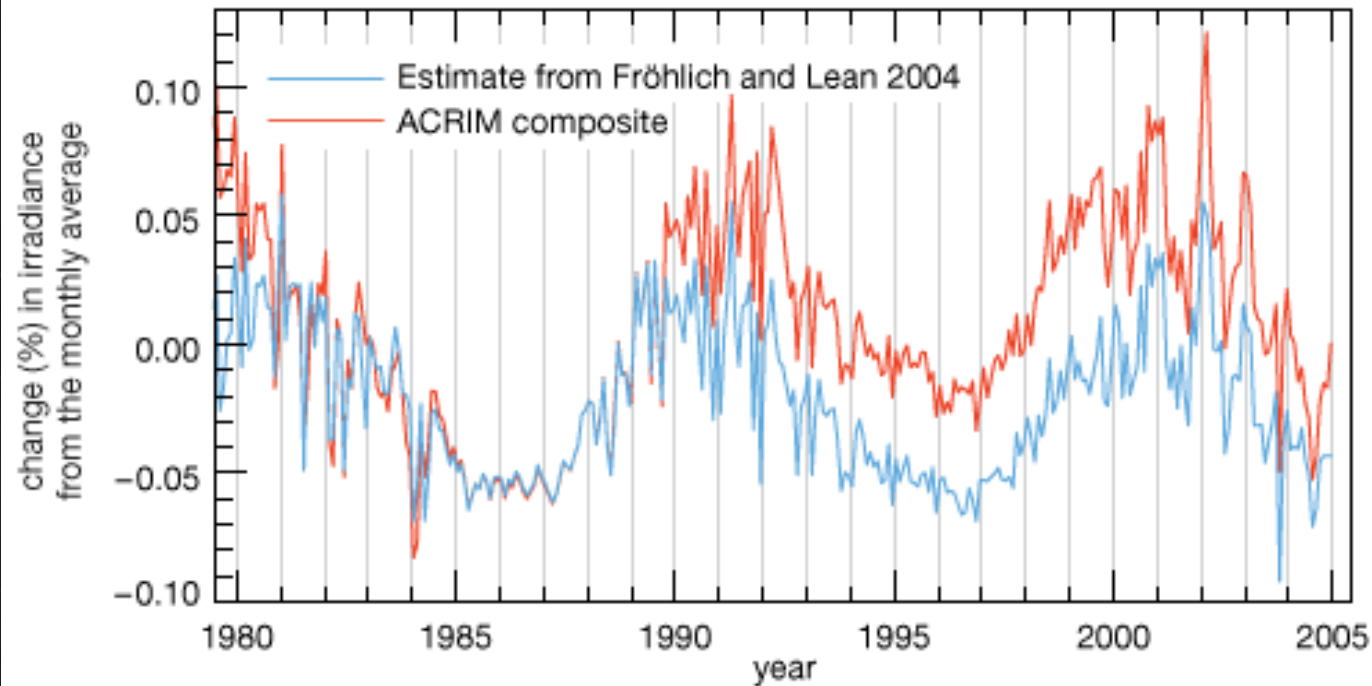
We know today that the irradiance also varies like the UV flux, although in much smaller extend.

Total Solar Irradiance



However, a look at the raw data is a call for care

Satellite measurements of total solar irradiance



Source : Climate Change 2007 : The Physical Science Basis , Summary for Policymakers , Intergovernmental Panel on Climate Change

And critical sense is requested when this is invoked to explain the global warming

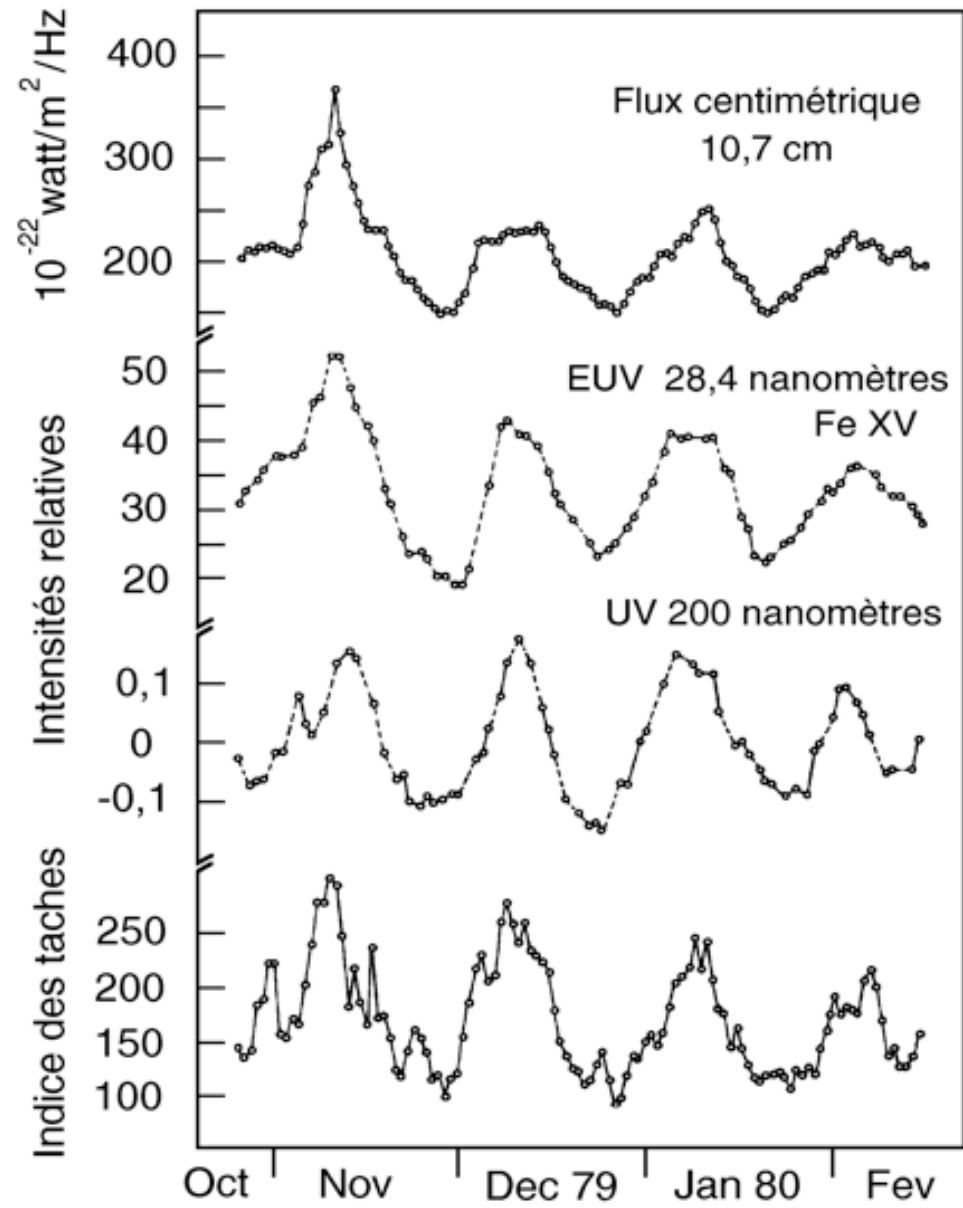
How to monitor the solar EUV flux and its variability ? By using indices (or ... proxies).

What is a index?

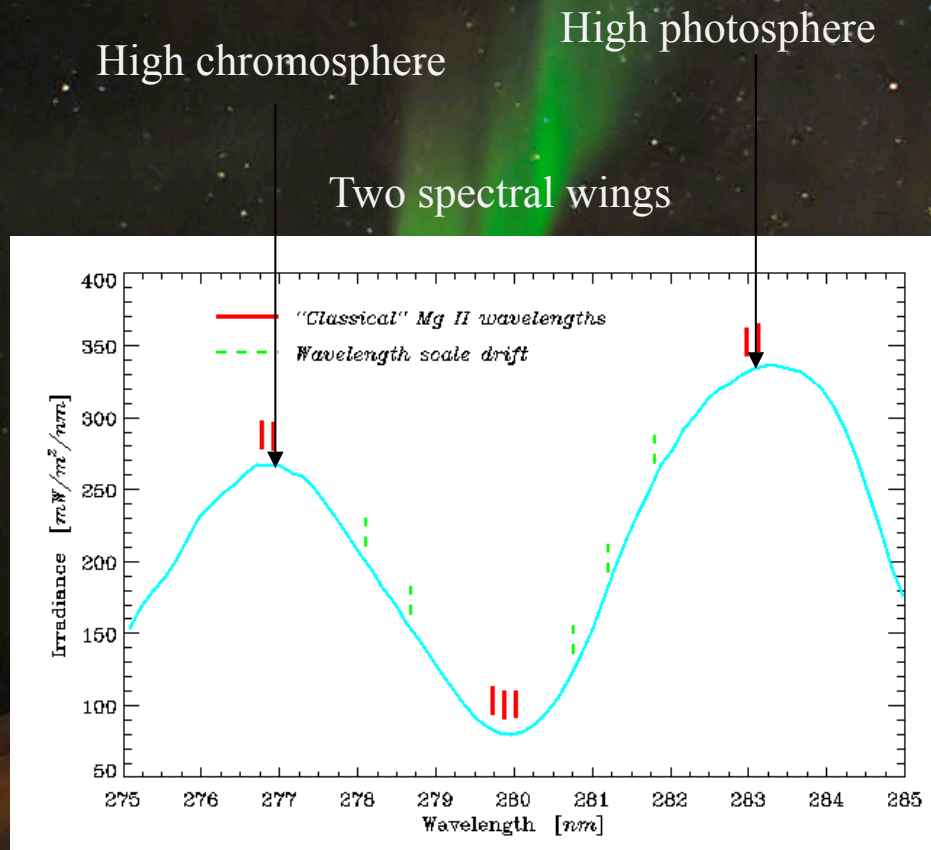
Indices have been introduced in order to give a simple yet almost exact description of massive data ensembles which vary with time (and eventually in space). Basically, an index is made up from a set of discrete values which provide as pertinent and reliable information as possible about the phenomenon in question by characterising it as a whole. Of course, the validity of the index basically depends on its definition, and on the choice of the described aspect of the phenomenon.

ISN, the international sunspot number (from SIDC, Brussels), which is not really a UV proxy but remains the most widely used gauge of solar activity.

f10.7 is the radio flux at 10.7 cm (from Penticton Observatory, Canada). This proxy is widely used as a solar input to ionosphere/thermosphere models, partly because it can be conveniently measured from ground.



MgII is the core-to-wing ratio of the Mg II line at 280 nm (from *SORCE/SOLSTICE*, version 9). This index probes the high chromosphere and is often advocated for the FUV [Heath and Schlesinger, 1986].



☒ Indice Mg d'activité solaire (Heath et Schlesinger, 1986) :
 = rapport d'irradiance à 280 nm et
 moyenne des ailes à 276 nm et 283 nm

Advantage : independant of the instrumental gain

SBUV / 2 discrete MgII k spectrum (Cebula et al., 1992)



CaK is the normalized intensity of the Ca II K-line at 393 nm (from National Solar Observatory at Sacramento Peak). This line originates at nearly the same altitude as the Mg II line and has also been advocated for the FUV [Lean et al., 1982].

MPSI is the magnetic plage strength index (from the Mt. Wilson 150-Foot Solar Tower), which quantifies the relative fraction of the solar surface that is covered by mild magnetic fields ($10 < jB_j < 100$ Gauss). By definition, MPSI index is a proxy for plages and faculae [Parker et al., 1998].

MWSI is the Mount Wilson sunspot index, defined as the MPSI, but for intense magnetic fields (100 Gauss). The MWSI is a proxy for active regions.

s10.7 is computed by Tobiska et al. [2008] out of the integrated 26 – 34 nm emission from the SEM radiometer onboard SoHO, and rescaled to the f10.7 index after a trend correction (version 3.9a). It is dominated by the emission from the chromospheric and transition region He II line at 30.4 nm. Is it a proxy ?

Lyman-a channel (ch-L) is the output of a photodiode from the LYRA radiometer [Hochedez et al., 2006] onboard the PROBA2 satellite, launched in 2010. This channel integrates emissions in the 110 – 210 nm band, with a peak around 125 nm.

Herzberg channel (ch-H) is the output of a photodiode from LYRA in the Herzberg band, here between 195 – 220 nm. Both the Herzberg and the Lyman-a channels are relevant inputs for upper atmospheric models.

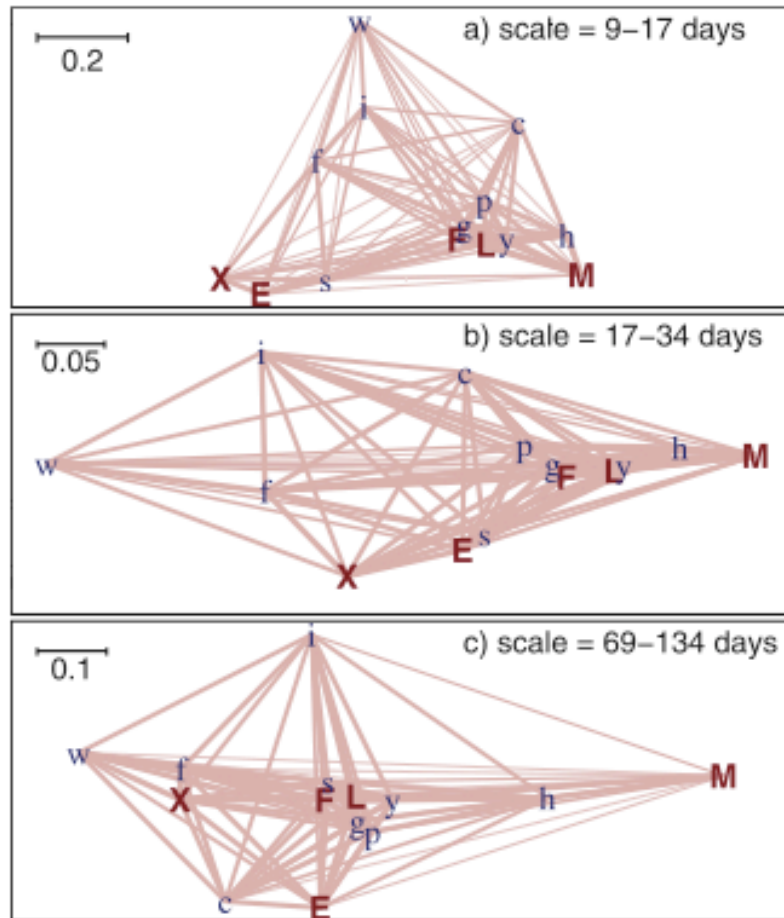


Figure 3. Correspondence maps for three characteristic scales. The distance between each pair of points corresponds to $1 - |r|$ (see text) and the line thickness is proportional to r . Capitals designate our 5 spectral bands: (X)UV, (E)UV, H I (L)yman- α , (F)UV and (M)UV. The other characters correspond to proxies: (i)sn, (f)10.7, (s)10.7, M(g)II, (c)aK, M(p)SI, M(w)SI, L(y)man- α channel, (h)erzberg channel.

Finding the best proxies for the solar UV irradiance, Dudok de Wit et al., Geoph. Res. Let., Vol. 36, L10107, doi: 10.1029/2009GL037825, 2009

What are the best proxies for reconstructing specific spectral bands?

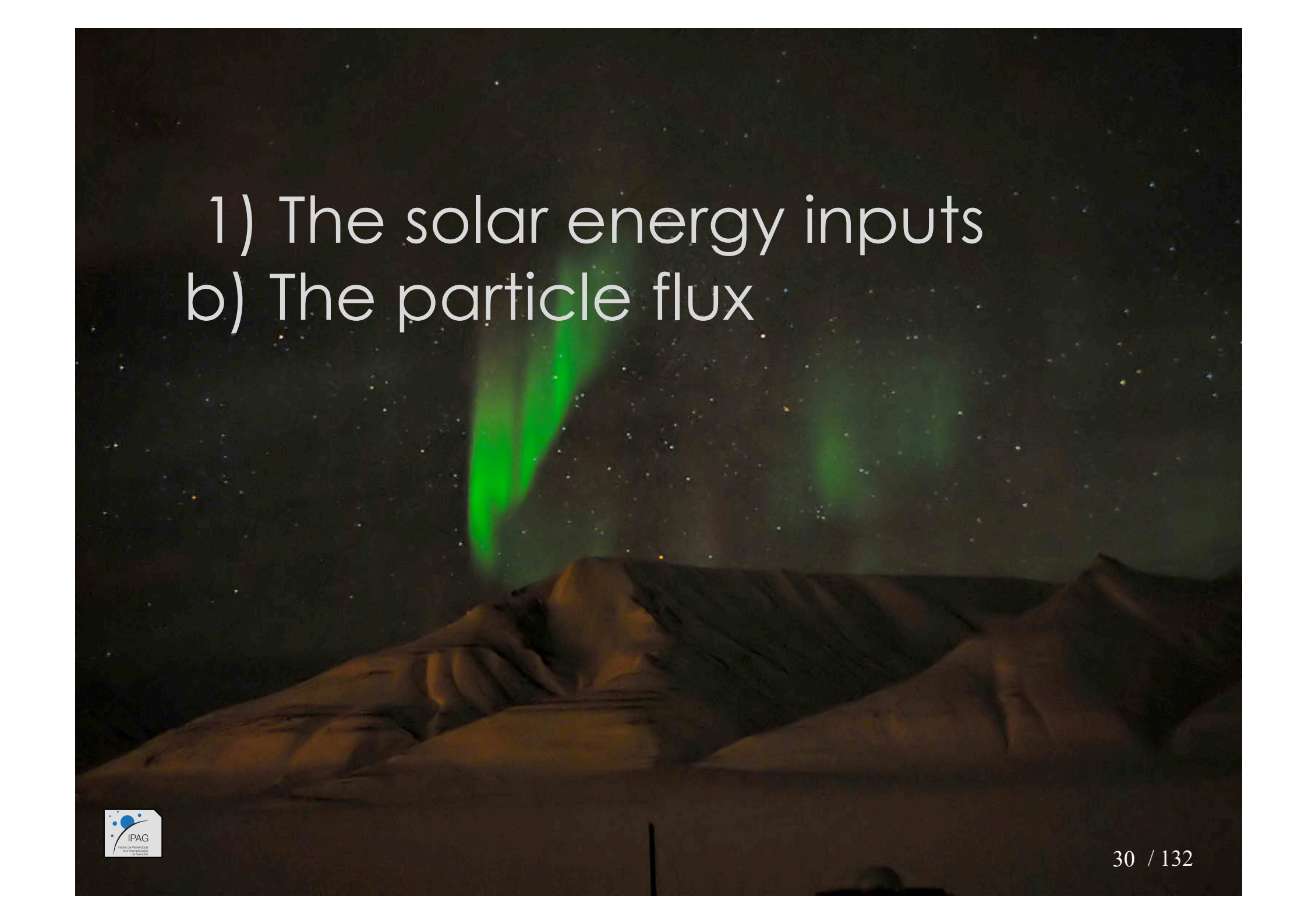
- The answer very much depends on the time-scale of interest.
- Proxies that are derived from real irradiance data do match their corresponding spectral band quite well. The correlation between the LYRA Lyman- α channel and the Lyman- α band, for example, always exceeds 0.95.
- The MgII index shows the best global performance since it is always located close to the center of the cloud of points. It is particularly well suited for the FUV band. The MPSI index is a backup solution, but is not measured continuously.
- Apart from these, no single spectral band can be properly reconstructed at all scales from one single proxy.
- There is no good (non irradiance-derived) proxy for the XUV and EUV bands. The f10.7 index would be the least bad solution.
- None of our proxies properly fits the MUV band, for which a better gauge of photospheric emissions is needed

<http://www.swpc.noaa.gov/ftpmenu/indices.html>

<http://www.stce.be/>

http://swc.nict.go.jp/sunspot/index_e.php

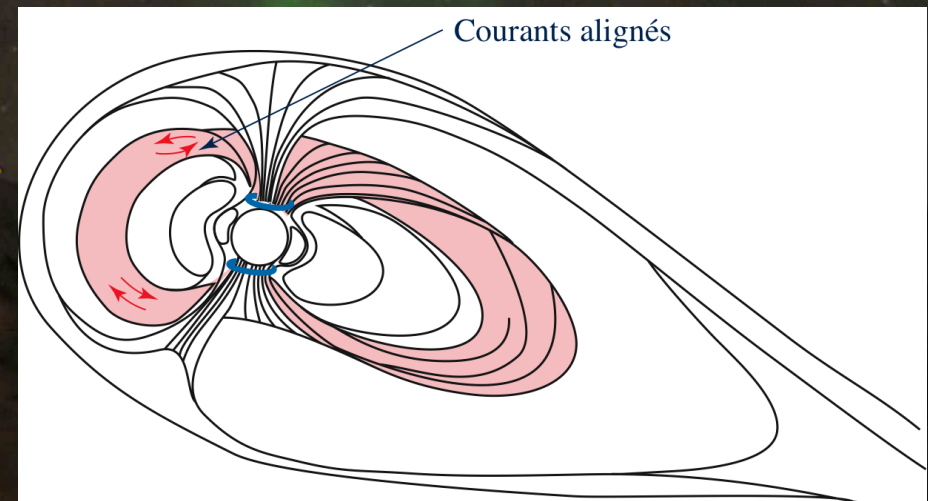
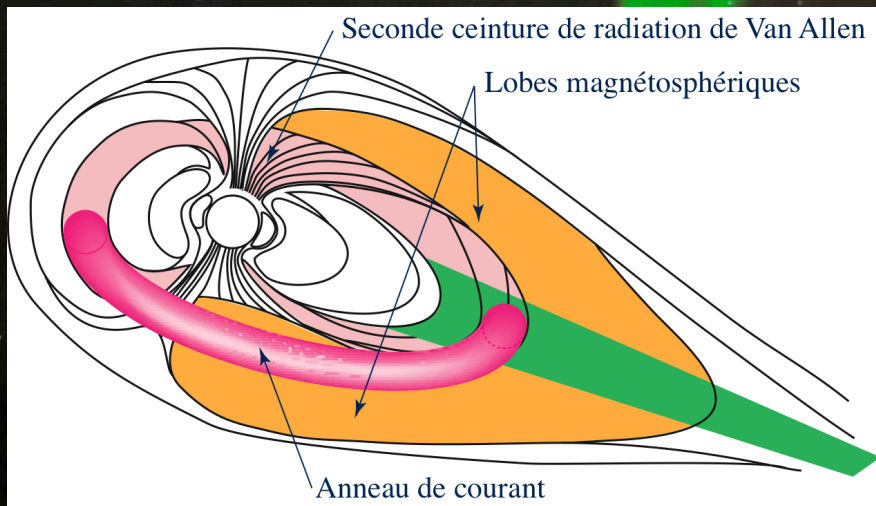
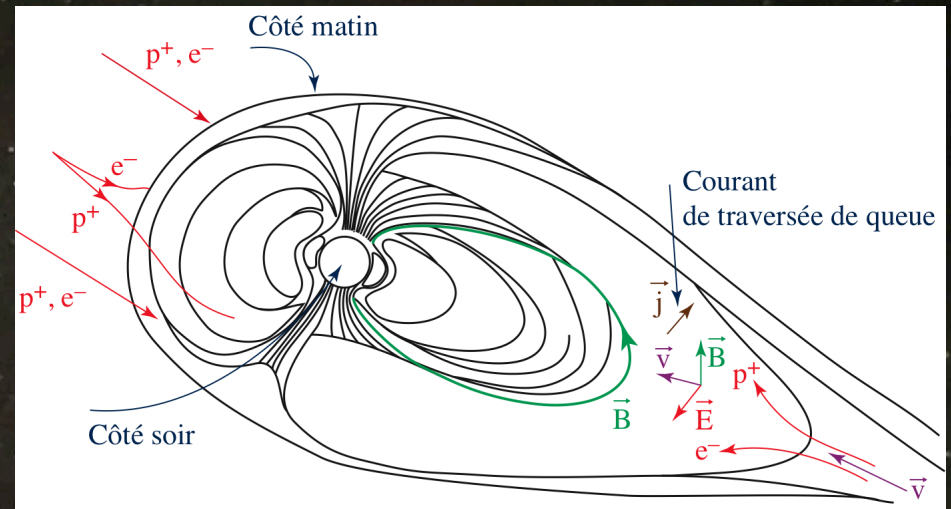
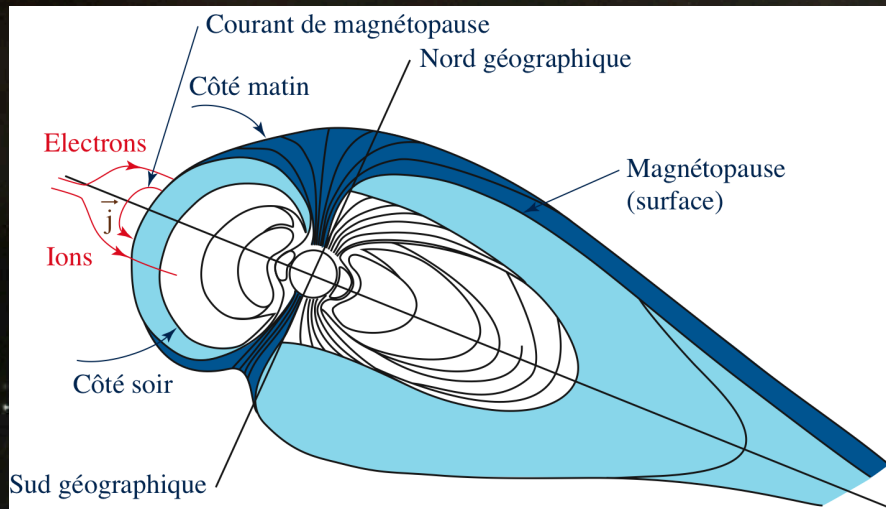
<http://lpc2e.cnrs-orleans.fr/~soteria/>

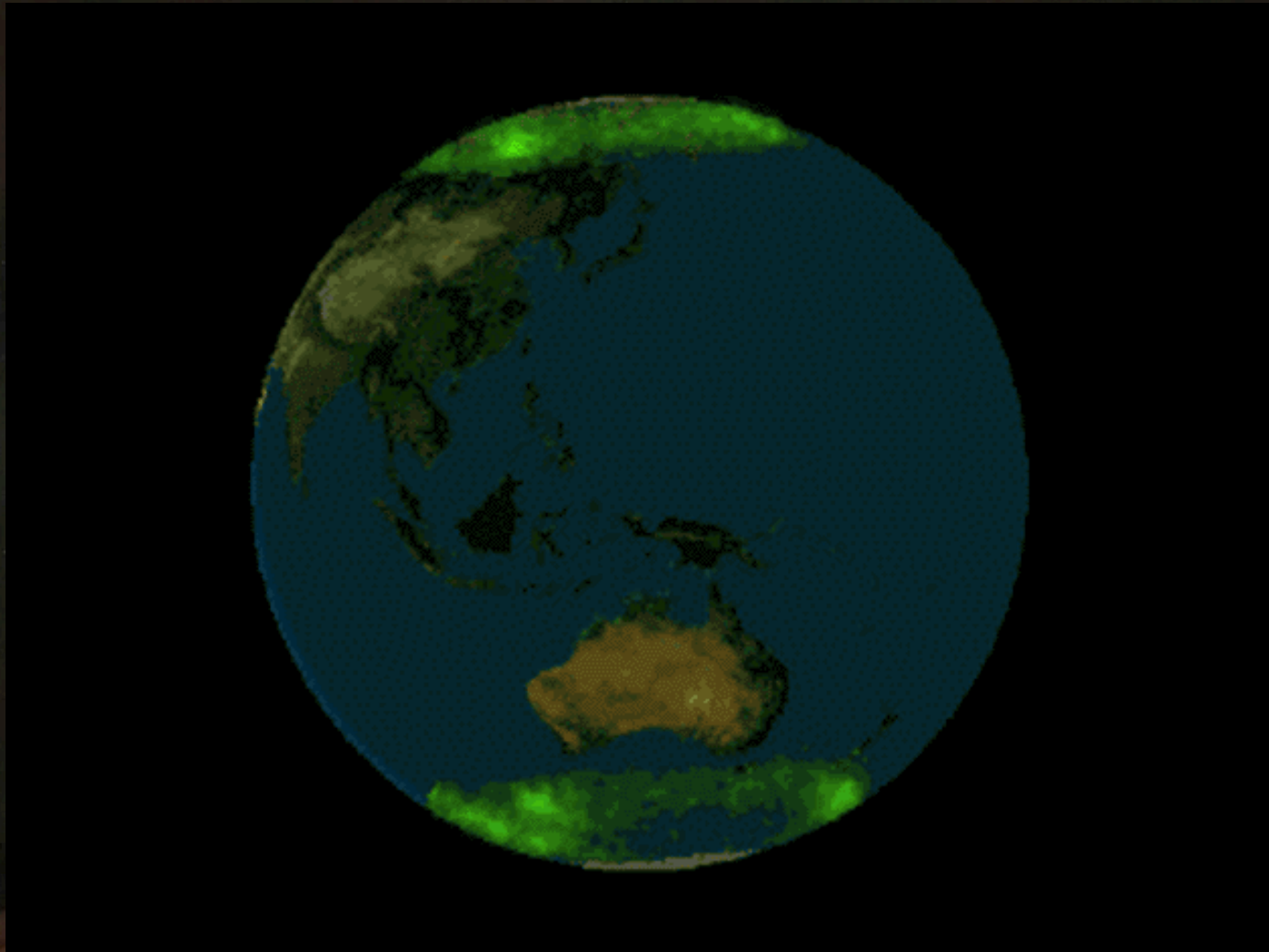
- 
- 1) The solar energy inputs
 - b) The particle flux



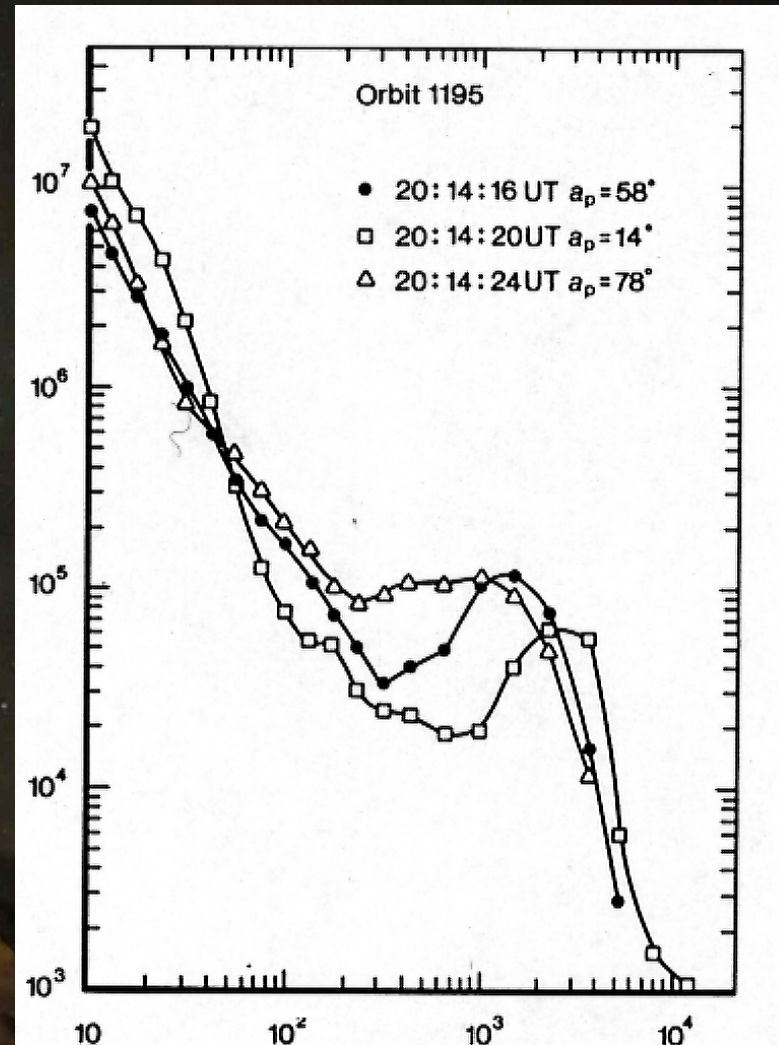
Where does it come from ?

See class by A. Aylward



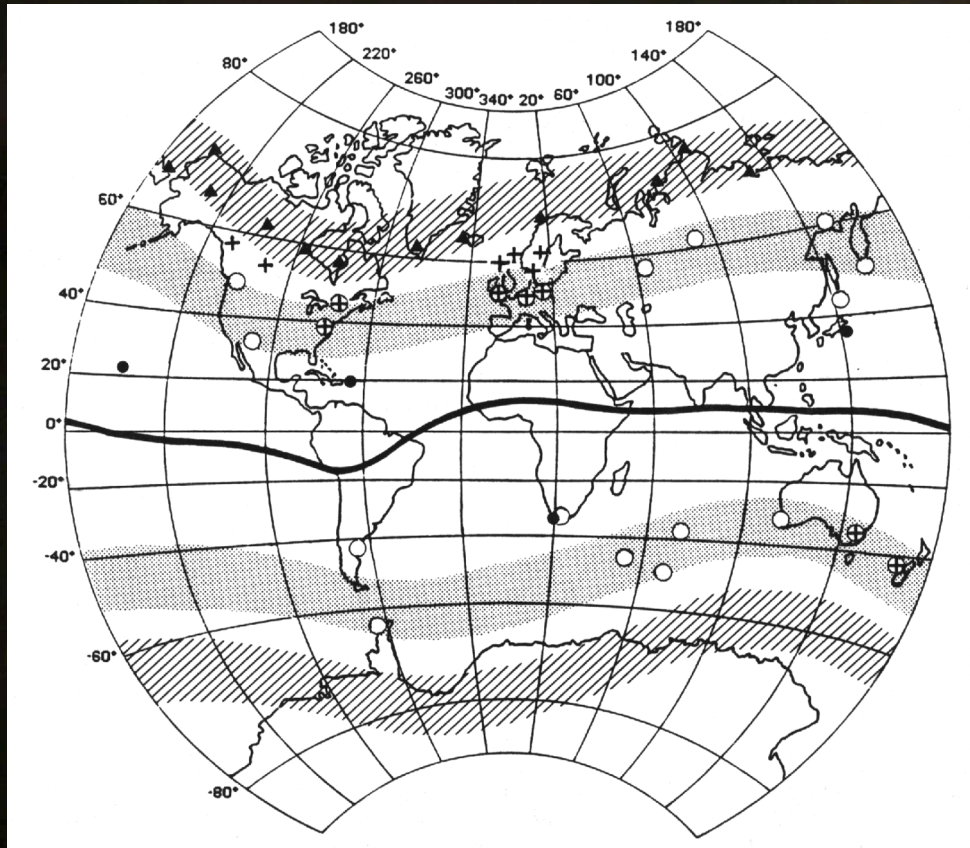


In the cusps, energies of typically 500 eV (polar rain), relatively constant (slightly depending on the solar activity)



In the auroral ovals, energies ranging from 100s' eV to 100s' keV, strongly depending on the solar activity

How to monitor the geomagnetic activity and its variability ? By using proxies again !



Geographical world map on which are indicated the positions of stations belonging to the different networks used in deriving geomagnetic indices: ▲ for AE, ● for Dst, + for Kp, ap, ○ for am, Km, and ⊠ for stations belonging to both Kp, ap, and am, Km networks. A solid line indicates the position of the dip equator. The average extension of the auroral zone is sketched by the hatched area, that of the subauroral region by the shaded area (after Berthelier, 1993).

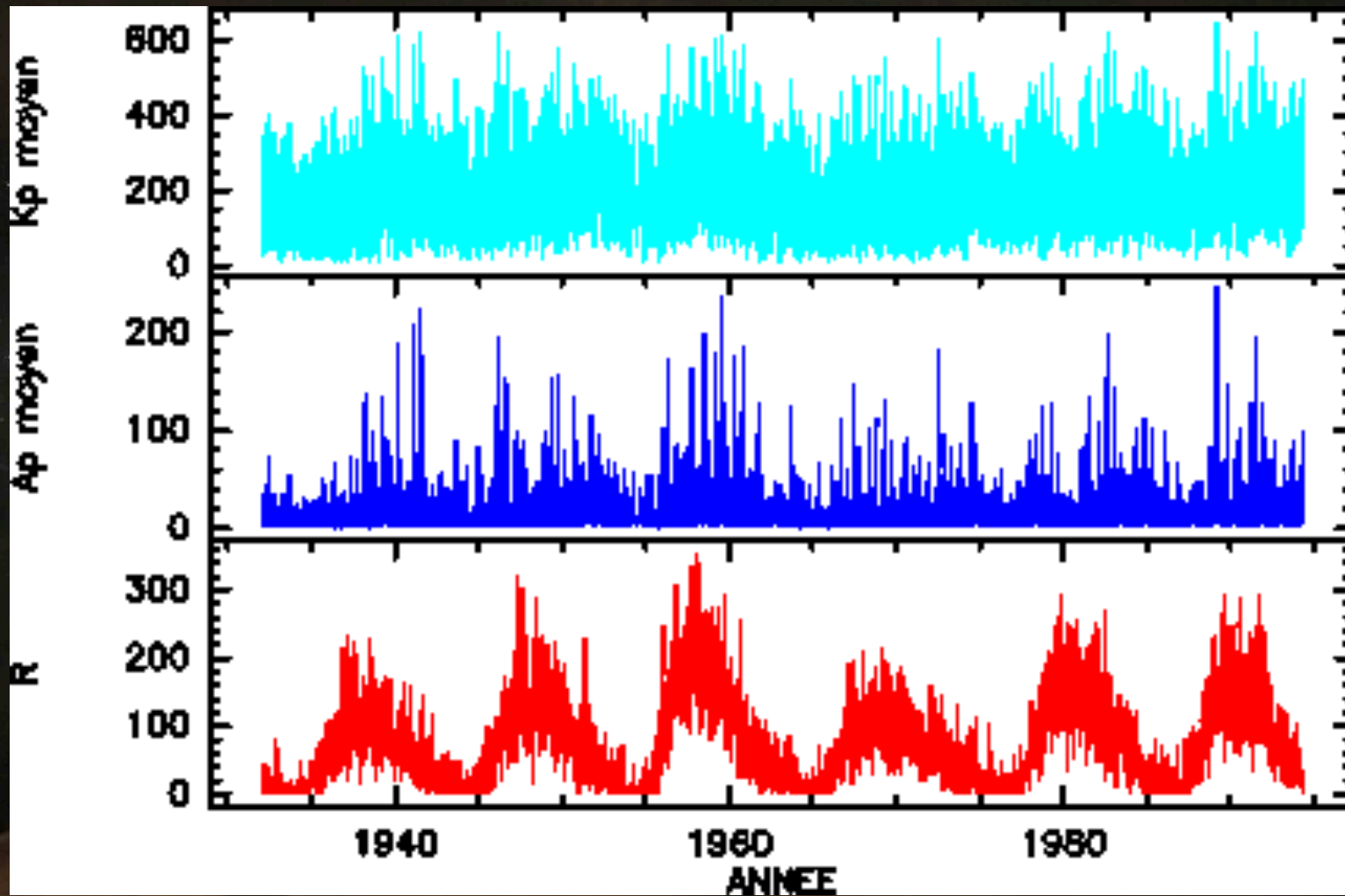
Indices <i>(beginning of the data series)</i>	(1) Measured quantity Baseline	(2) Time interval	(3) Network	(4) Derivation process
<i>Auroral indices</i> AE, AU, AL, A0	Deviation ΔH (nT) of the horizontal component Baseline: Sq* variation (see text)	1 minute (since 1978)	Network of stations in the boreal auroral zone Modification of the network in 1966 (see Figure 8 the network since 1966)	<u>AU</u> : largest observed value of $\Delta H(t)$ at the network stations and at time t (upper envelope) <u>AL</u> : smallest observed value of $\Delta H(t)$ (lower envelope) AE = AU + AL A0 = (AU + AL) / 2 Unit: nT
<i>(Since July 1957 ; missing data in 1976-1977)</i>				
<i>Equatorial index</i> Dst (since 1957)	ΔH (nT) variation of the horizontal component; Baseline: secular variation	1 hour	Network of 4 low latitude stations (see Figure 8)	Hourly values of the perturbation D are computed at each station : D = $\Delta H - Sq^{**}$ (see text) Dst = Moy(D) / Moy(cos ϕ) ϕ : dipolar latitude of the stations Unit: nT

Indices <i>(beginning of the data series)</i>	(1) Measured quantity Baseline	(2) Time interval	(3) Network	(4) Derivation process
<i>Local indices</i>	Amplitude of the	3 hours (UT);	K indices are defined	K is a code (a number: 0 to 9)
K	<u>irregular variations:</u> <u>ranges</u>	00-03, 03-06,, 18-21, 21-24	<u>everywhere, but</u> <u>their meaning is</u> <u>the best at</u> <u>subauroral latitudes</u>	<u>corresponding to the class in which</u> <u>falls the measured range.</u> The limits of the classes are defined <u>according to a quasi logarithmic scale</u> <u>(see text and Figure 8)</u> <u>$a_K(nT)$ is the mid-class amplitude</u> <u>associated to the K value.</u>
	Baseline: S_R variation <u>(see text)</u>			

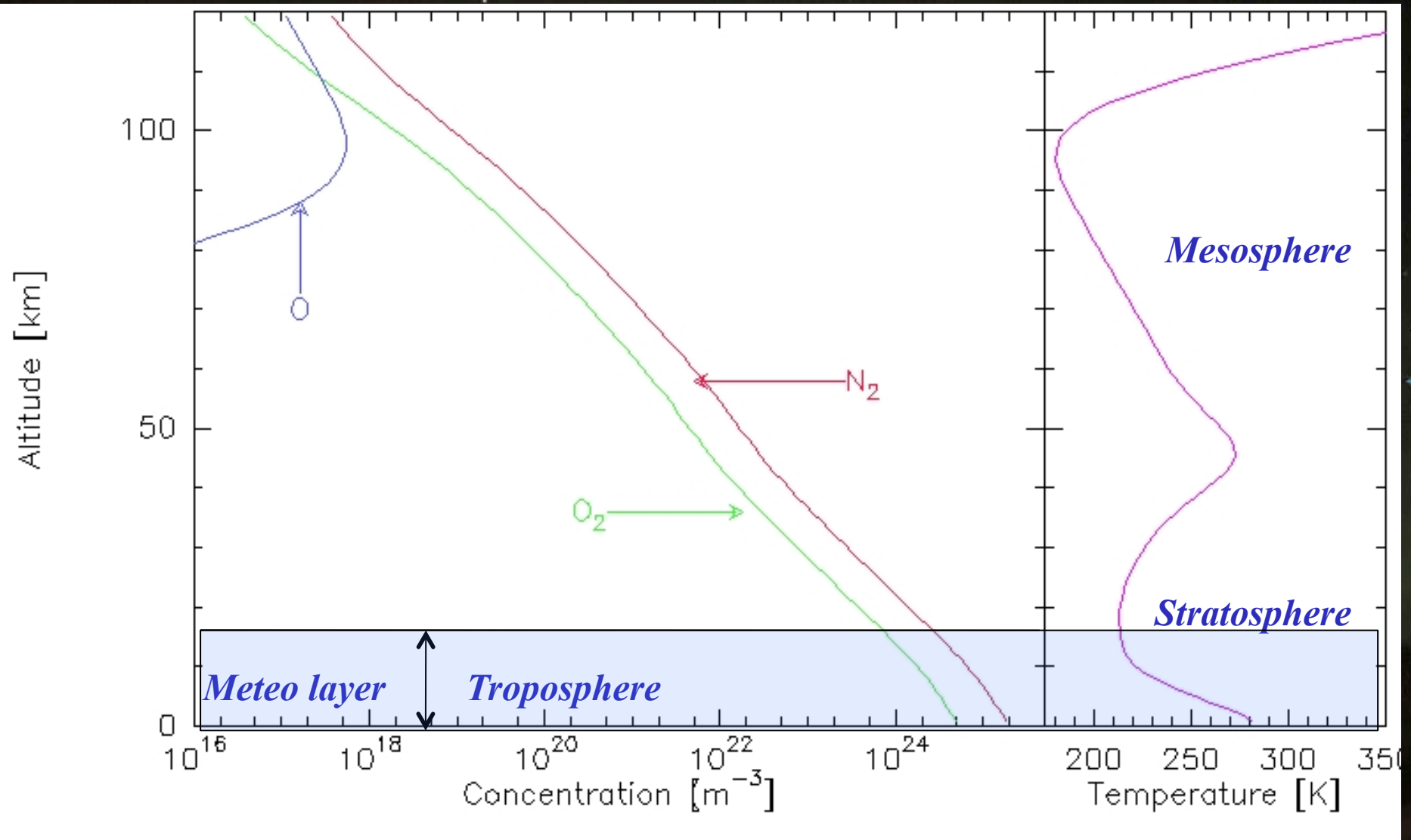
Indices <i>(beginning of the data series)</i>	(1) Measured quantity Baseline	(2) Time interval	(3) Network	(4) Derivation process
<i>Planetary indices</i>	K indices	3 hours (UT)	Network of	K codes from each station are
K _p			13 <u>stations</u> :	<u>converted to standardised codes "3Ks"</u>
<u>a_p</u> , A _p		<i>(cf. K indices)</i>	11 boreal ones and	$3K_p = \sum 3K_s / 12$
			2 austral ones.	3K _s et 3K _p : integers, 0 to 27
<i>(since 1932)</i>				K _p : 0 _o , 0+, 1-, to 9 _o
			<i>(see Figure 8)</i>	<u>a_p</u> : deduced from K _p through conversion tables (<i>unit: 2nT</i>)
				A _p : daily mean value of a _p

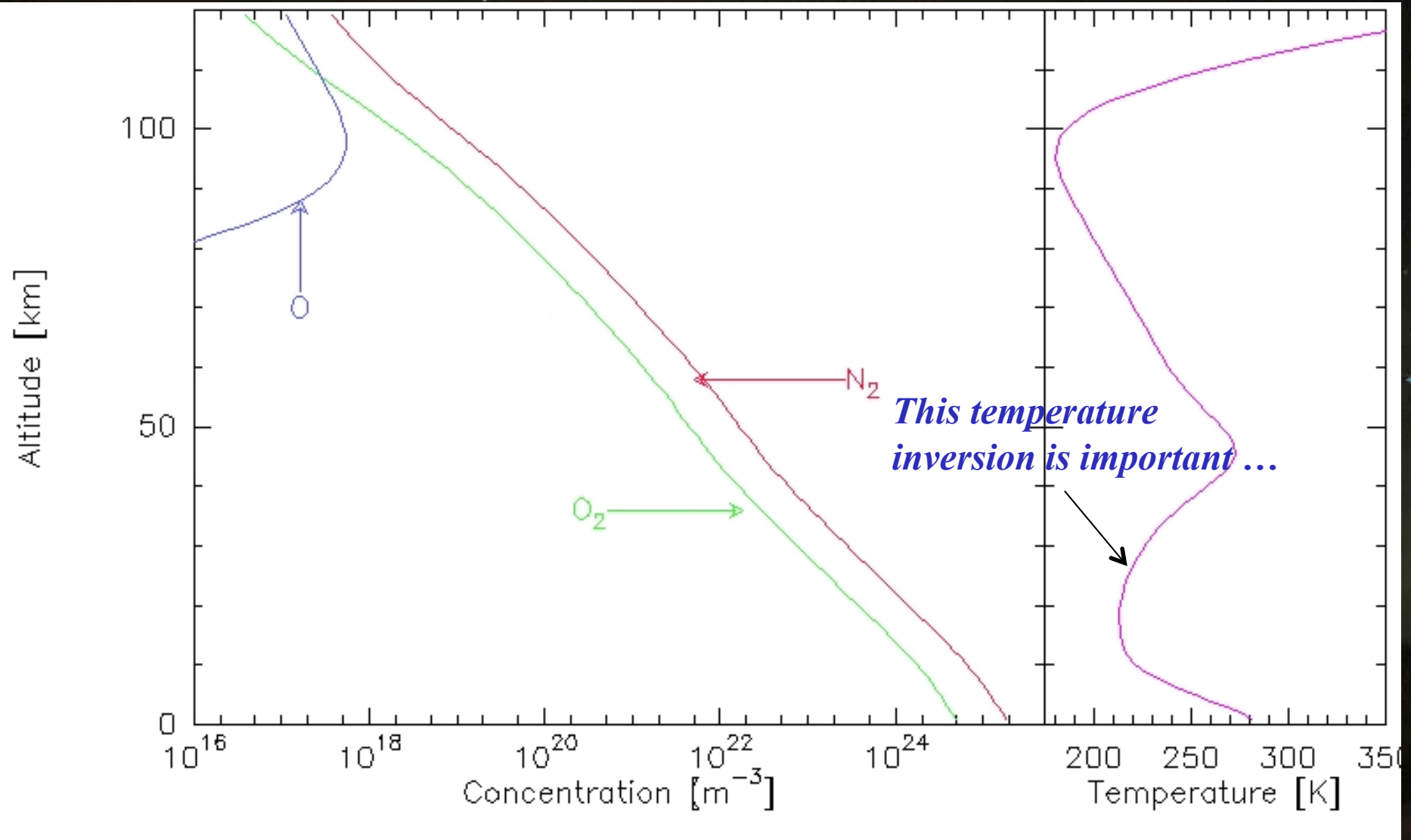
Indices <i>(beginning of the data series)</i>	(1) Measured quantity Baseline	(2) Time interval	(3) Network	(4) Derivation process
<i>Planetary indices</i> a_n , a_s and a_m A_n , A_s and A_m K_{pn} , K_{ps} and K_{pm} <i>(since 1959)</i>	Amplitudes deduced from K indices	3 hours (UT) <i>(cf. K indices)</i>	Network of subauroral latitude stations: 13 boreal ones and 10 austral ones arranged in groups each group representing a longitude sector <i>(see Figure 8)</i>	For each longitude sector G_i , the average of Ks is converted to equivalent amplitudes: $a_{G_i}(nT)$ $a_n: \sum \lambda_{G_i} a_{G_i}$ (boreal hemisphere) $a_s: \sum \lambda_{G_i} a_{G_i}$ (austral hemisphere) λ_{G_i} : weighting factor accounting for the longitude width of G_i $a_m = (a_n + a_s) / 2$ A_n, A_s, A_m : daily mean values of a_n, a_s, a_m K_{pn}, K_{ps}, K_{pm} : deduced from a_m, a_n, a_s through conversion tables <i>Unit for a_m, a_n, a_s: nT</i> <i>Unit for K_{pn}, K_{ps}, K_{pm}: Kp unit</i>

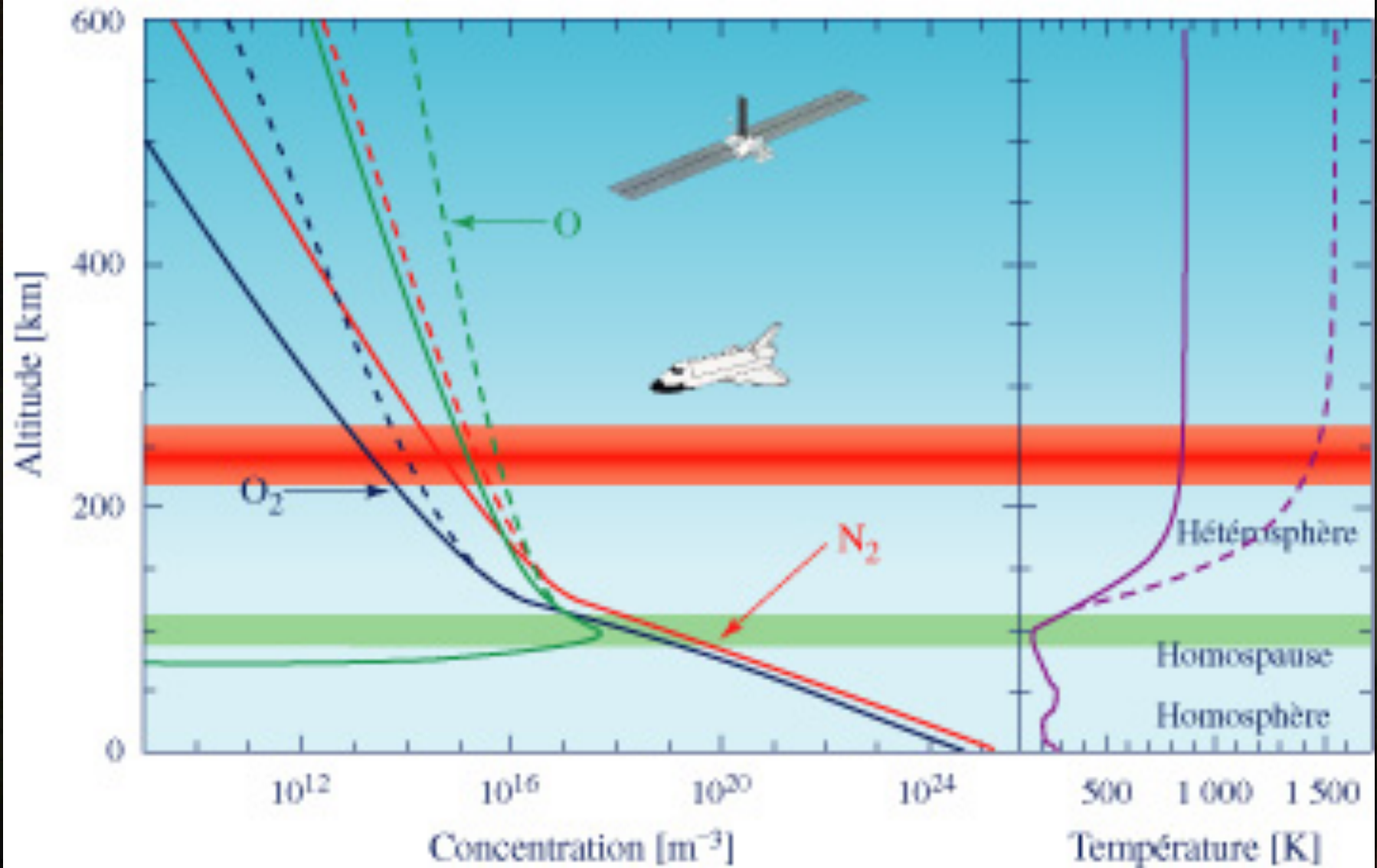
Indices <i>(beginning of the data series)</i>	(1) Measured quantity Baseline	(2) Time interval	(3) Network	(4) Derivation process
<i>Planetary index</i> <u>aa</u>	Amplitudes deduced from K indices	<u>derivation:</u> 3 hours (UT)	Network of 2 <u>antipodal</u> <u>subauroral latitude</u> <u>stations:</u> HAD and CAN (see Figure 8)	For each station, the a_K values are corrected to take into account the small differences between the latitudes of the 2 stations <u>aa</u> : average of the 2 corrected amplitudes <i>Unit: nT</i>
<i>(since 1868)</i>		<u>meaningful when</u> <u>averaged over</u> <u>at least 4</u> <u>intervals</u>		



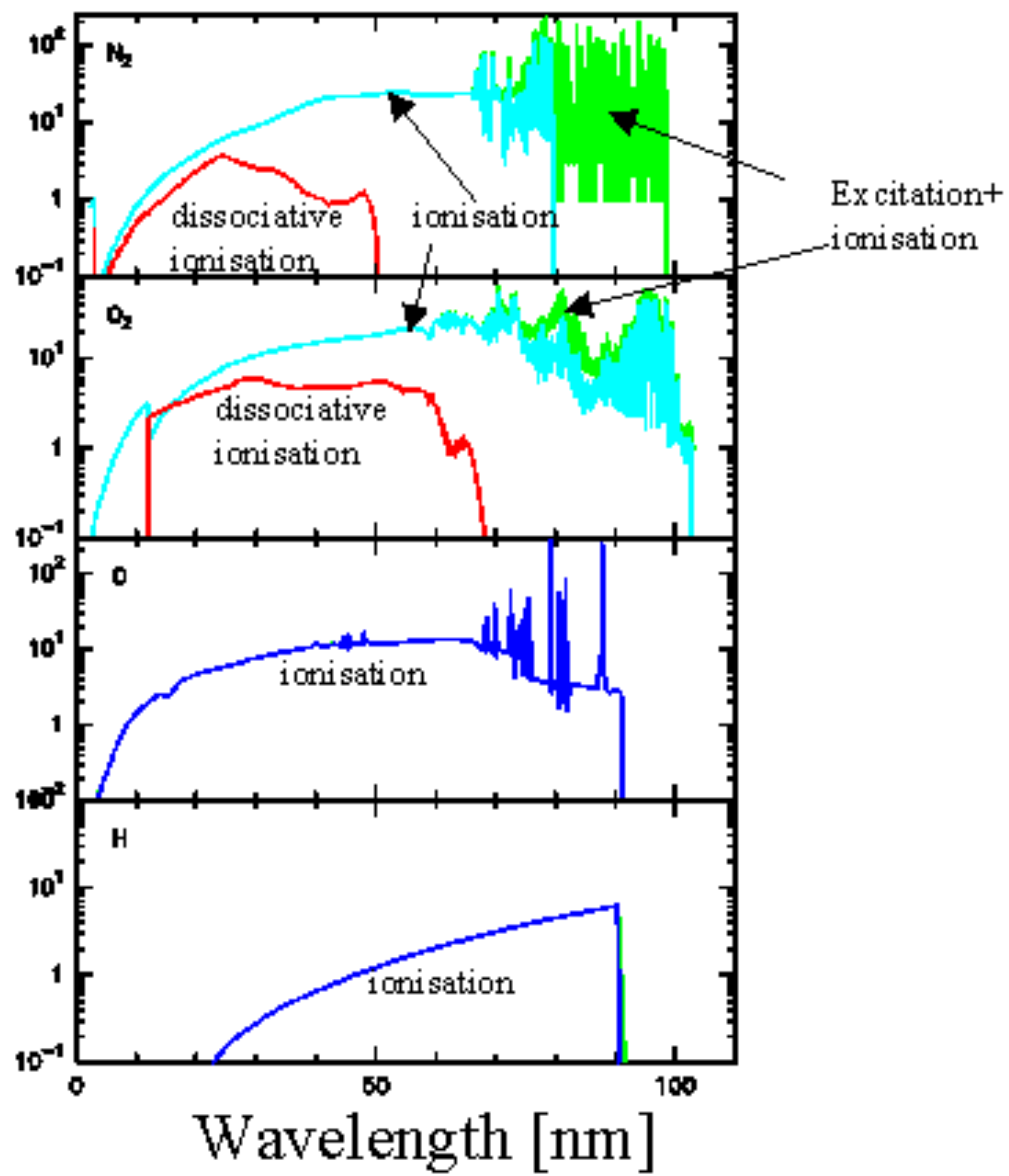
2) The Earth Atmosphere



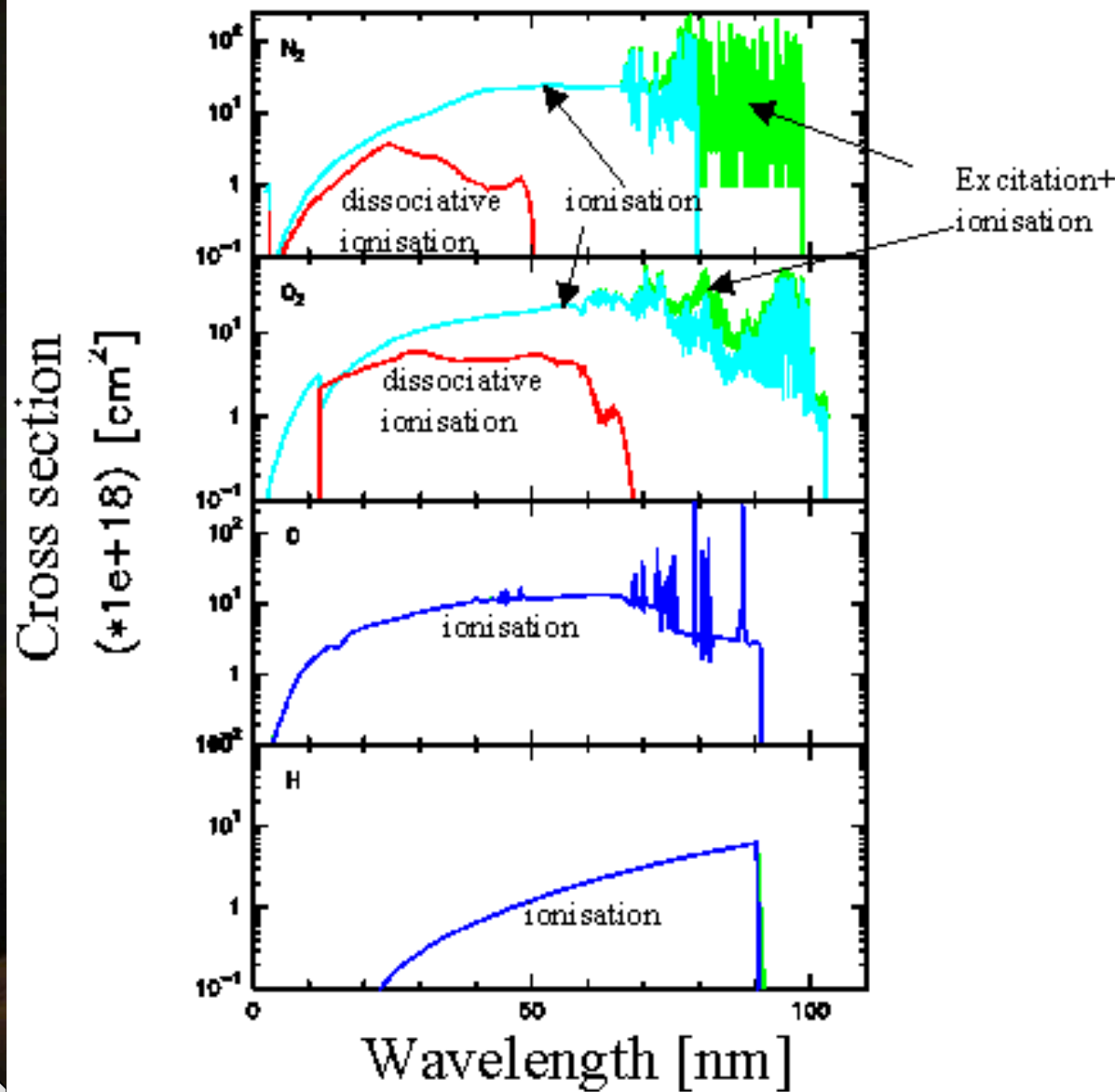




Cross section
(*1e+18) [cm²]



Note that cross sections are much bigger than Van der Waals sections

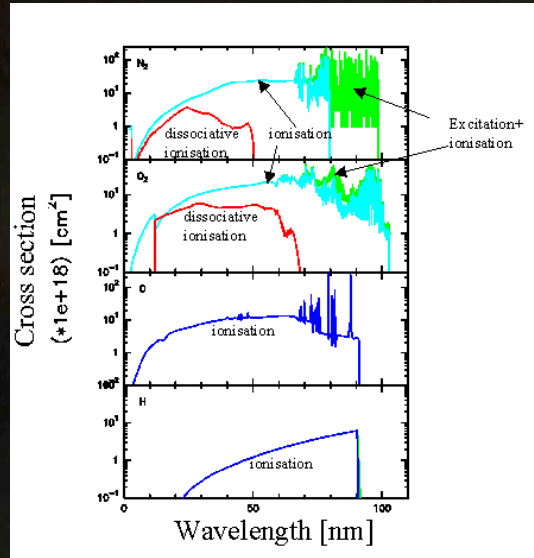


$$L(\text{N}_2) = 0.1098 \text{ nm}$$
$$S \approx 0.15 \cdot 10^{-22} \text{ cm}^2$$

$$L(\text{O}_2) = 0,292 \text{ nm}$$
$$S \approx 1.07 \cdot 10^{-22} \text{ cm}^2$$

$$L(\text{O}) = 0,066 \text{ nm}$$
$$S \approx 0.55 \cdot 10^{-23} \text{ cm}^2$$

$$L(\text{H}) = 0,025 \text{ nm}$$
$$S \approx 0.79 \cdot 10^{-24} \text{ cm}^2$$



For atmospheric gazes, keep in mind values of :

$$S \approx 1 \text{ to } 20 \cdot 10^{-24} \text{ cm}^2 = 1 \text{ to } 20 \cdot 10^{-28} \text{ m}^2$$

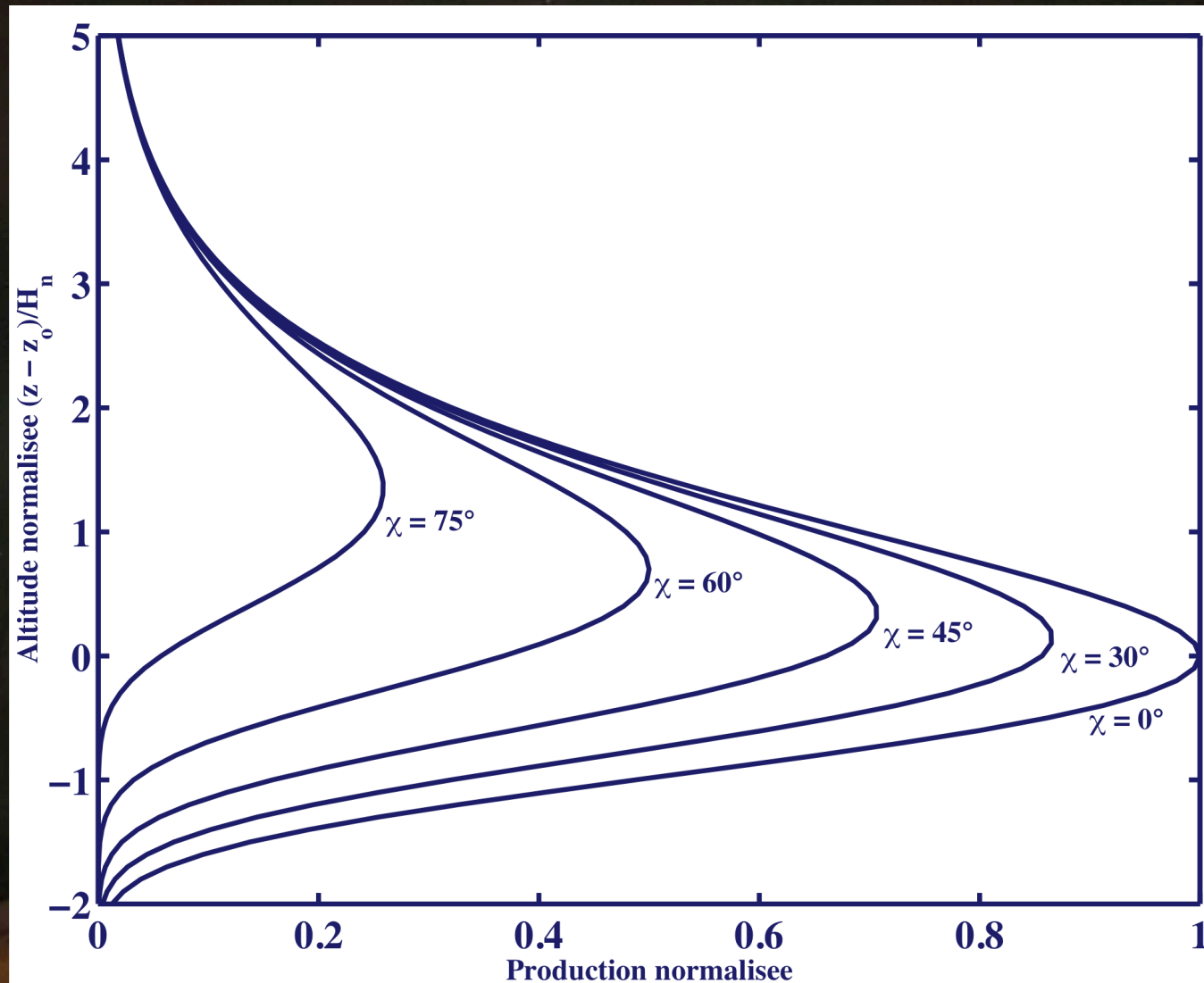
$$= 1 \text{ to } 20 \text{ barn}$$

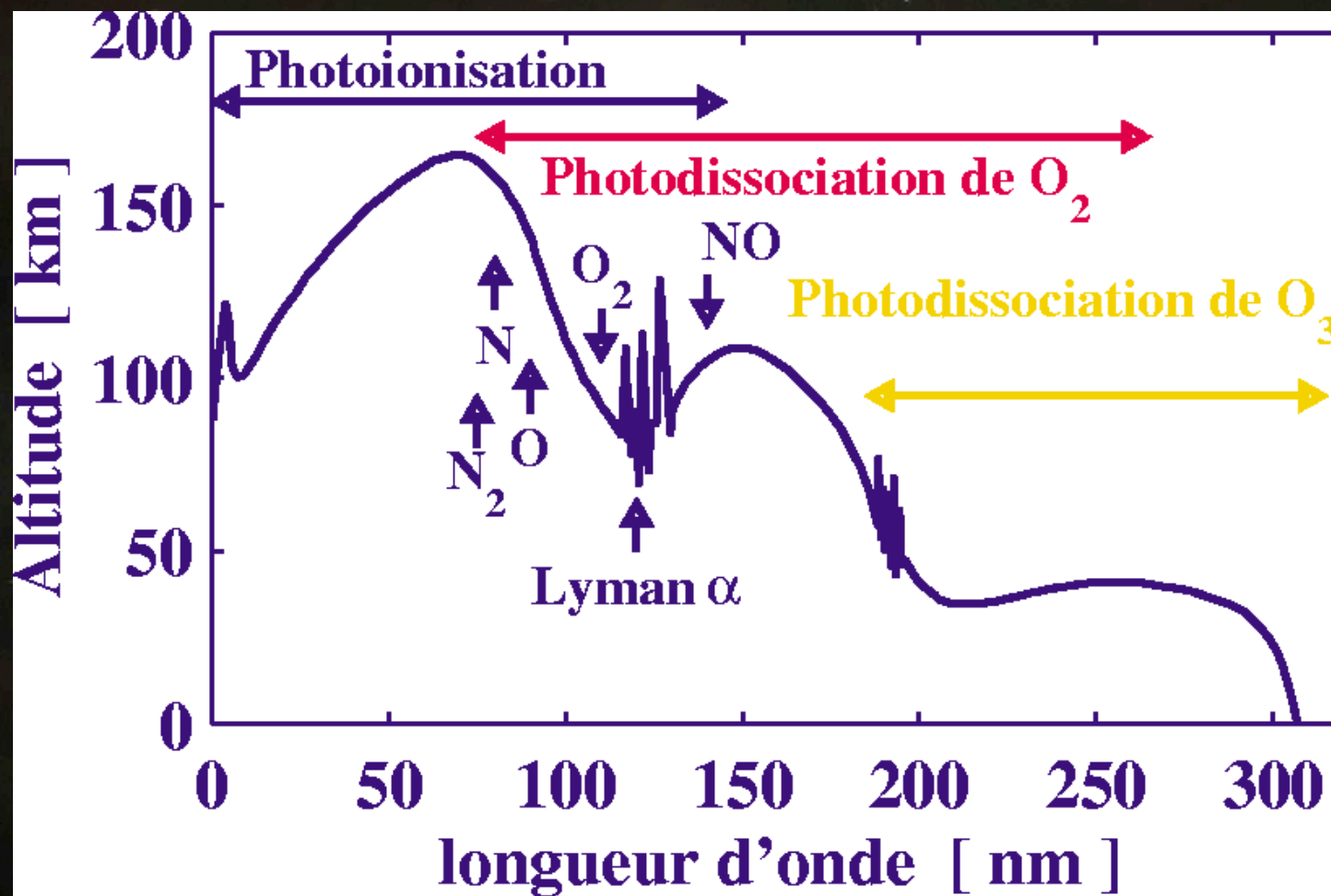
$$\sigma_{\text{ion}} \approx 10^{-17} \text{ cm}^2 = 10^{-21} \text{ m}^2$$

$$\sigma_{\text{dissoc}} \approx 10^{-18} \text{ cm}^2 = 10^{-22} \text{ m}^2$$

We can now start making some computations (on the board).

The hydrostatic equilibrium, the scale height
and the Chapman theory





However, it is not that simple ...

Let's have a look to the kinetic theory
(on the board first)

... and see also class by Valentini and
Mignone

For instabilities: see class by Califano

For modeling: see class by Lapenta

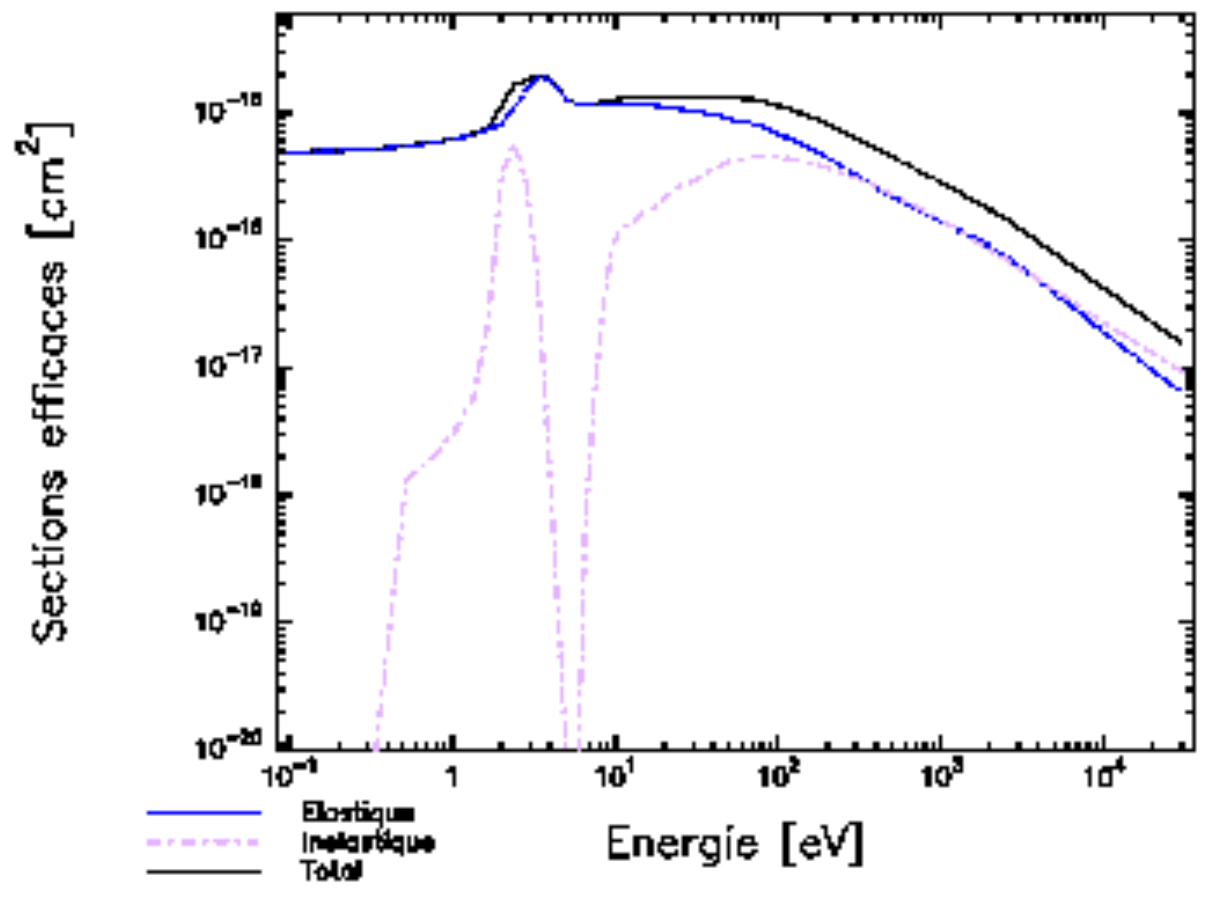
Kinetic Boltzmann equation for dissipative forces

$$\frac{\partial f}{\partial t} + \frac{\partial \vec{v} f}{\partial \vec{r}} + \frac{\partial \vec{F}}{m} f = \left(\frac{\delta f}{\delta t} \right)_{\text{collisions}}$$

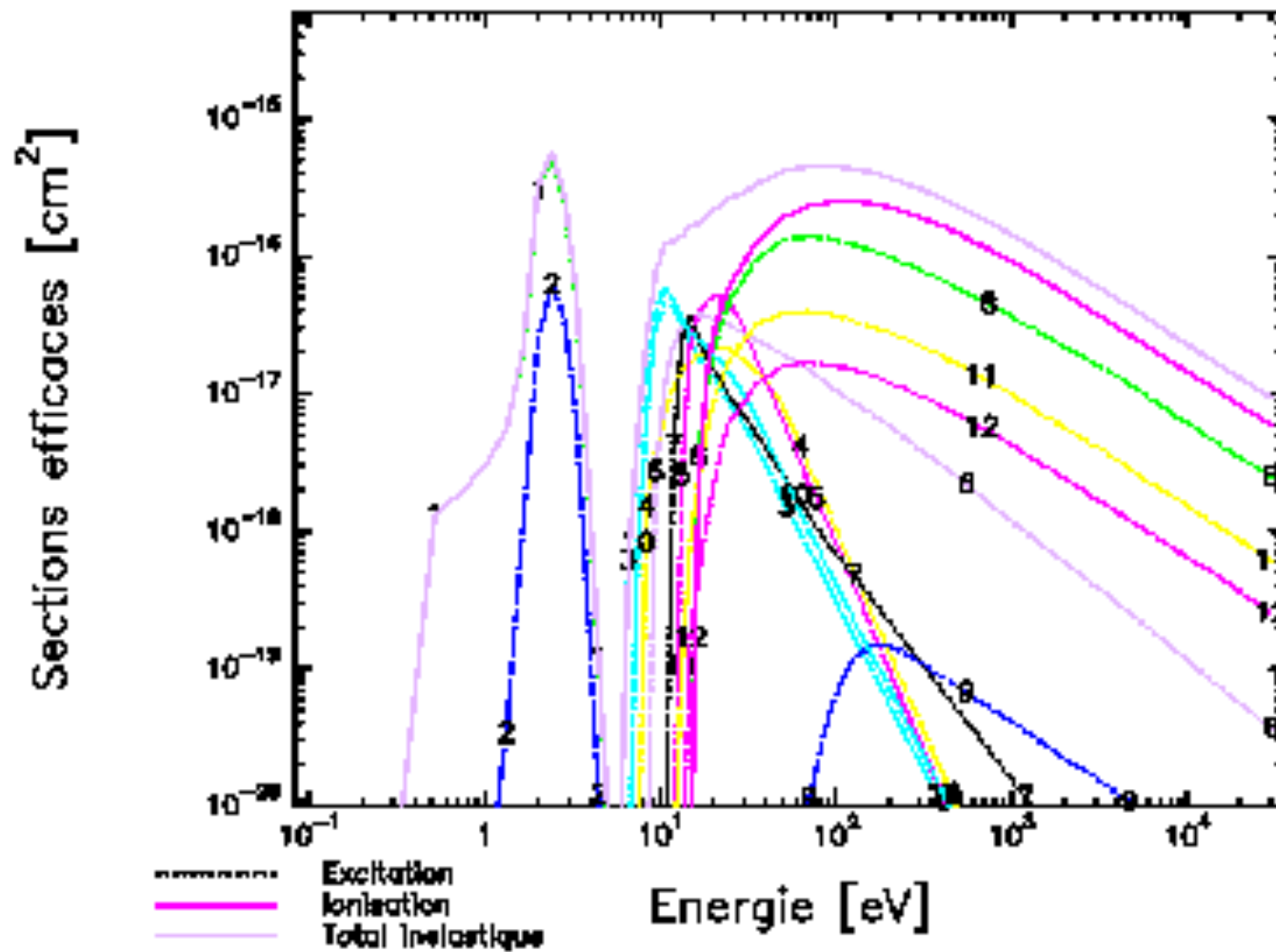
For the study of the ionosphere, use of the :
stationnary particle flux

$$\Phi(z, E, \mu) = \frac{|\vec{v}|^2}{m} f(t, \vec{v}, \vec{r})$$

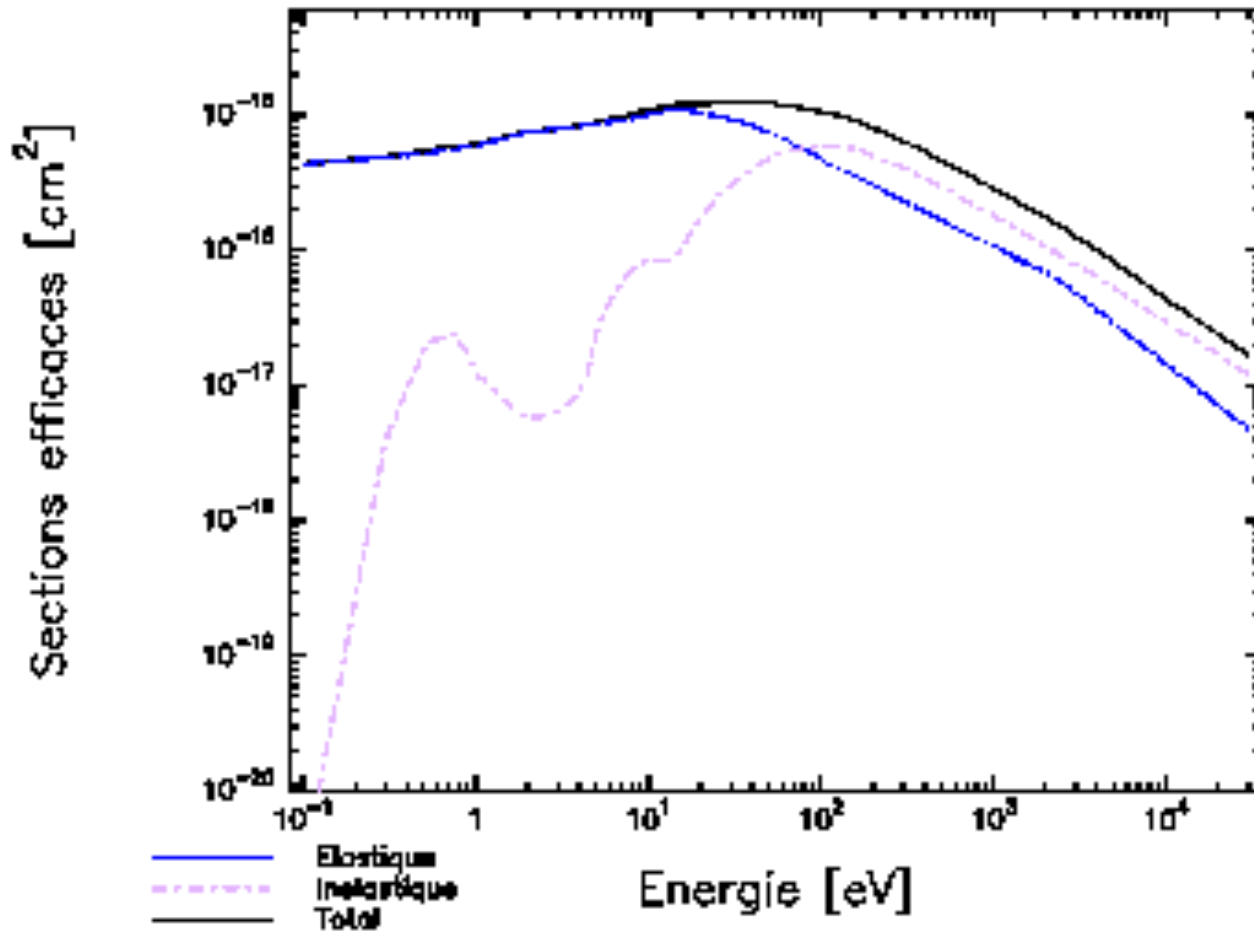
COLLISIONS ELECTRONS - [N2]



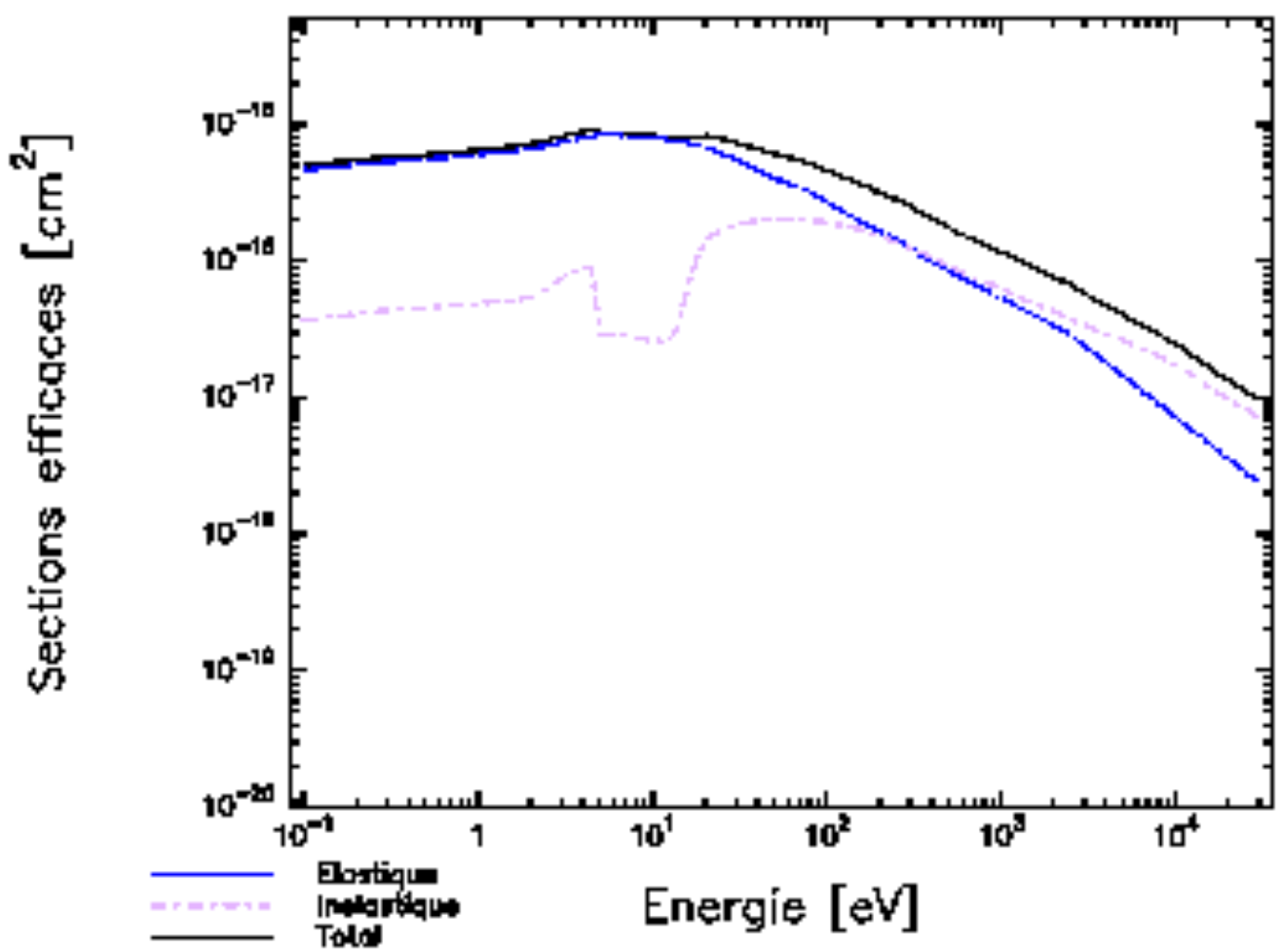
COLLISIONS ELECTRONS - [N2]

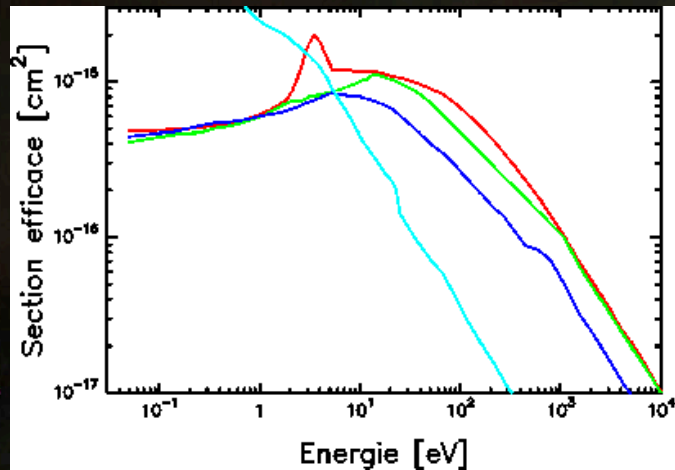


COLLISIONS ELECTRONS - [02]



COLLISIONS ELECTRONS - [O]





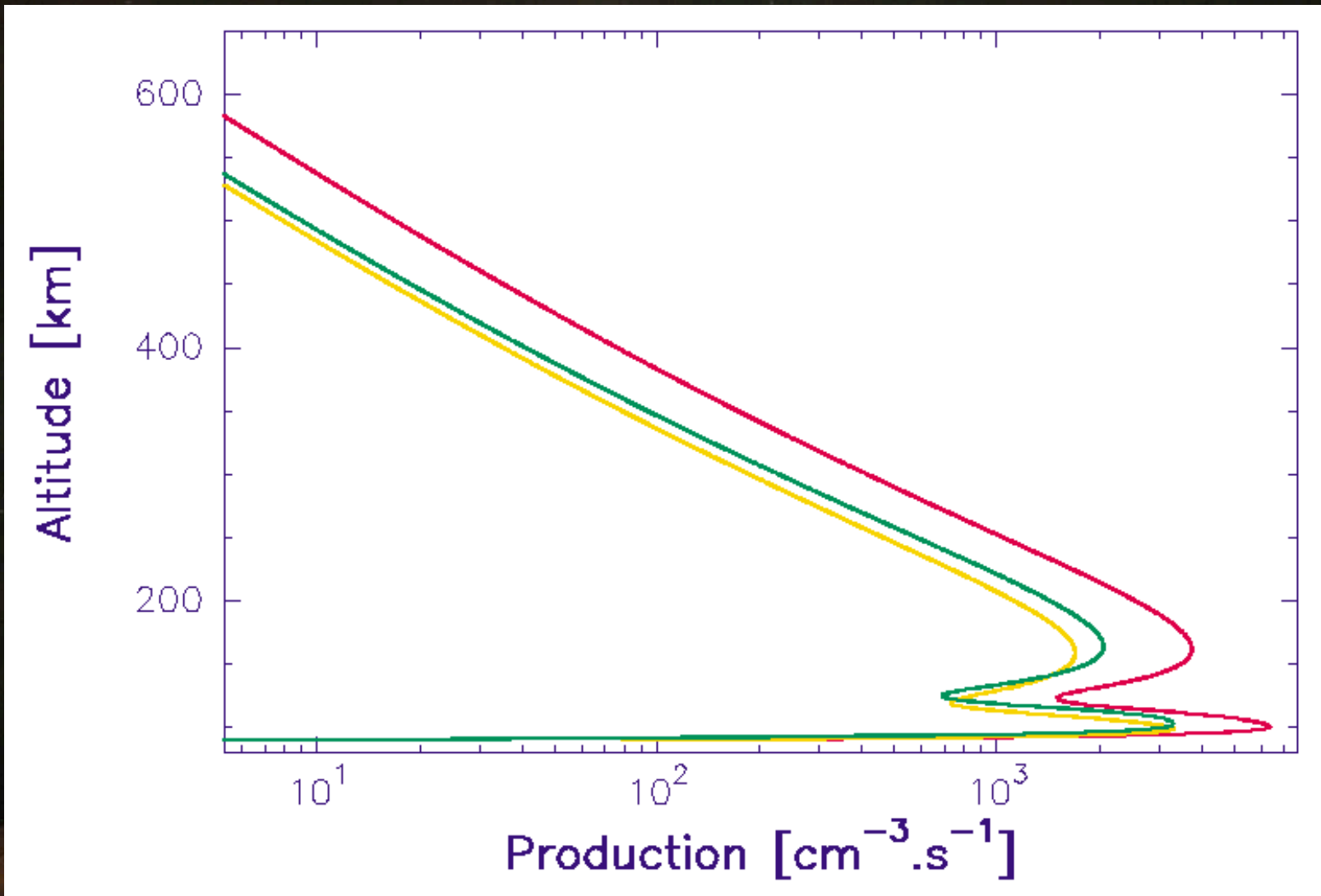
For atmospheric gazes, keep in mind values of :

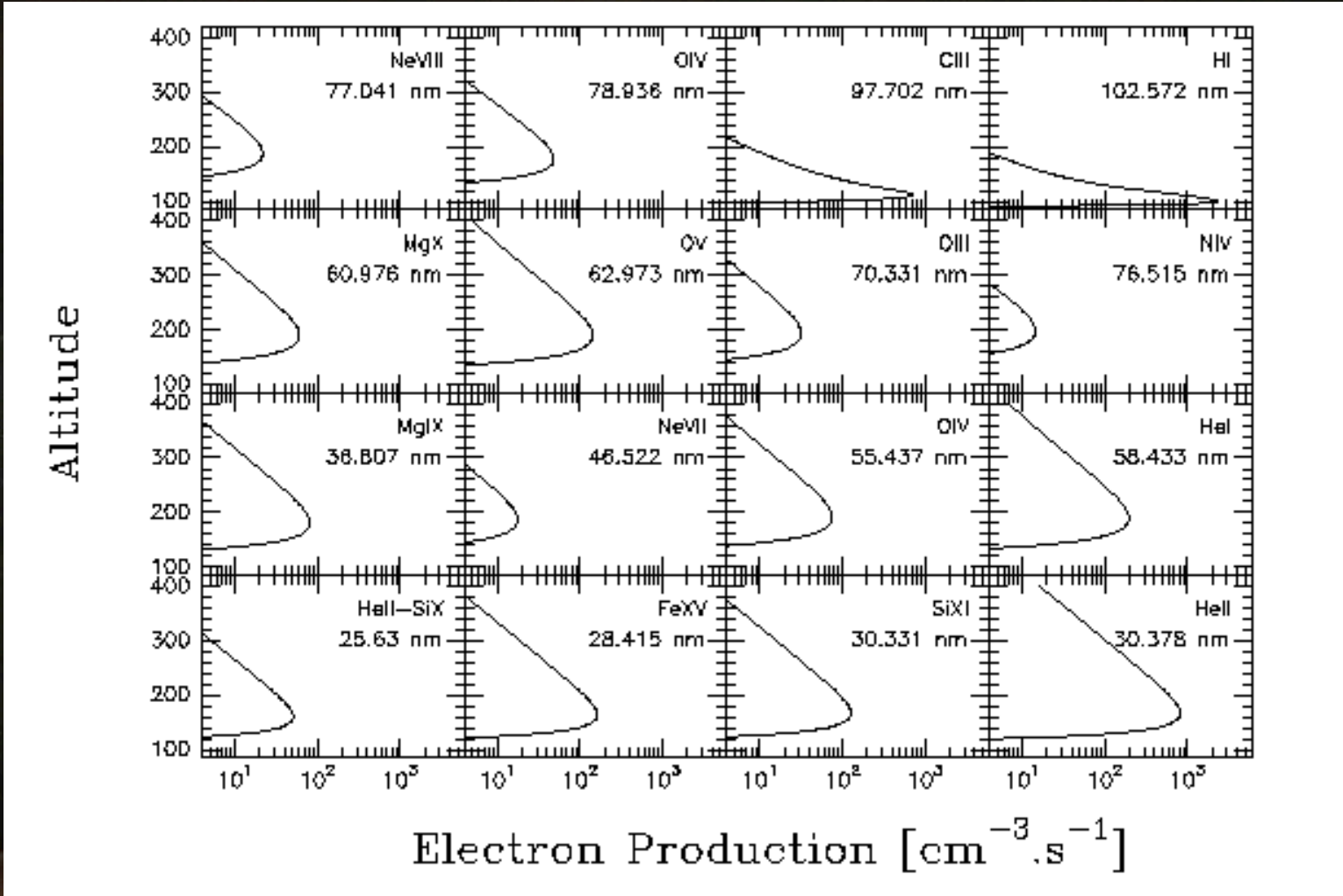
Collision cross sections about 10 times bigger than absorption cross sections

$$\sigma \approx 10^{-16} \text{ to } 10^{-15} \text{ cm}^2 = 10^{-20} \text{ to } 10^{-19} \text{ m}^2$$

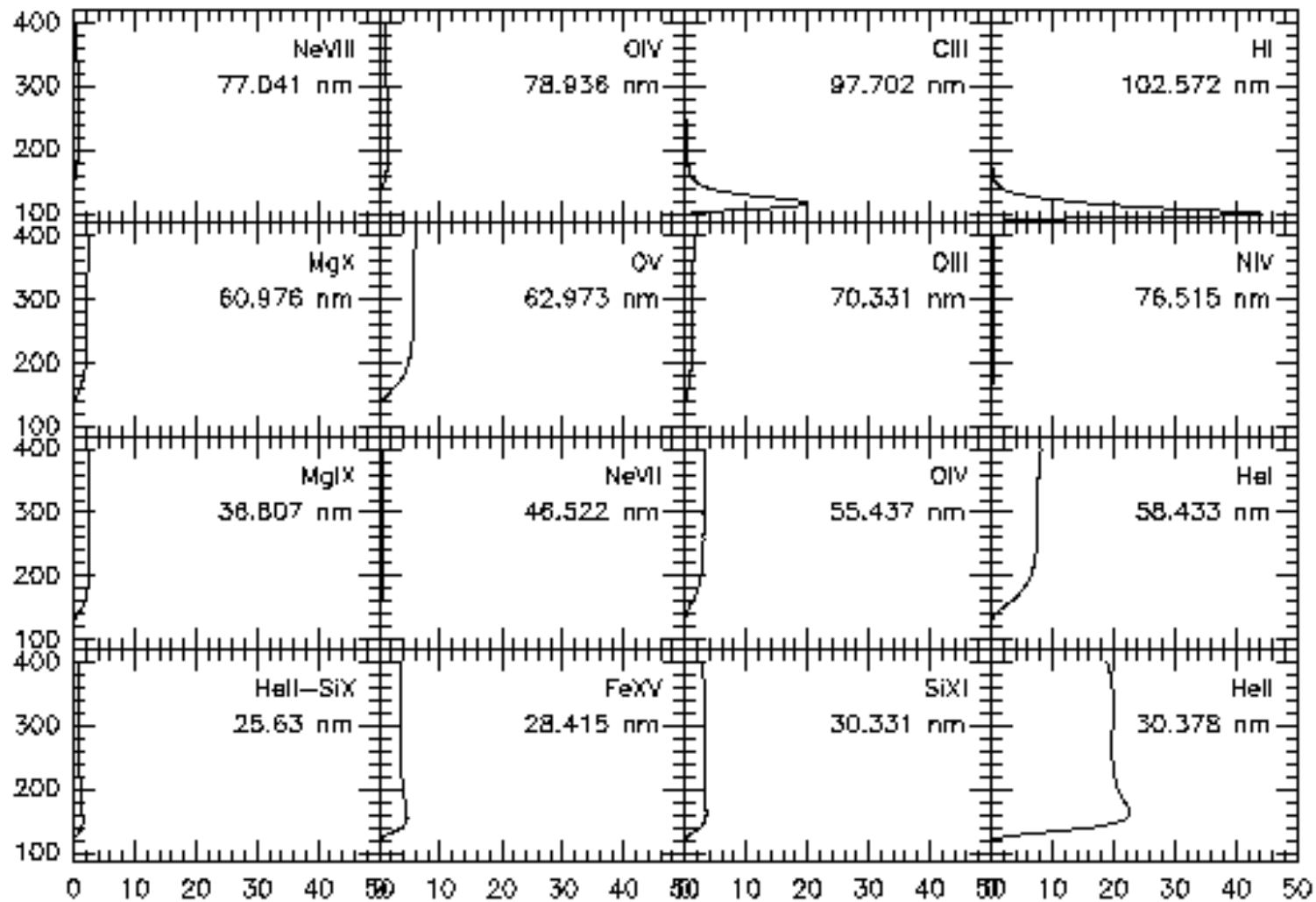
Note also that the collision frequency concept is linked to the cross sections:

$$v_{\text{coll}} = \sigma_{\text{tot}} N v$$



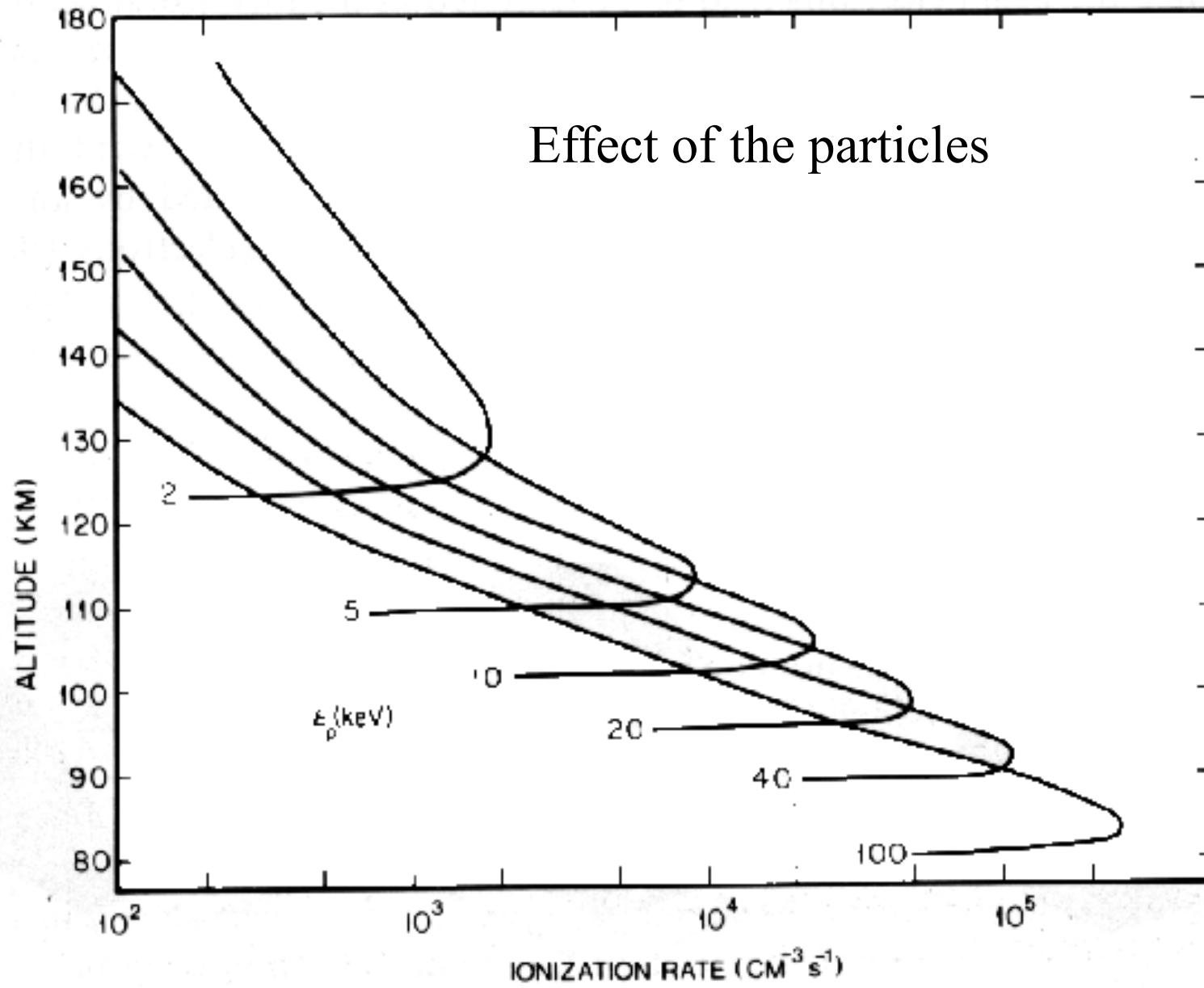


Altitude

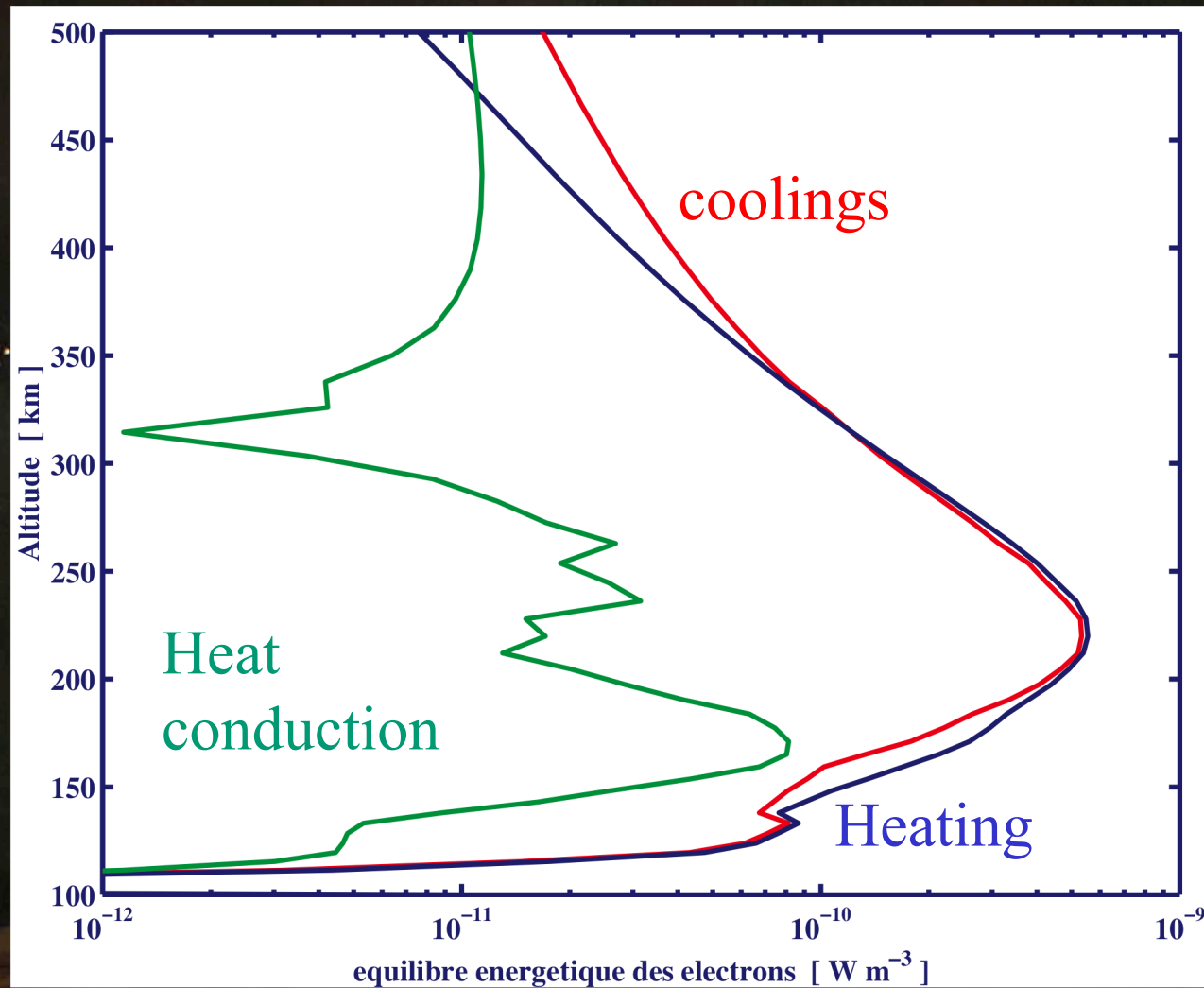


Contribution to the electron production [%]

Effect of the particles



The heating rate



Here for
high solar
activity

Note that this is efficient above about 100 km

To quote EISCAT people (see
class by Pierrard) :

Heating creates expansion

This is of primary importance
for space weather

Radiative de-excitation creates the polar lights



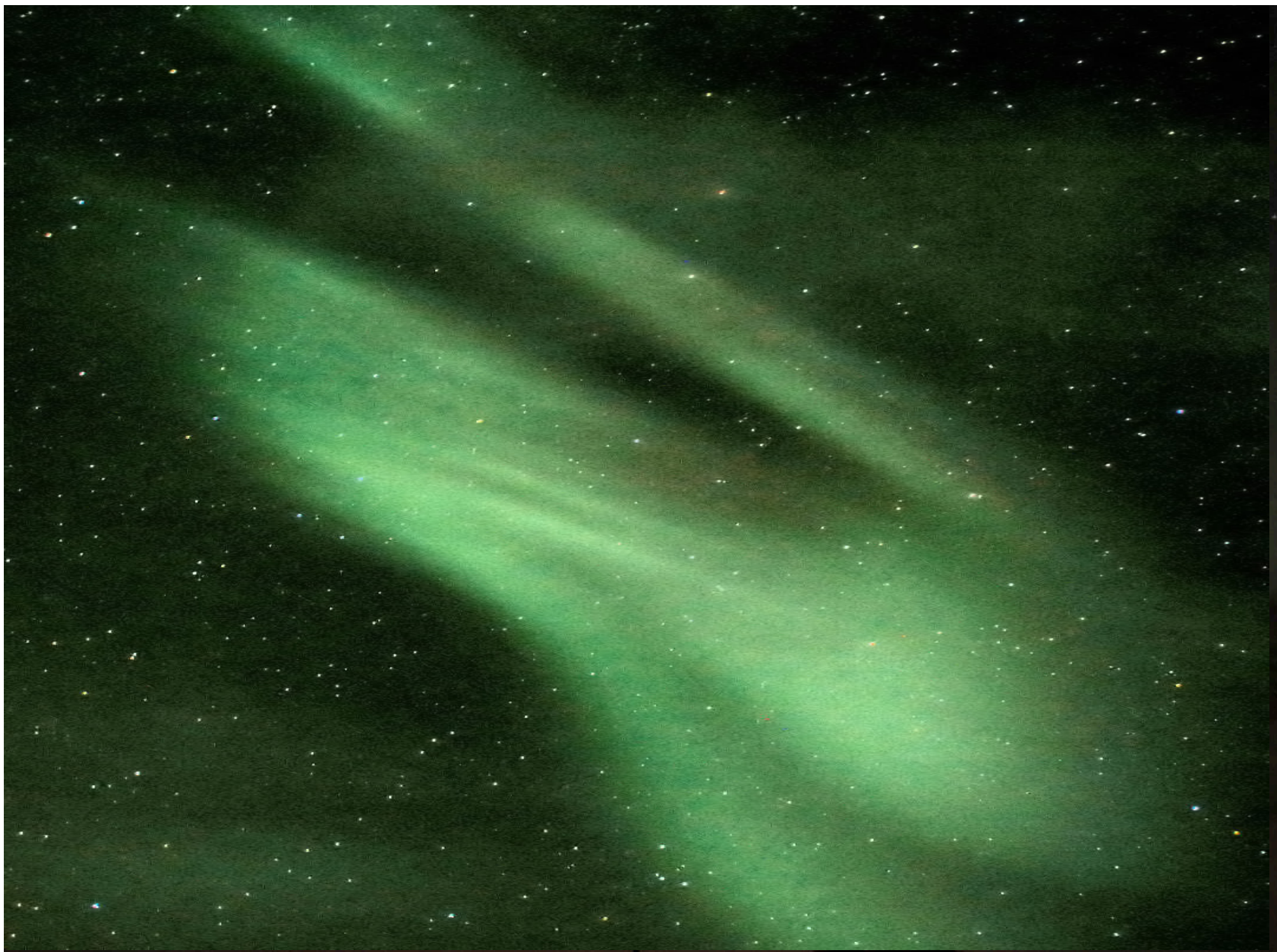
Tom Eklund



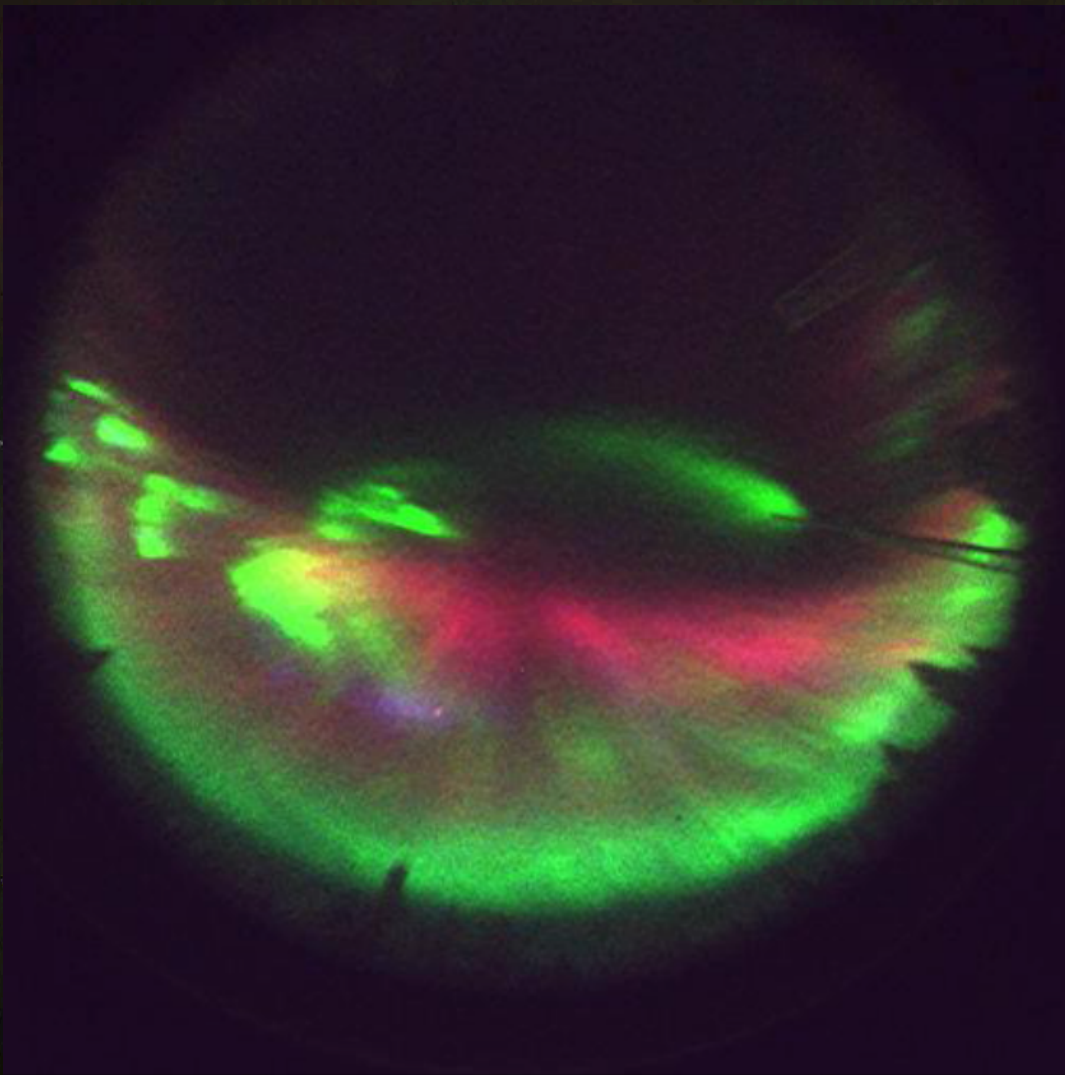
Tom Eklund







\\\\Meantimages\Aurores_et_ravonnement\films\Thomas_Ulich_20020119_20.mov



21:34:40 UTC

SGO/OY All Sky Camera Image

Station SODANKYLA, N67.37 E26.63

19 Jan 2002

Filter: 550 nm

Exposure: 1000 ms

N

W + E

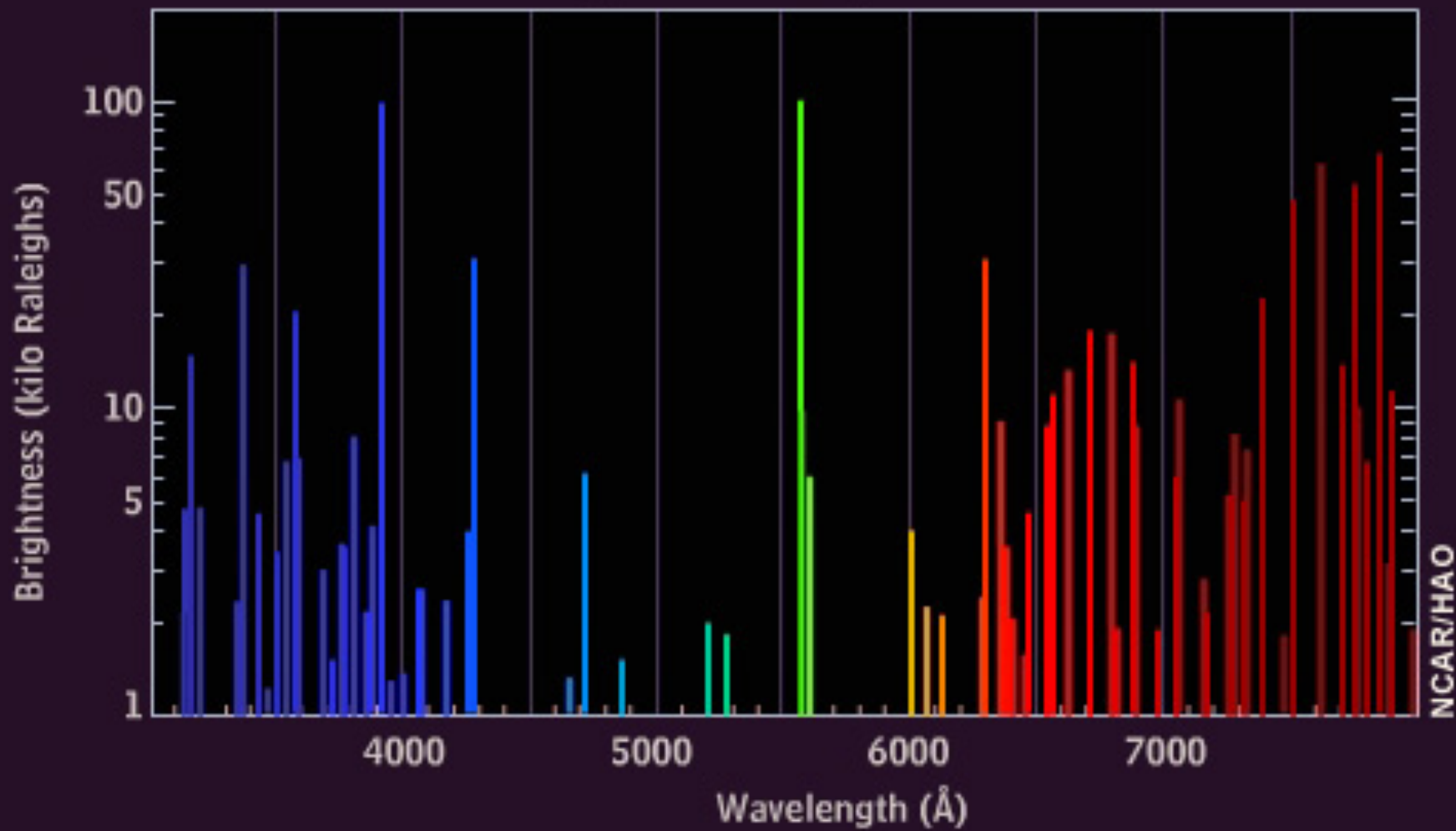
S







Typical Auroral Spectrum



In order to go from the flux,
production and rates to measurable
parameters such as density or
temperatures, one needs to consider
the fluid approach (see class by
Valentini)

Kinetic \rightarrow microscopic
Fluid \rightarrow macroscopic

Kinetic \rightarrow distribution
function

Fluid \rightarrow integral of the
distribution function

Boltzmann fluid equations:

Integrals of the kinetic equation over $v^a dv$

0th order momentum = continuity equation

1st order momentum = force equation

2^d order momentum = energy equation

3^d order momentum = heat flux equation

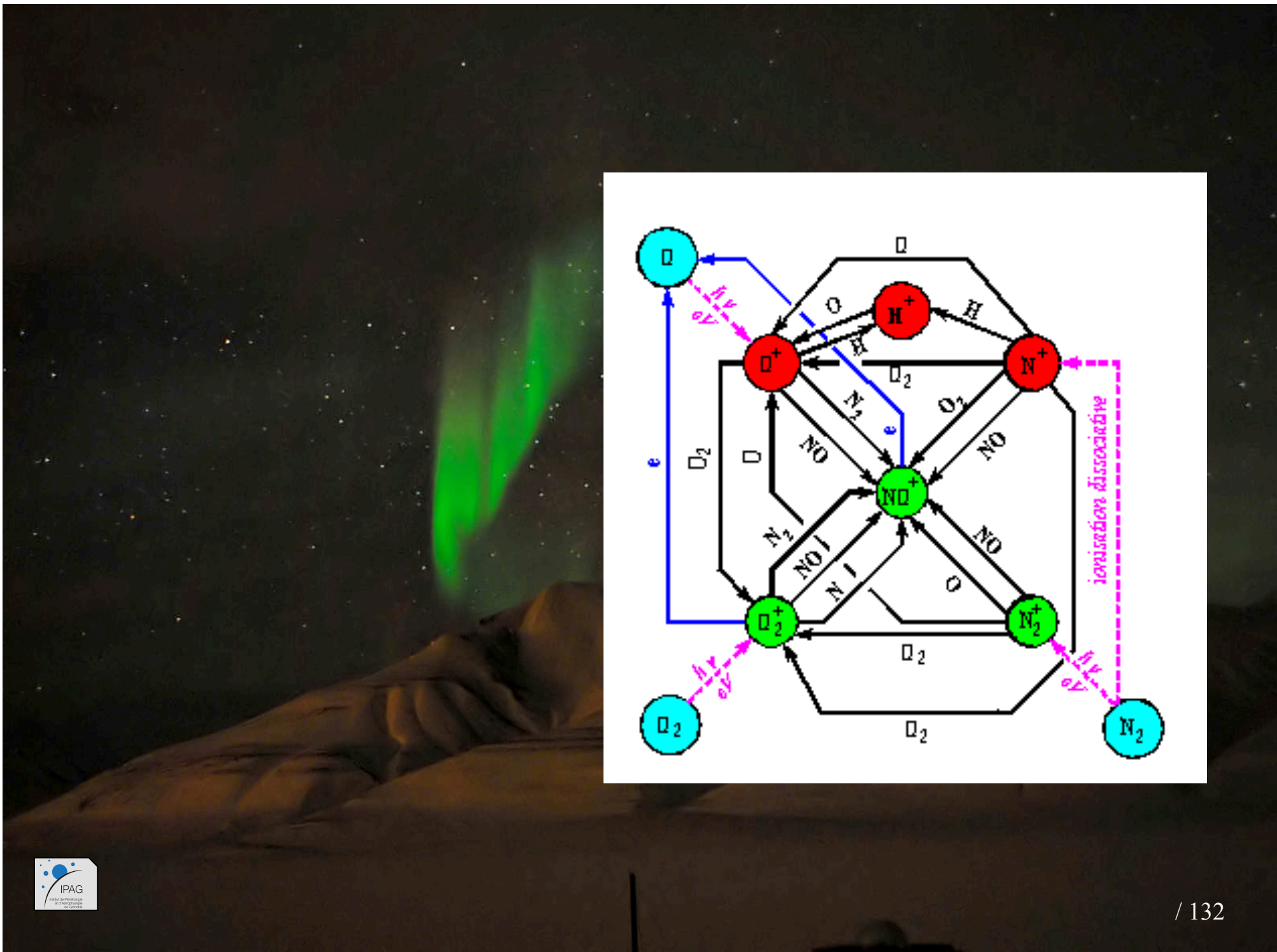
The distribution function is a maxwellian for thermal particles :

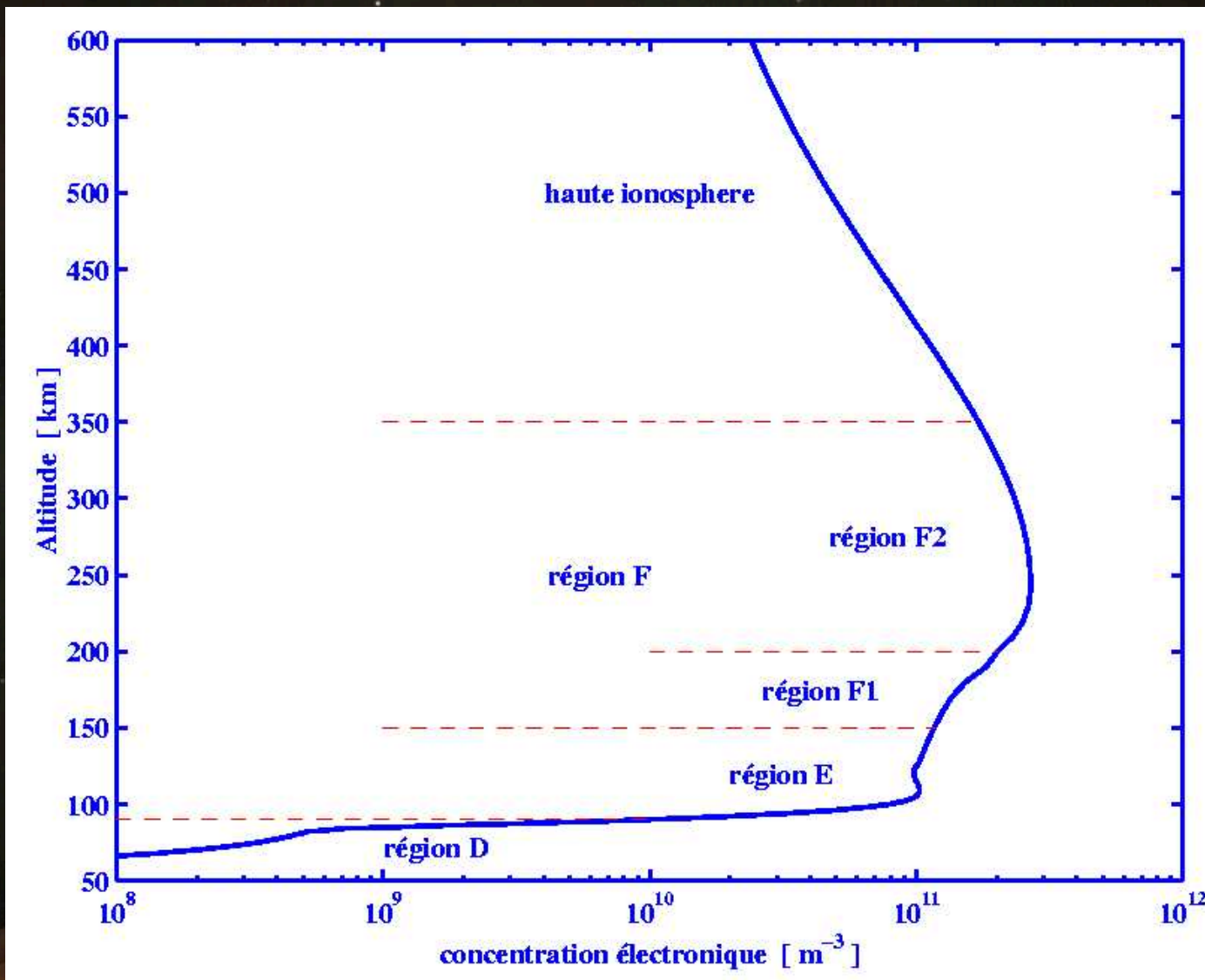
0th order momentum \rightarrow densities (scalars)

1st order momentum \rightarrow velocities (vectors)

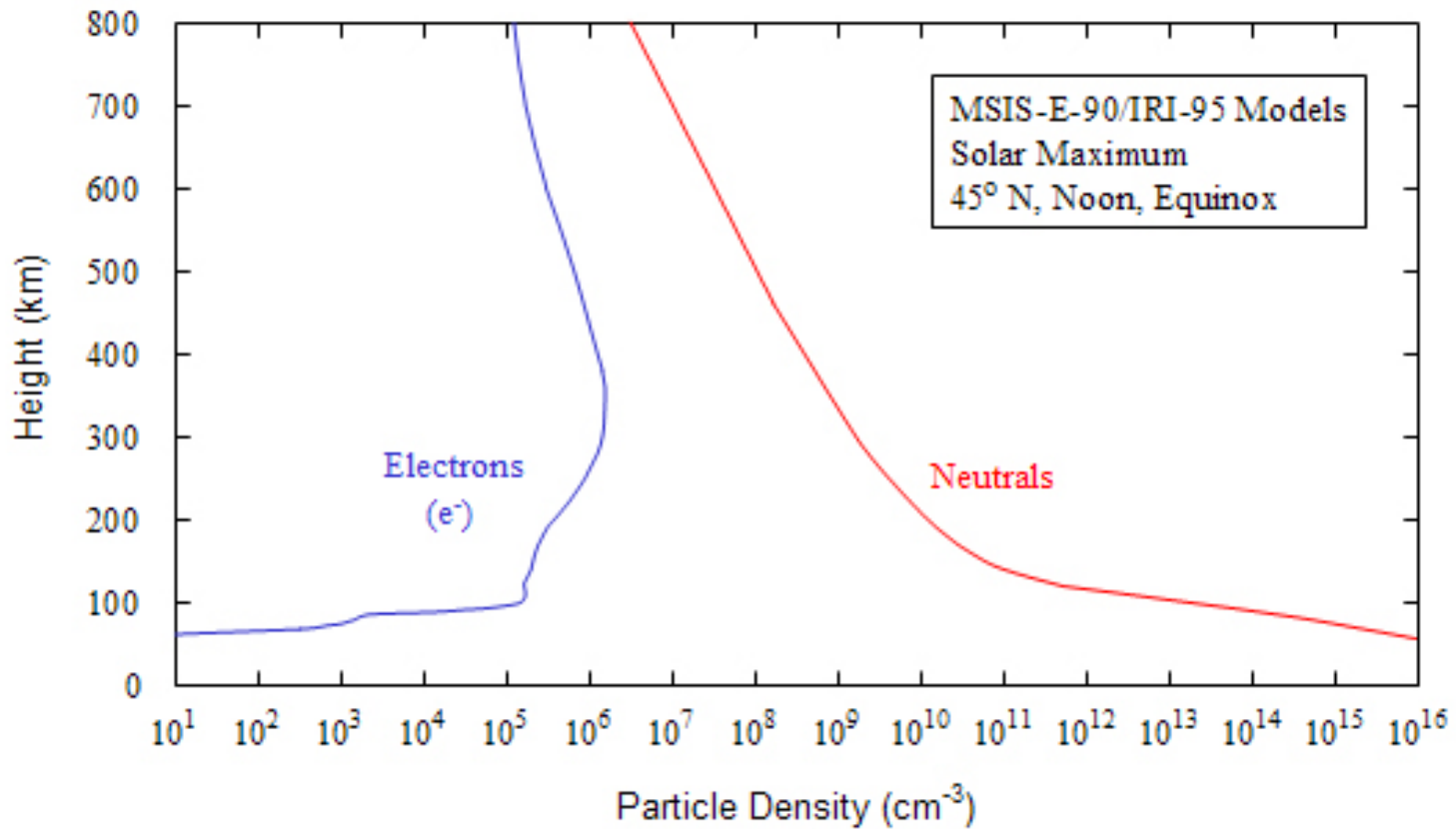
2^d order momentum \rightarrow temperatures (scalars)

3^d order momentum \rightarrow heat flux (vectors)

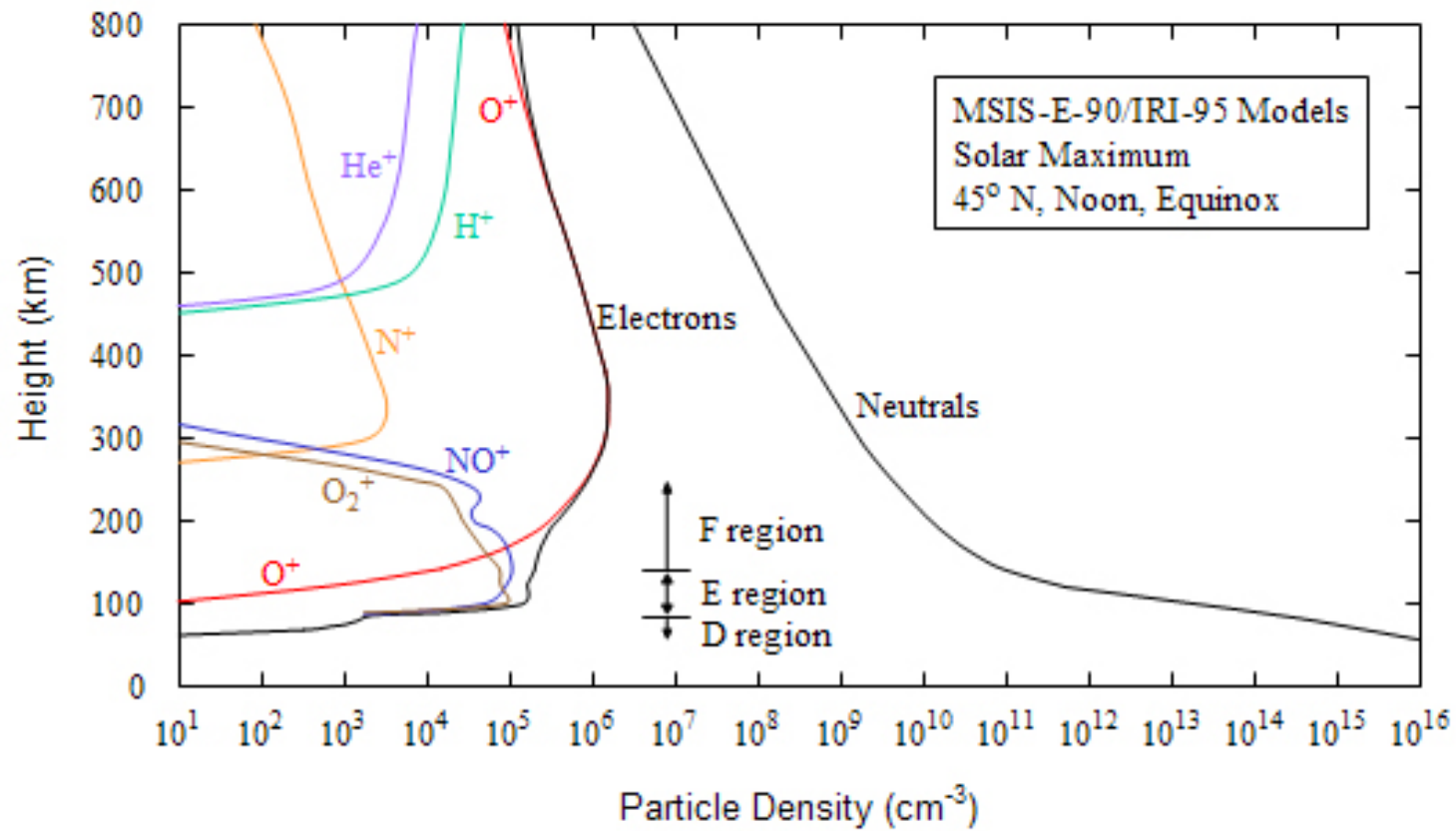




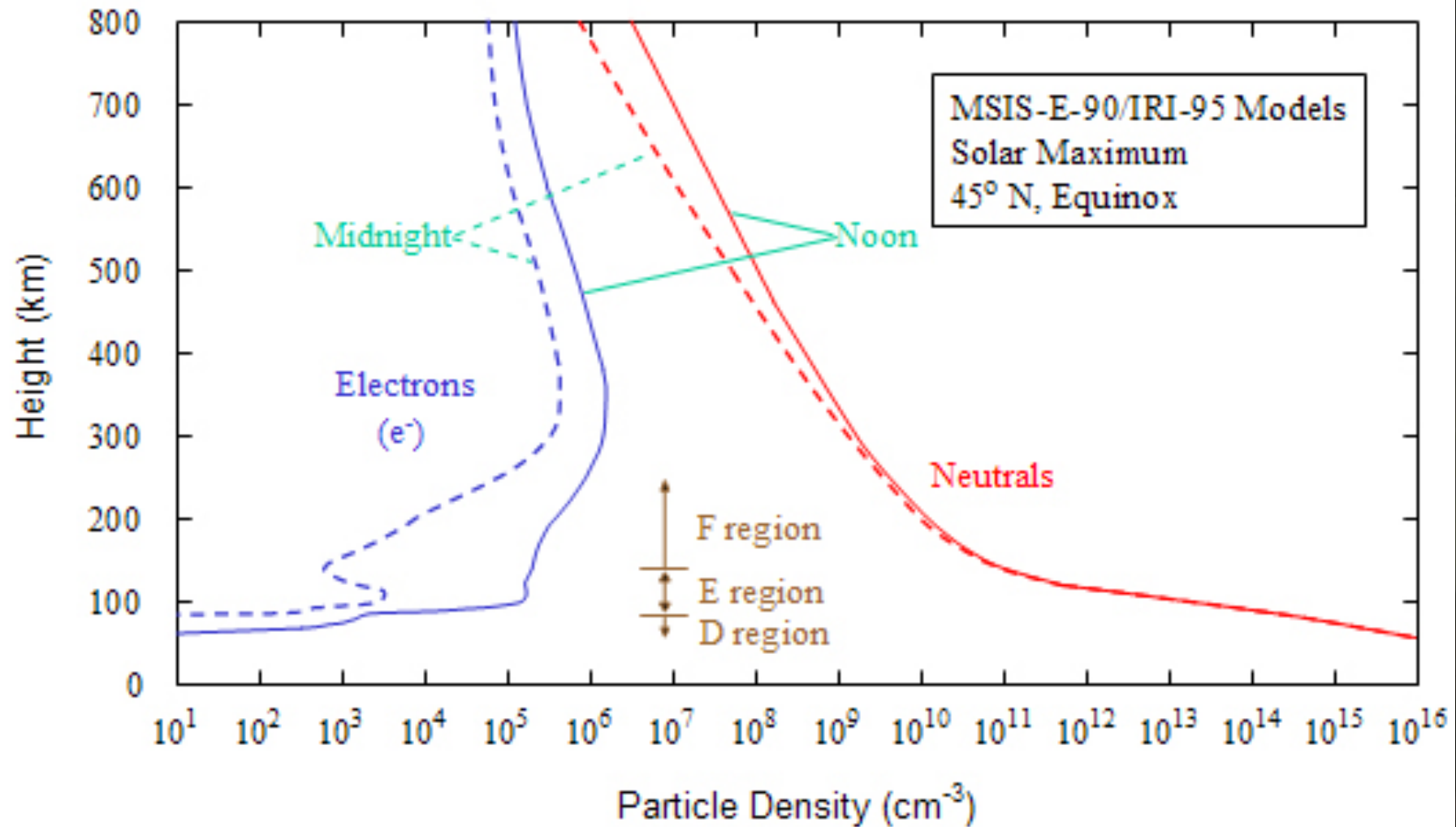
The Weakly Ionized Plasma of the Ionosphere

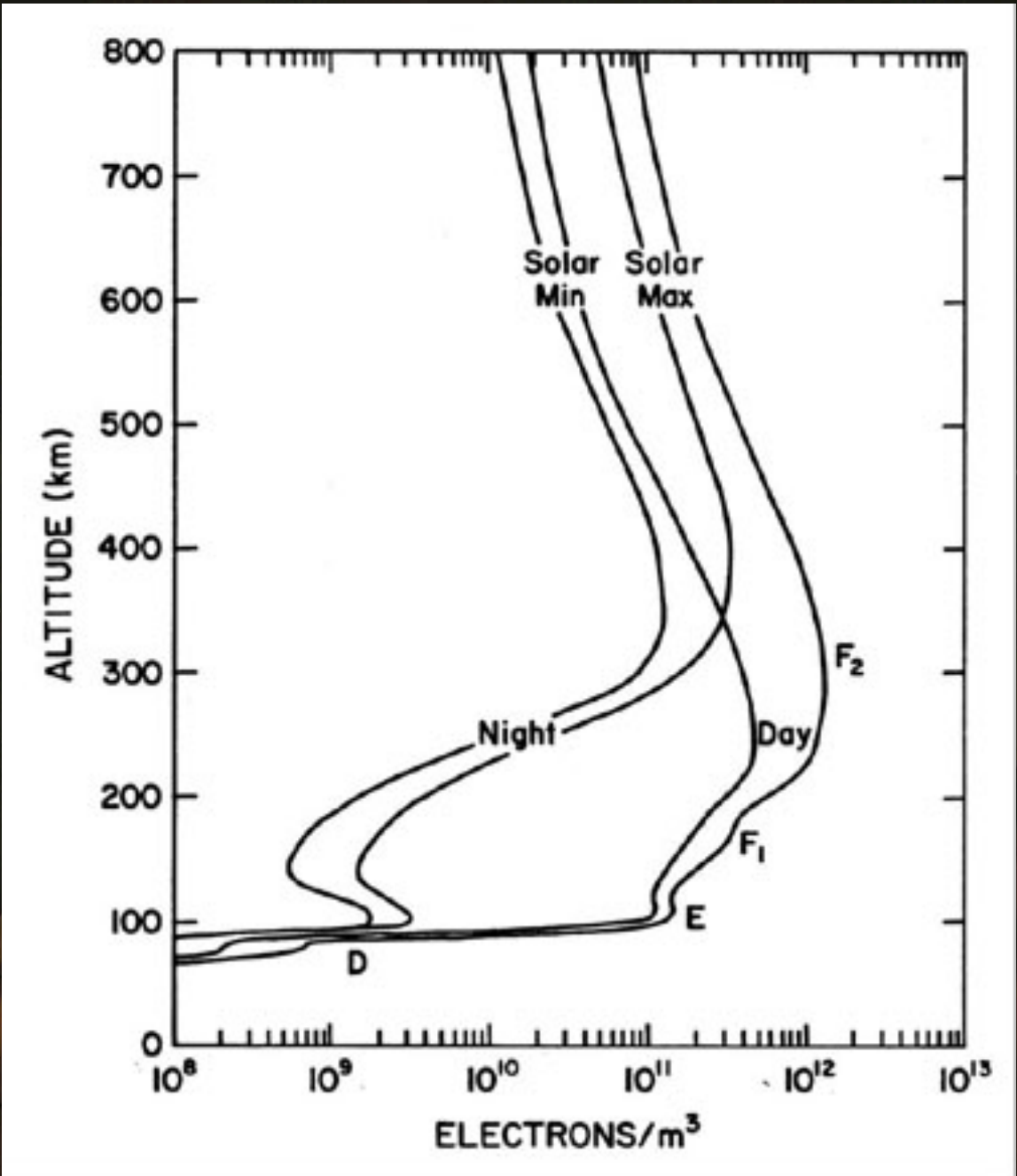


Principal Constituents of the Ionosphere

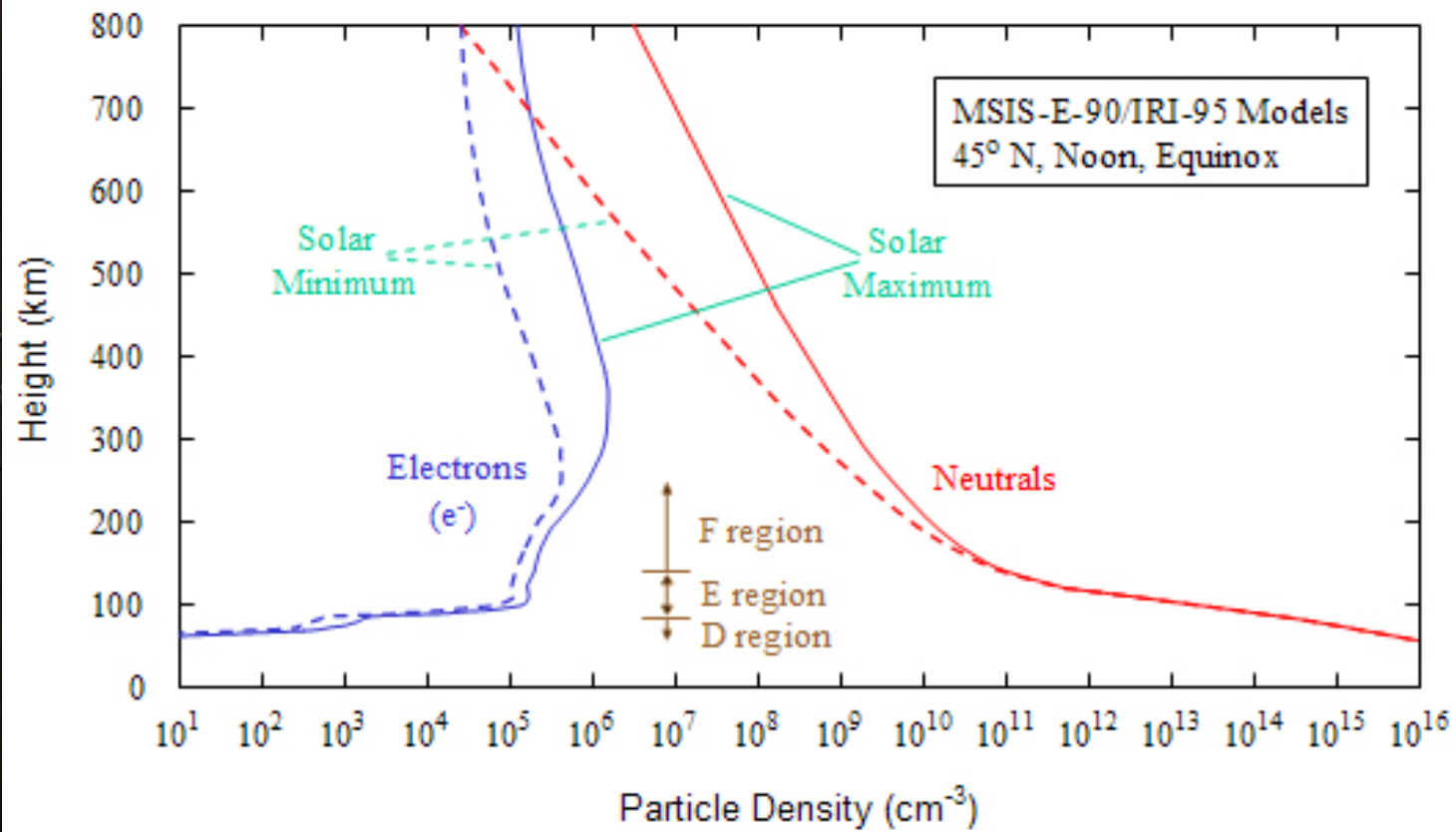


Day-Night Variation of Ionospheric Density

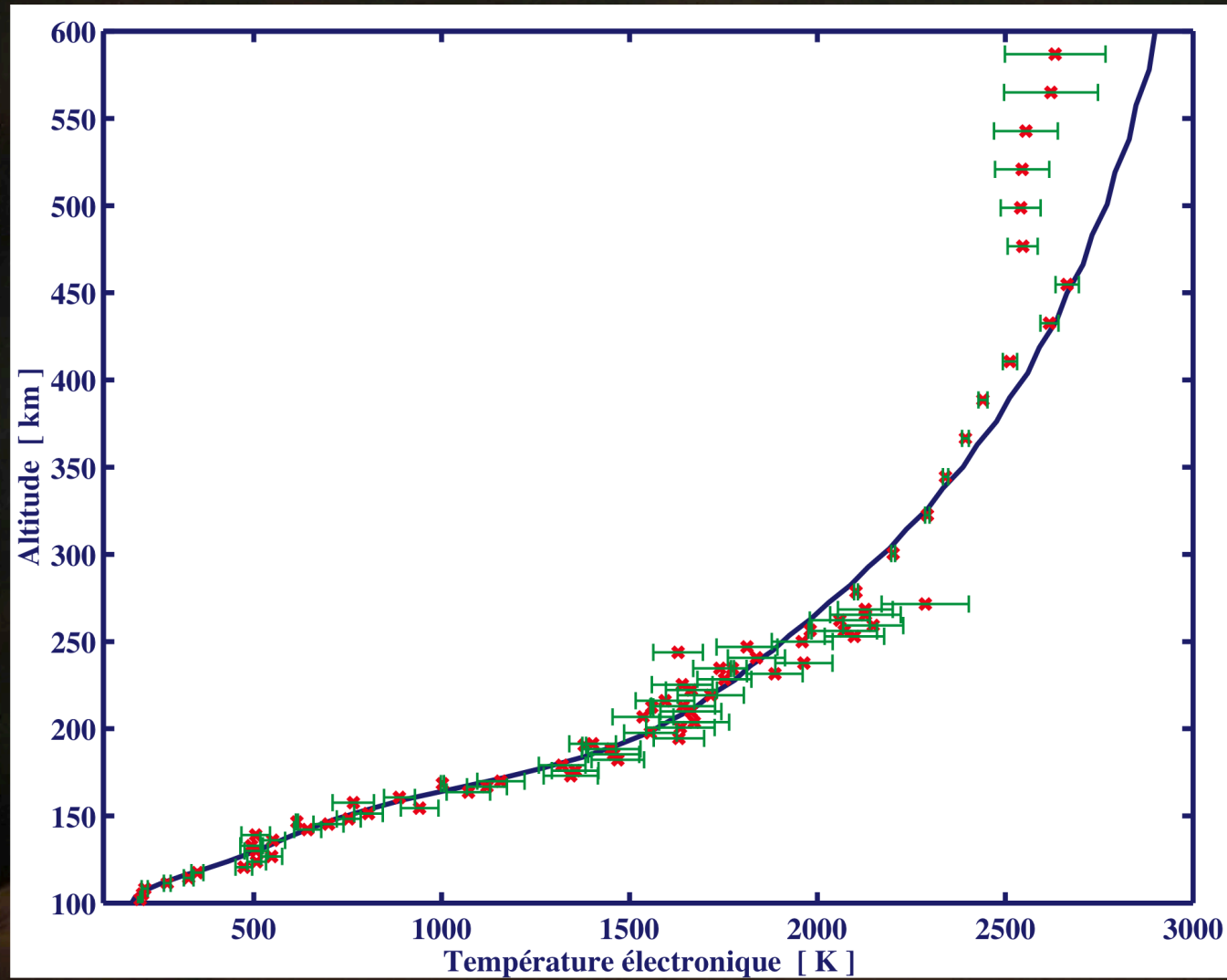




Solar-Cycle Variation of Ionospheric Density

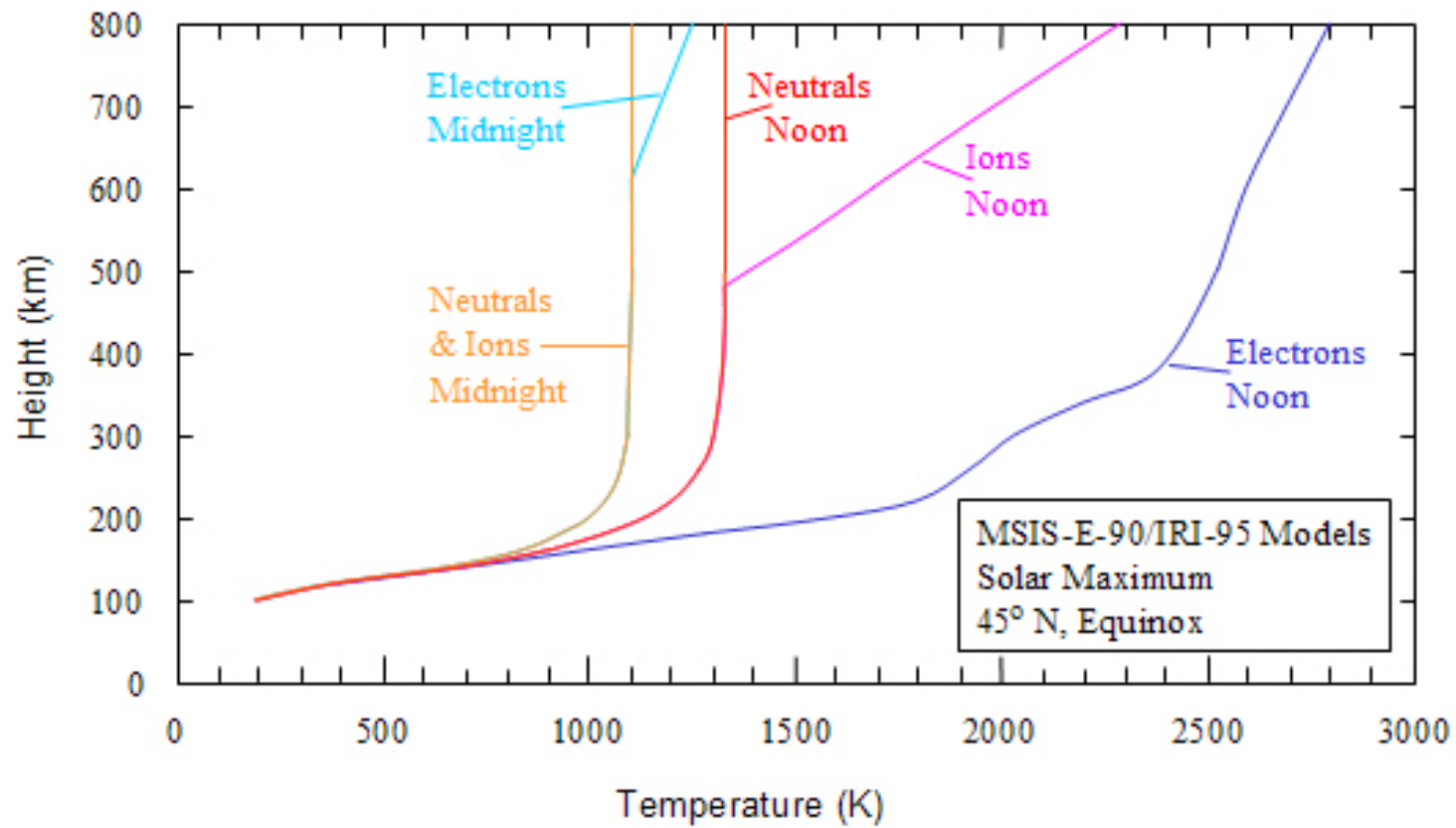


Temperatures



T electrons:
1500 K to
3000 K

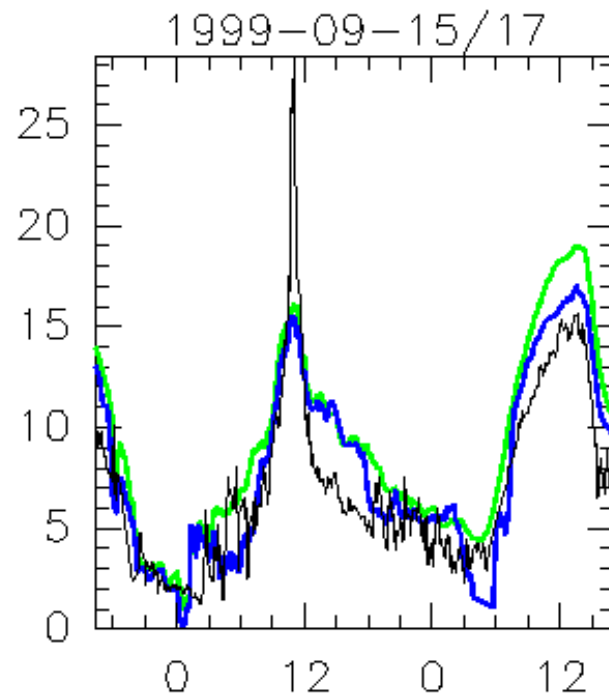
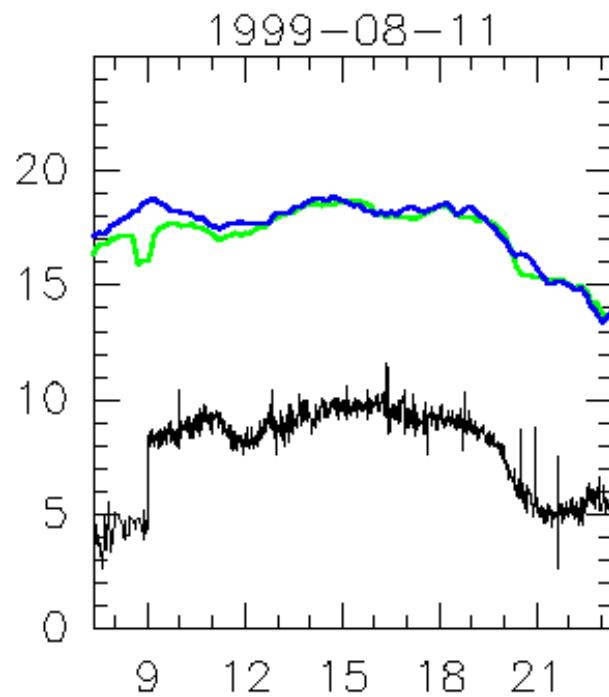
Day-Night Variation of Ionospheric Temperature



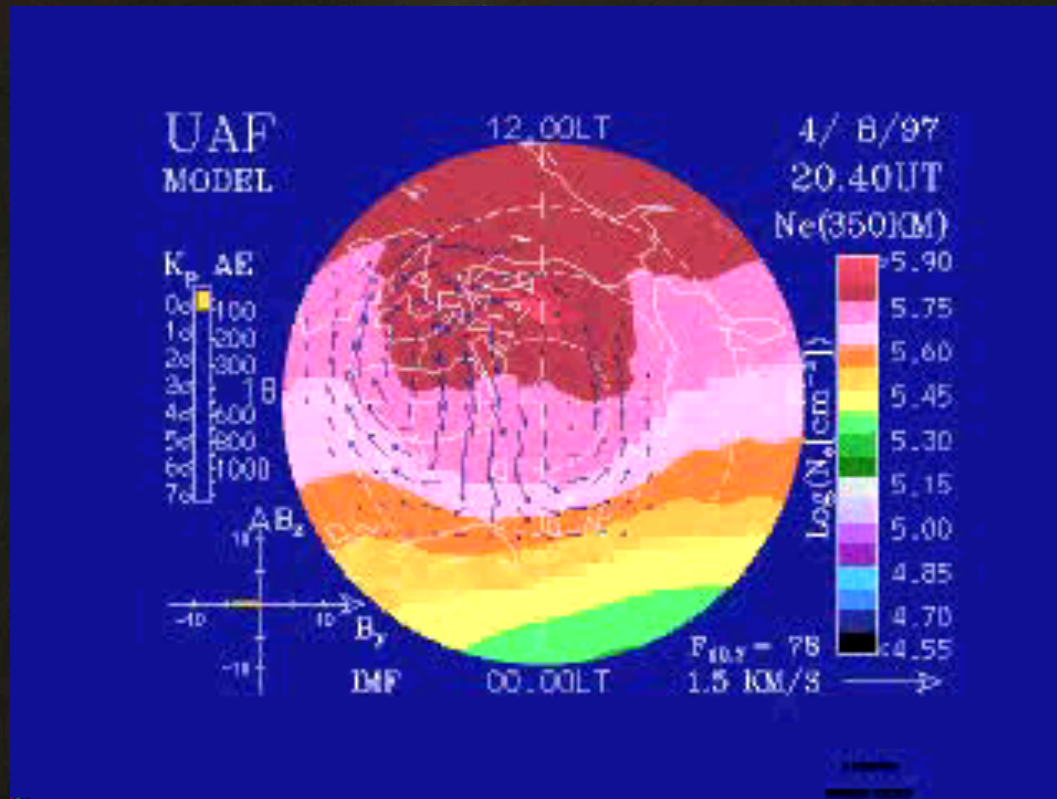
Note that local precipitation create mainly (but not totally) local perturbations : the blobs or patches resulting in scintillations (see class by S. Califano). These are of primary importance for space weather

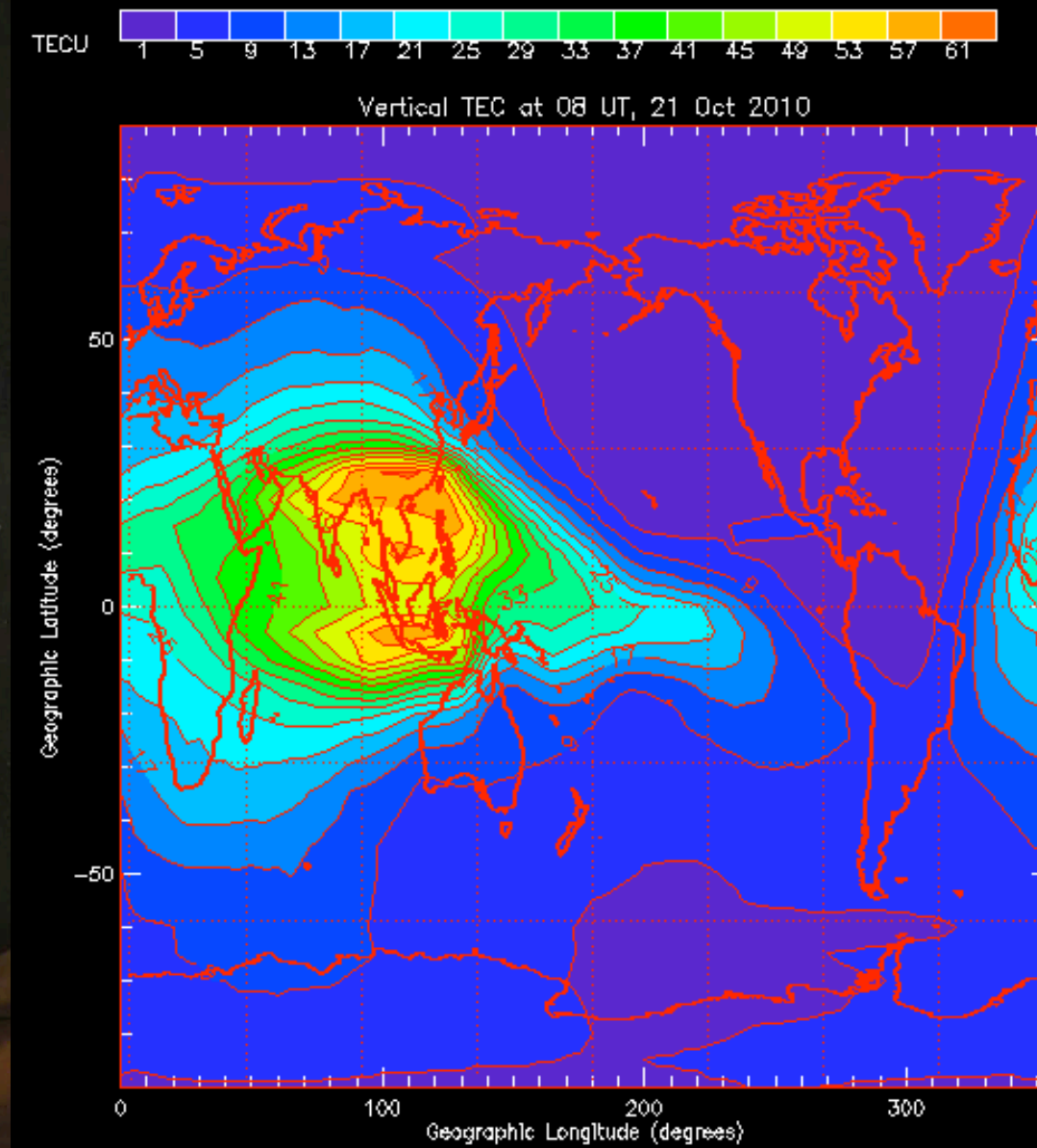
Integrating the electron density
over the altitudes gives the Total
Electron Content of primary
importance for space weather

TEC [10^{16} m^{-2}]



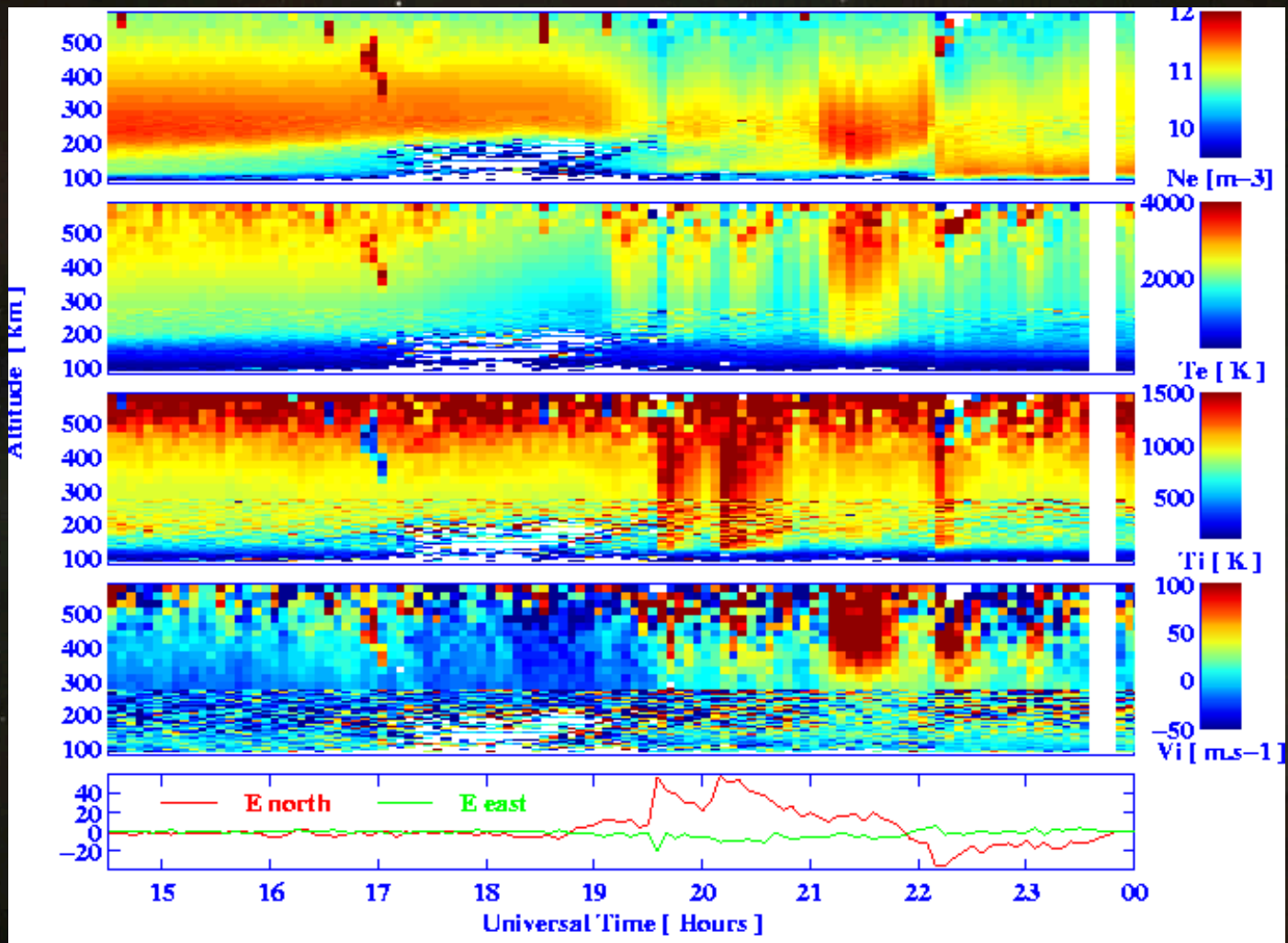
Local Time

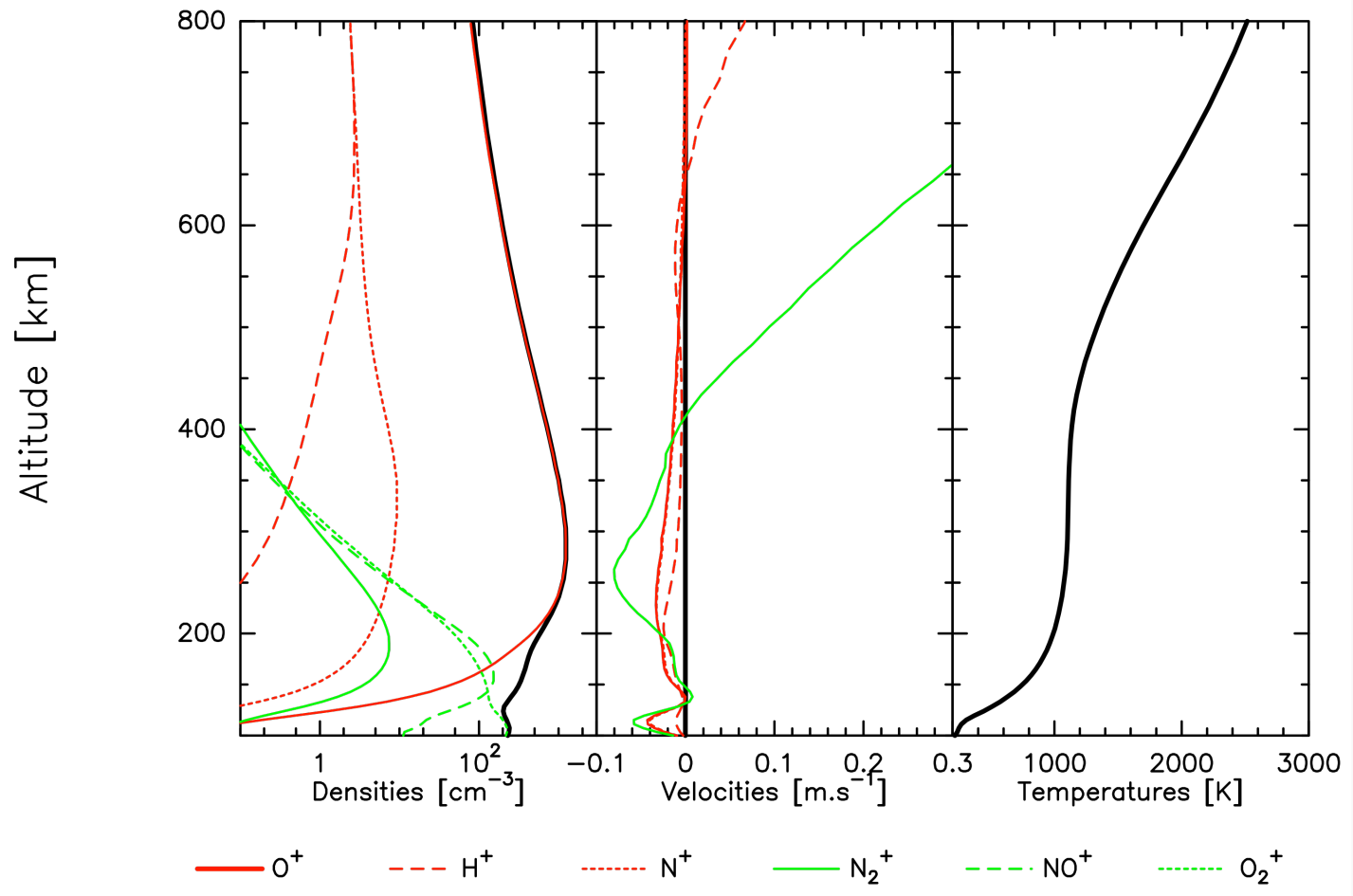




This is the origin of the densities,
temperatures and winds observed in
the ionospheres

Altitude [km]	75	100	150	200	400	800	1200	3000
« couche »	D	E	F1	F2		F sup		
N_n [m^{-3}]	10^{21}	10^{18}	$5 \cdot 10^{16}$	$8 \cdot 10^{15}$	10^{14}	10^{12}	$2 \cdot 10^{11}$	10^{10}
N_e / N_n	10^{-12}	$3 \cdot 10^{-9}$	$4 \cdot 10^{-6}$	10^{-4}	$4 \cdot 10^{-3}$	$4 \cdot 10^{-2}$	10^{-1}	1
T_e	200	200	700	1500	2500	3000	3200	3500
T_i	200	200	600	800	1000	2500	3000	3400





Sources of variations of the thermosphere :

- X rays and EUV fluxes
- Particle precipitation
- E fields

Physical processes involved :

- photo-absorption
- particle collisions
- Joule heating
- frictional heating

Result (amongst other phenomena) in rapid variations and creations of small scale disturbances

Result (amongst other phenomena) in a dilatation of the thermosphere (density may increase by a factor of 10 at the altitude of the International Space Station)

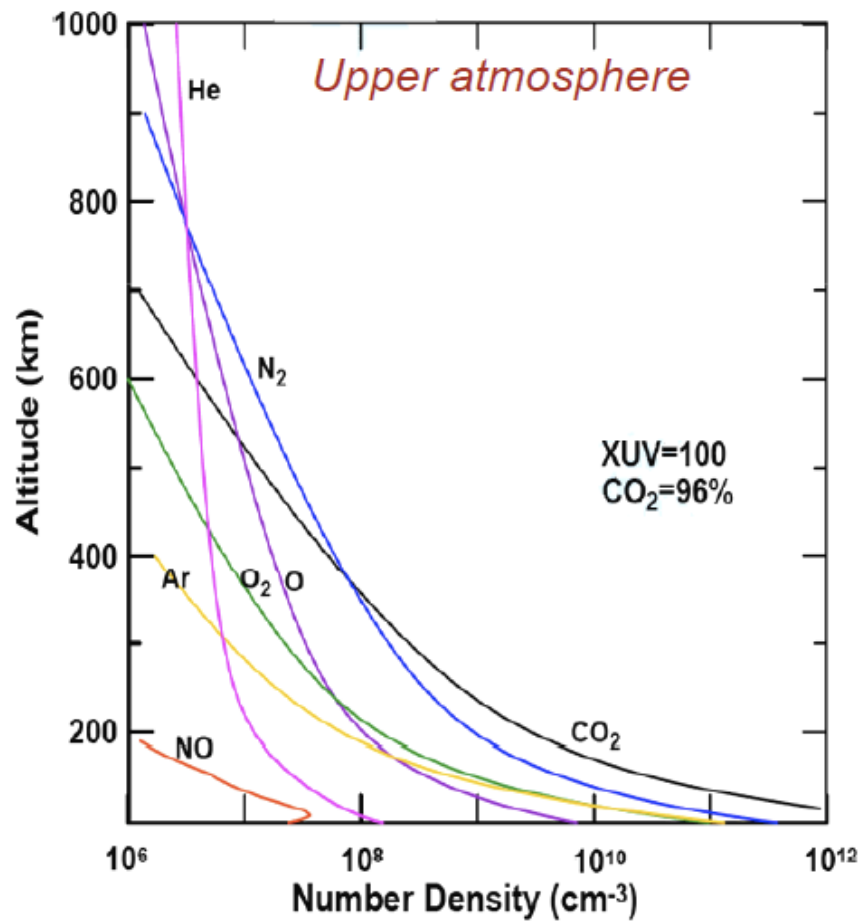
Dynamics and electric
circuit with the upper
layers : see class by V.
Pierrard and A. Aylward

What about the other planets?

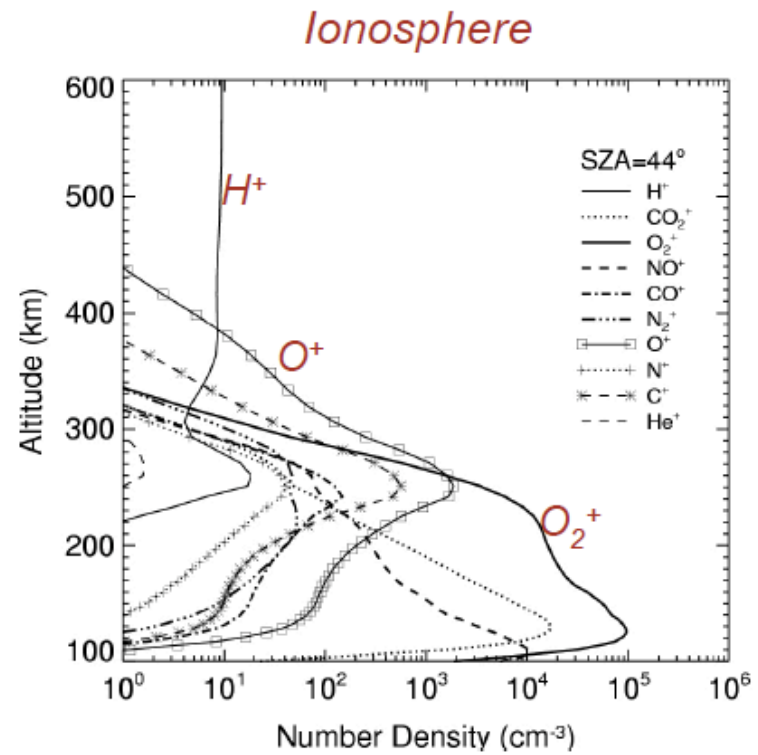
An example of a planet
without a magnetic field :
Mars...

- Ground pressure 5.3 - 7 mb
- Ground scale height: 10,8 km
- Composition (6.1 mb)

CO ₂	95,32%
N ₂	2,7%
Ar	1,6%
O ₂	0,13%
CO	0,07%
H ₂ O	0 – 0.1%



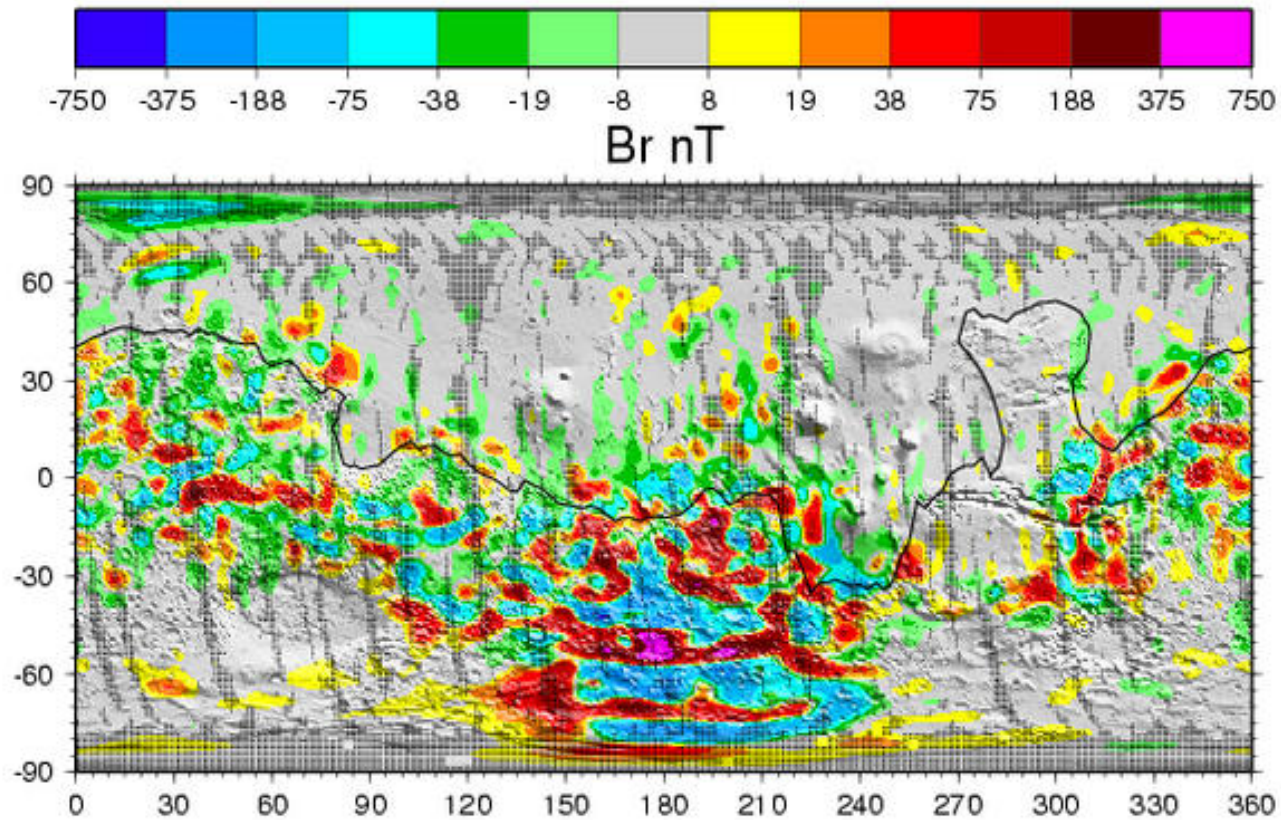
(Shinagawa and Cravens, 1989)

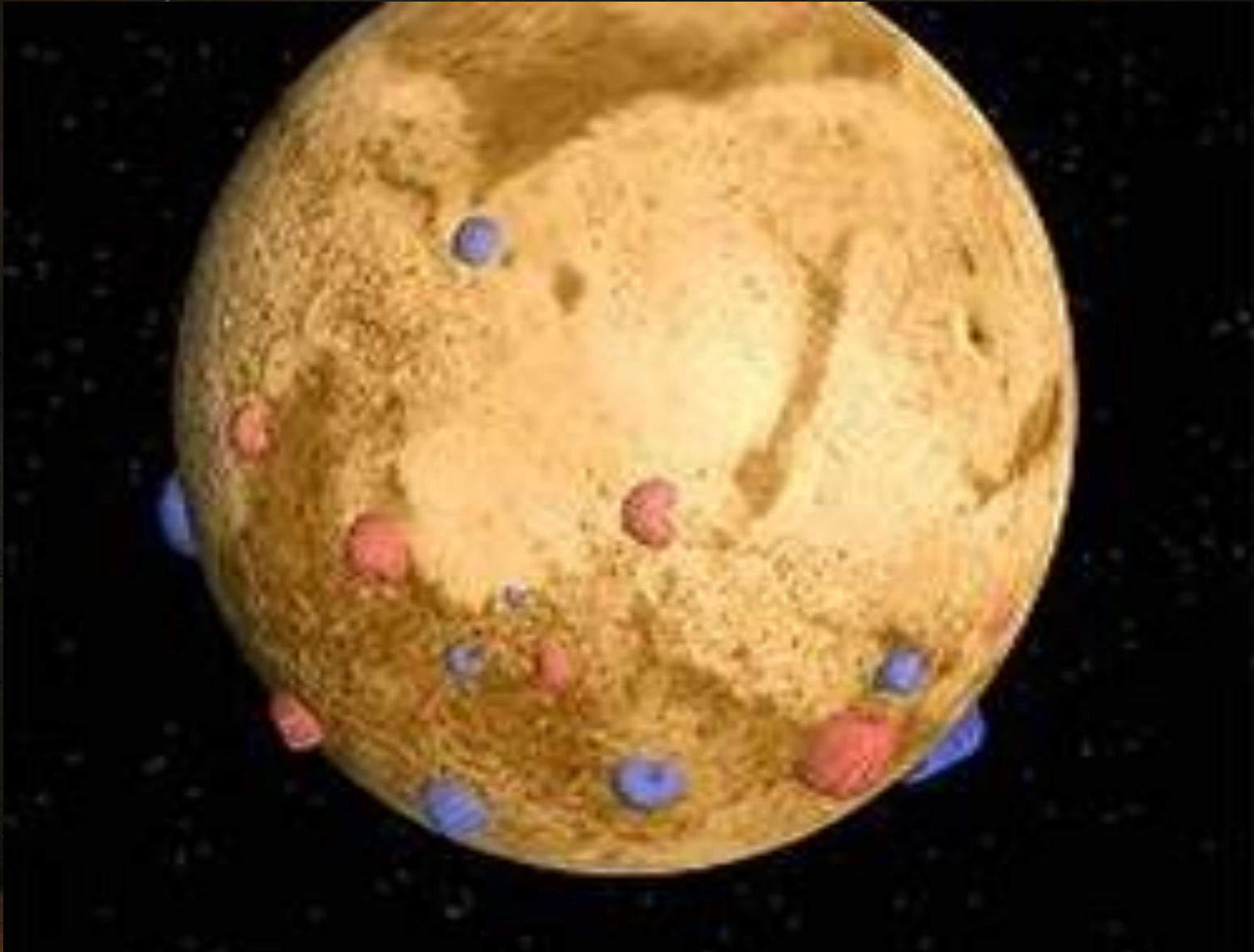


(Terada et al, 2009)

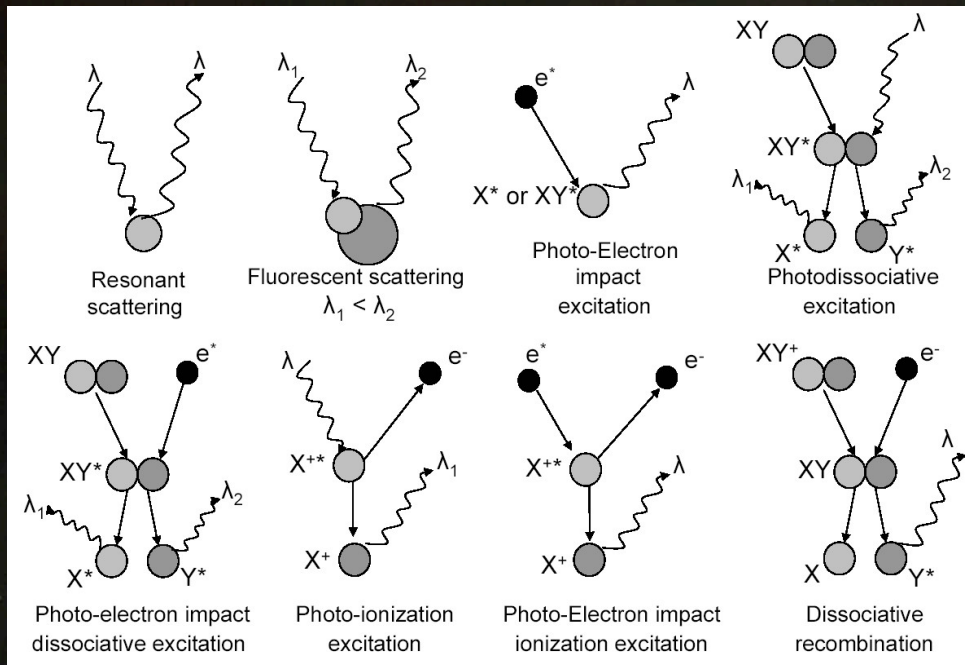
Le champ magnétique recalculé à 200 km

(les zones sans données au-dessous de 200 km sont grisées)

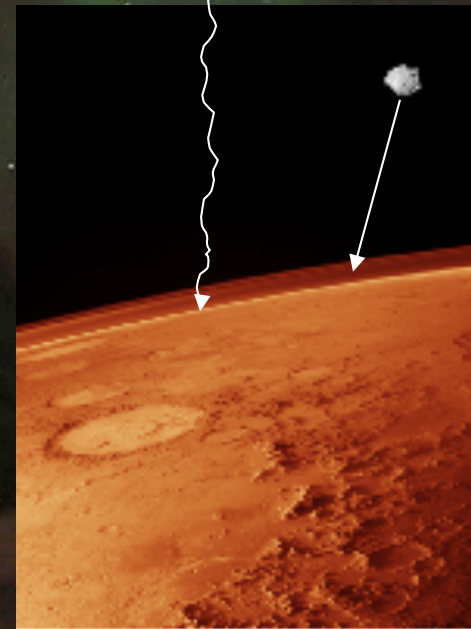




There are several origins for the martian ionosphere and its glow

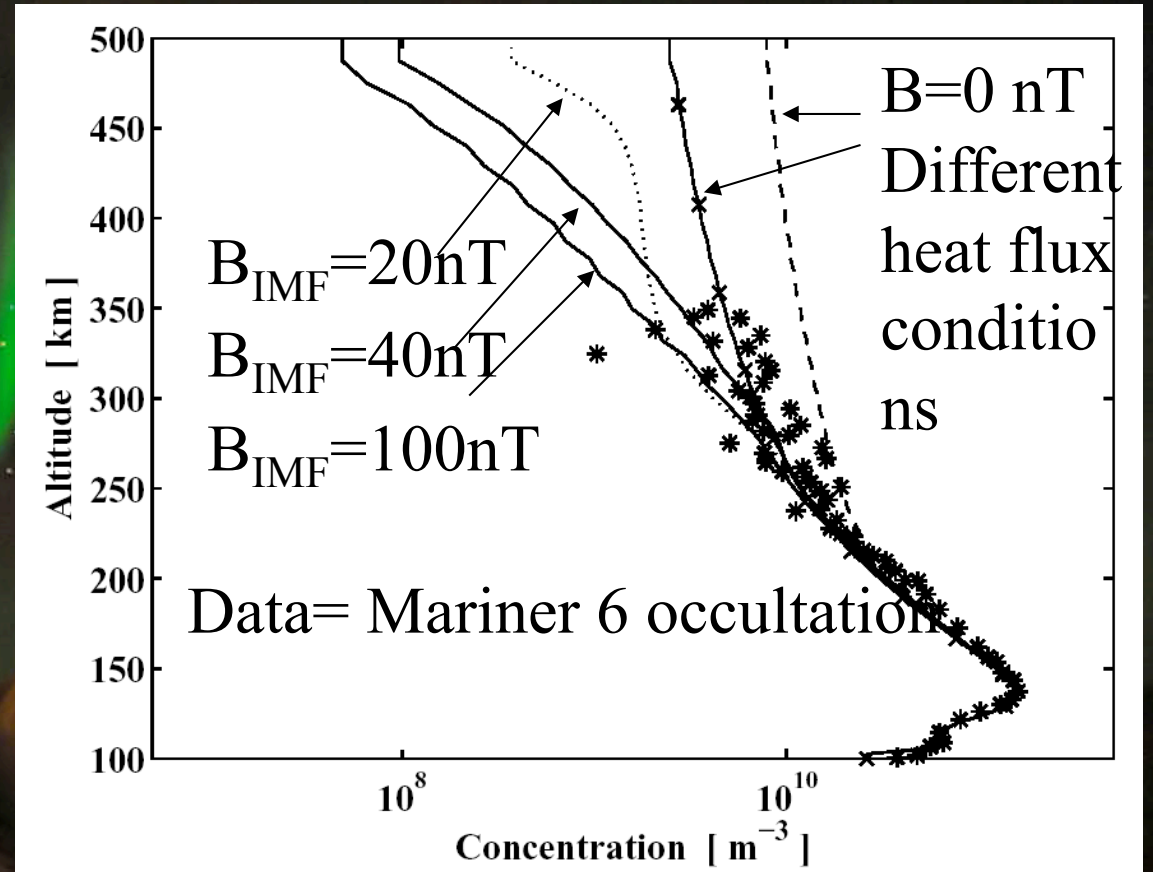
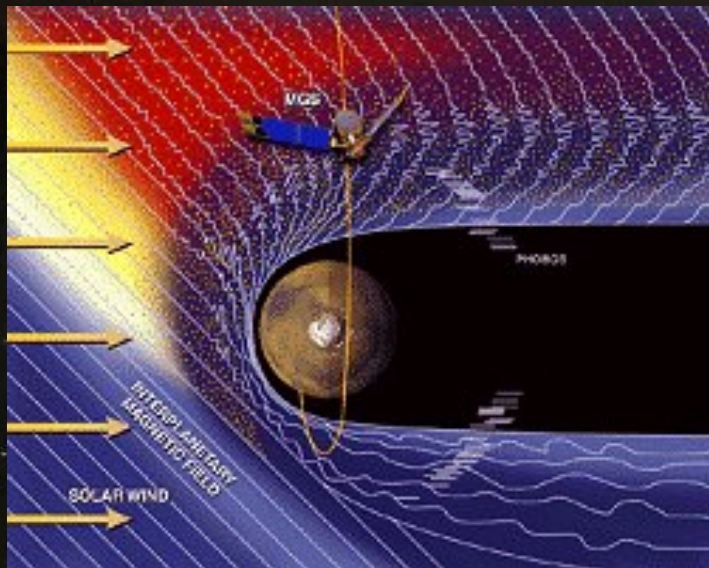


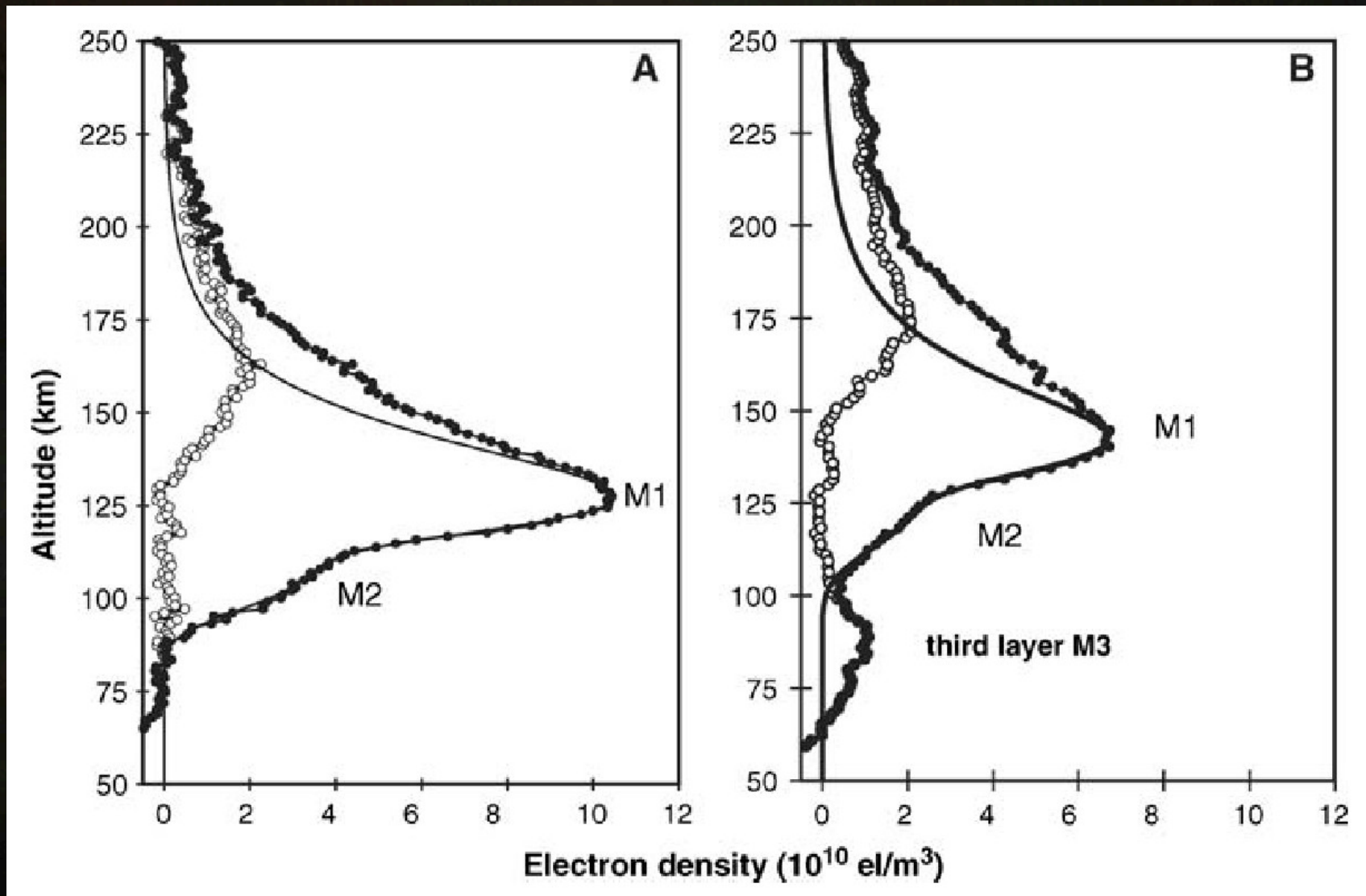
Cosmic rays



Meteoritic ablation

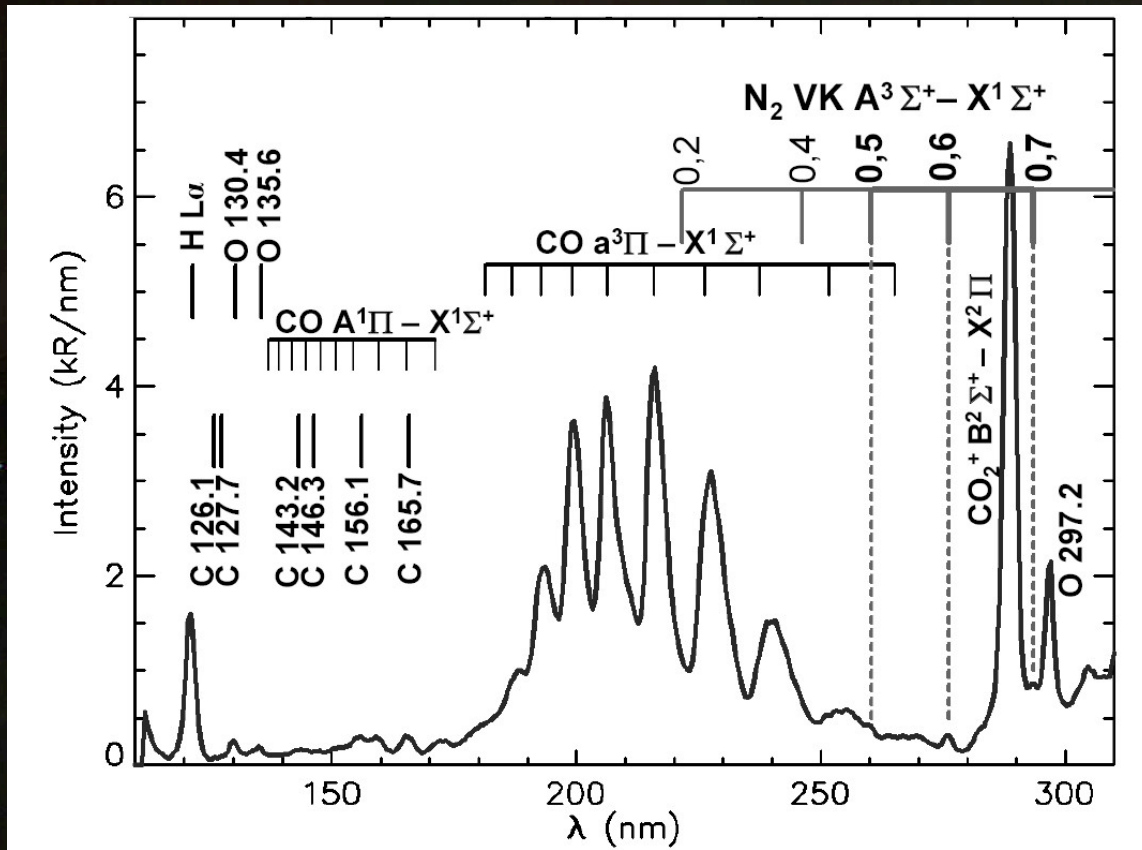
Since there is no global martian magnetic field, the interaction with the IMF is of first importance in the case of Mars.





MARSIS, Pätzold et al., Science, 2005

Leblanc et al., 2005



Orbit 44 (01/23/2004)

SZA = 34.6°, LT = 13h40, Latitude = 15°

Altitude = 111 – 128 km

kR/nm

O 130.4
O 135.6

CO a³Σ⁺ – X¹Σ⁺ (Cameron Band)

CO A¹Σ⁺ – X¹Σ⁺

CO⁺ B²Σ⁺ – X²Σ⁺

CO₂⁺ B²Σ⁺ – X²Σ⁺

O 297.2

C 156.1

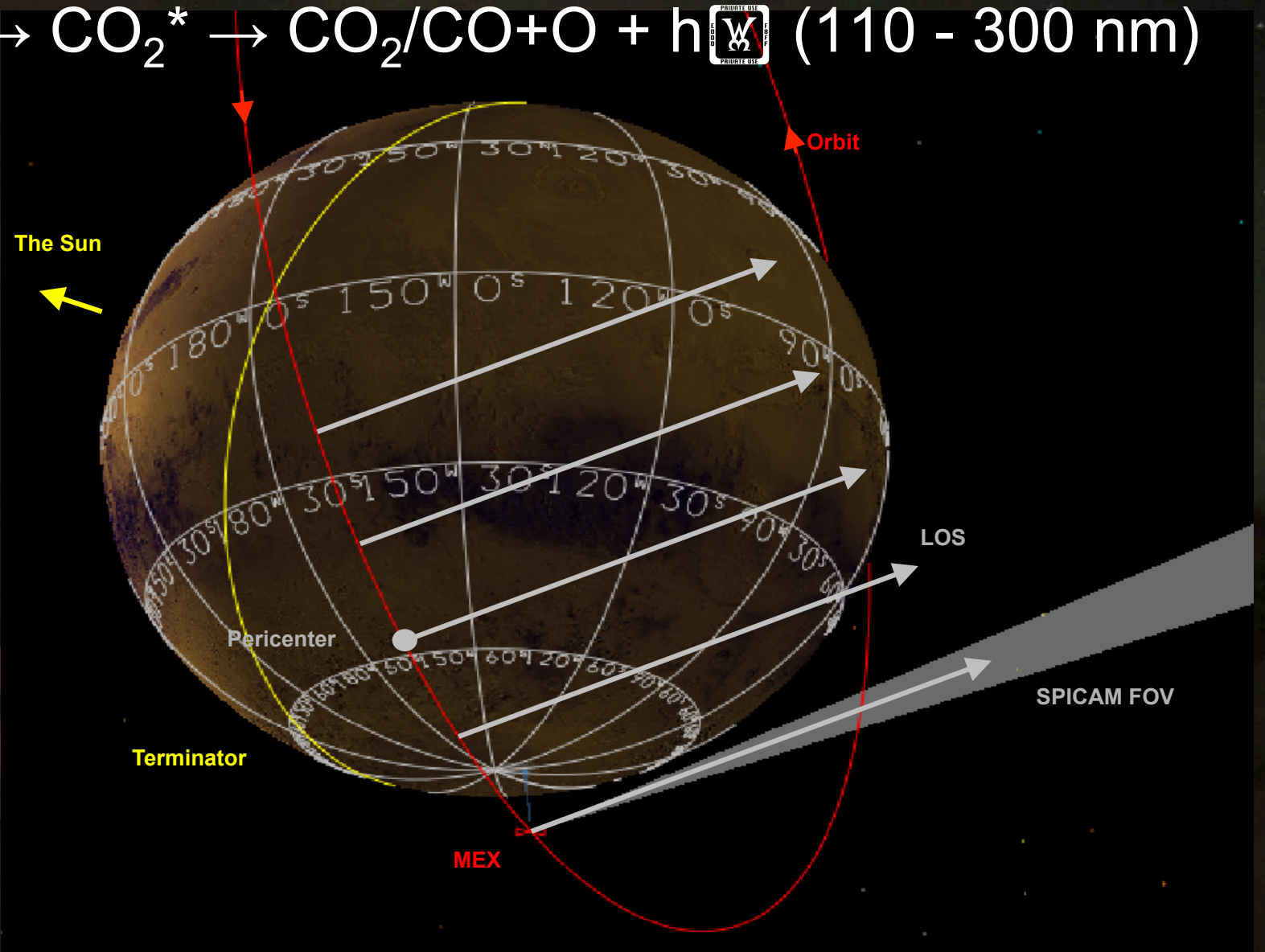
C 165.7

H 121.6
suppressed
by DCNU
construction

Wavelength nm

SPICAM discovery of a Martian Aurora

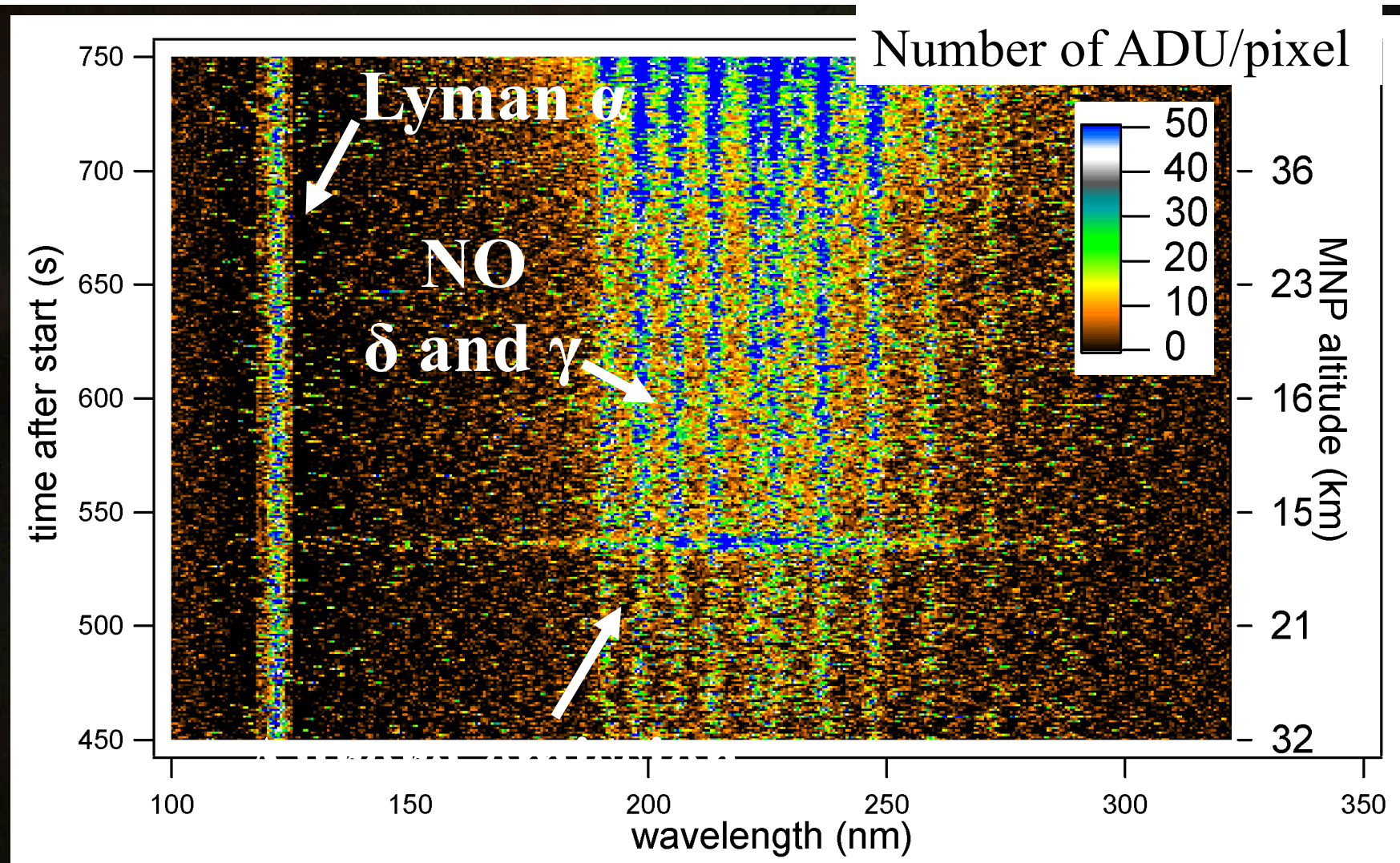
Charge particle precipitation into Mars' atmosphere



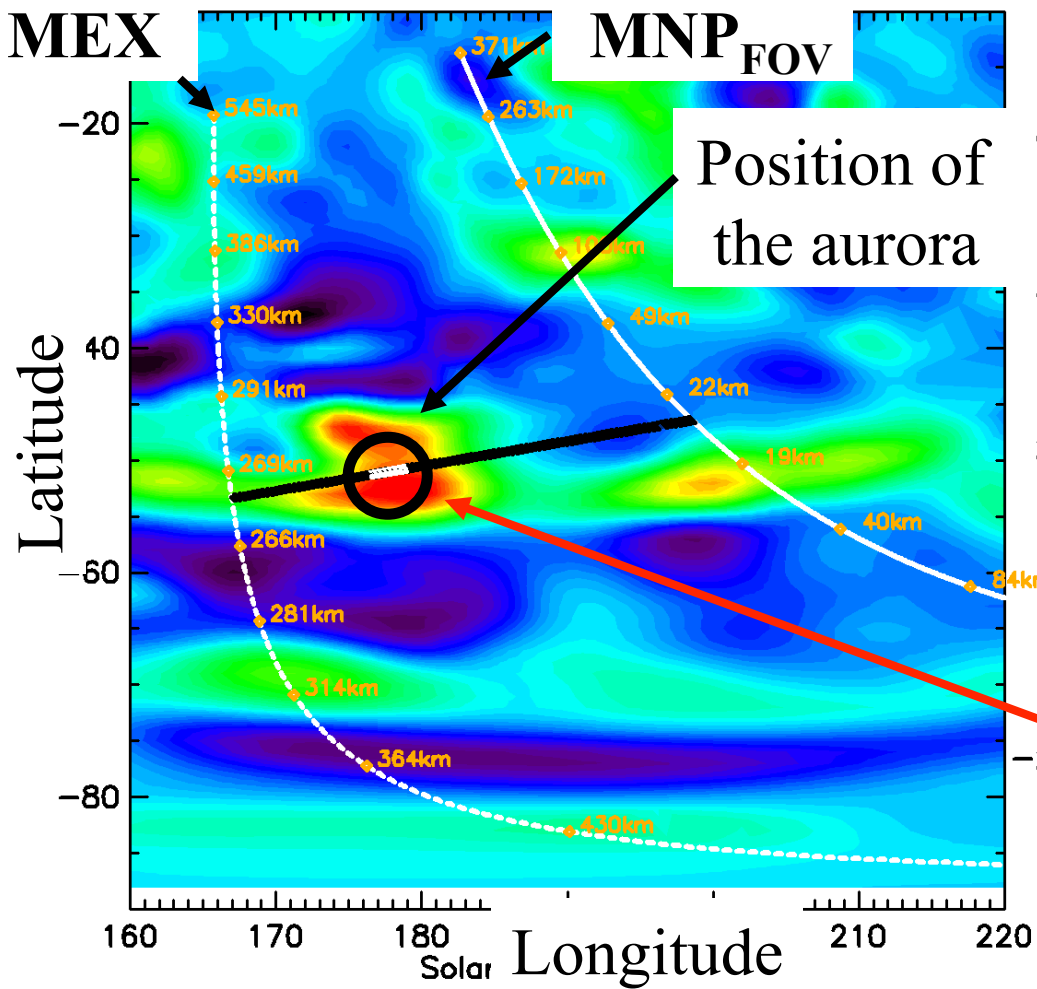
Bertaux et al.
Nature,
435, 790-794,
2005

Orbit 716,
08/11/2004





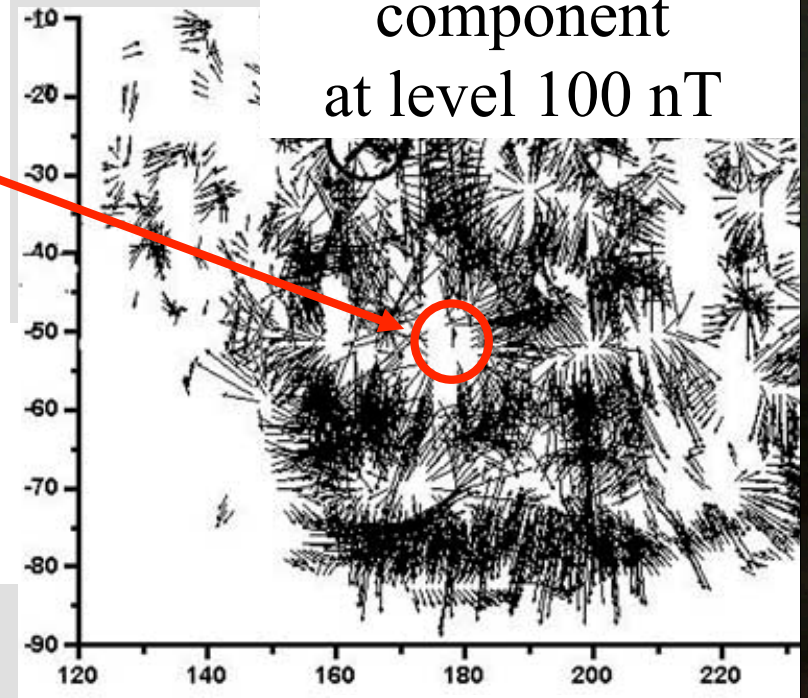
**Aurora emission lasts ~ 7 seconds
= 7 successive integrations**



From Purucker et al. (2000)

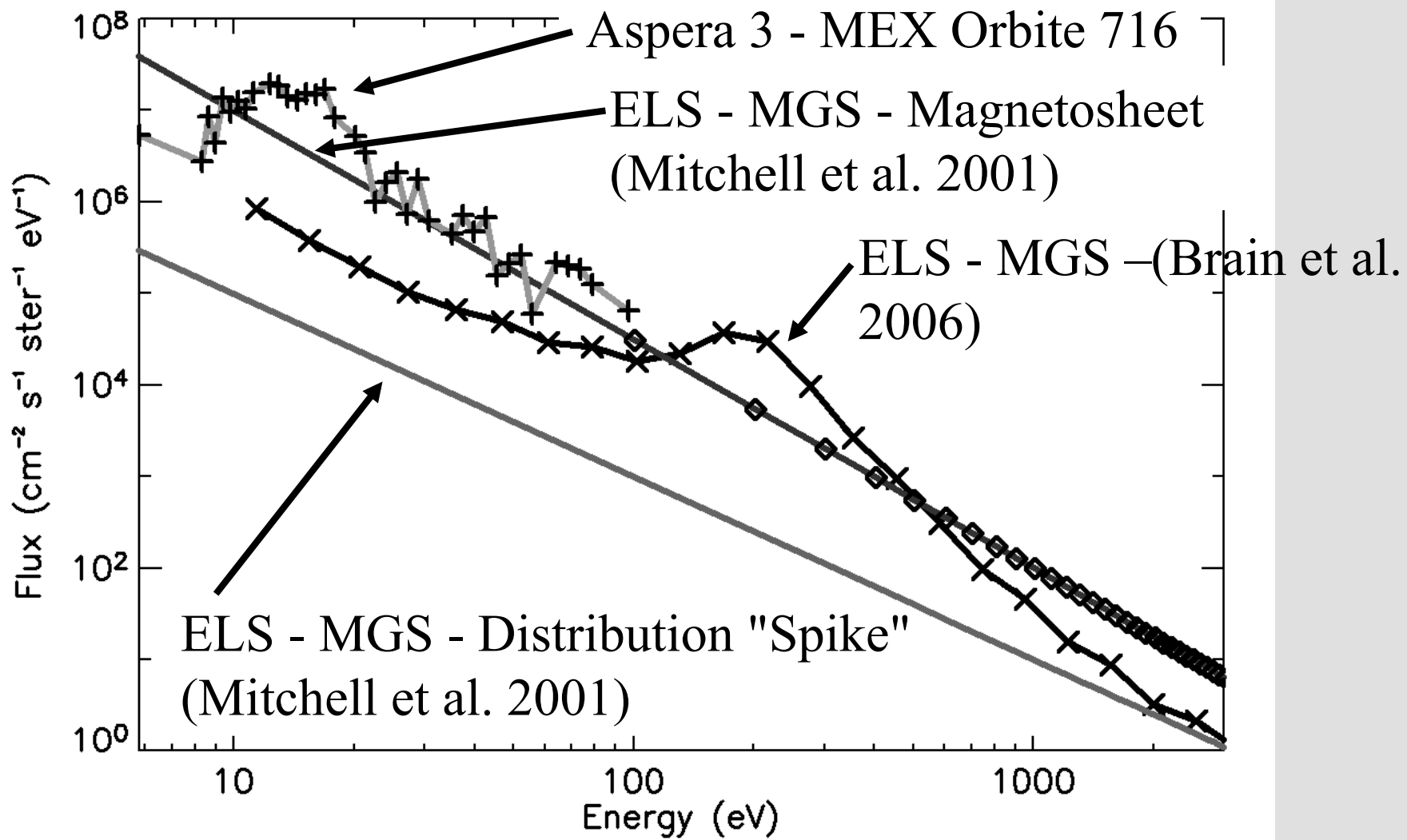
Crustal radial component (nT) at 400 km

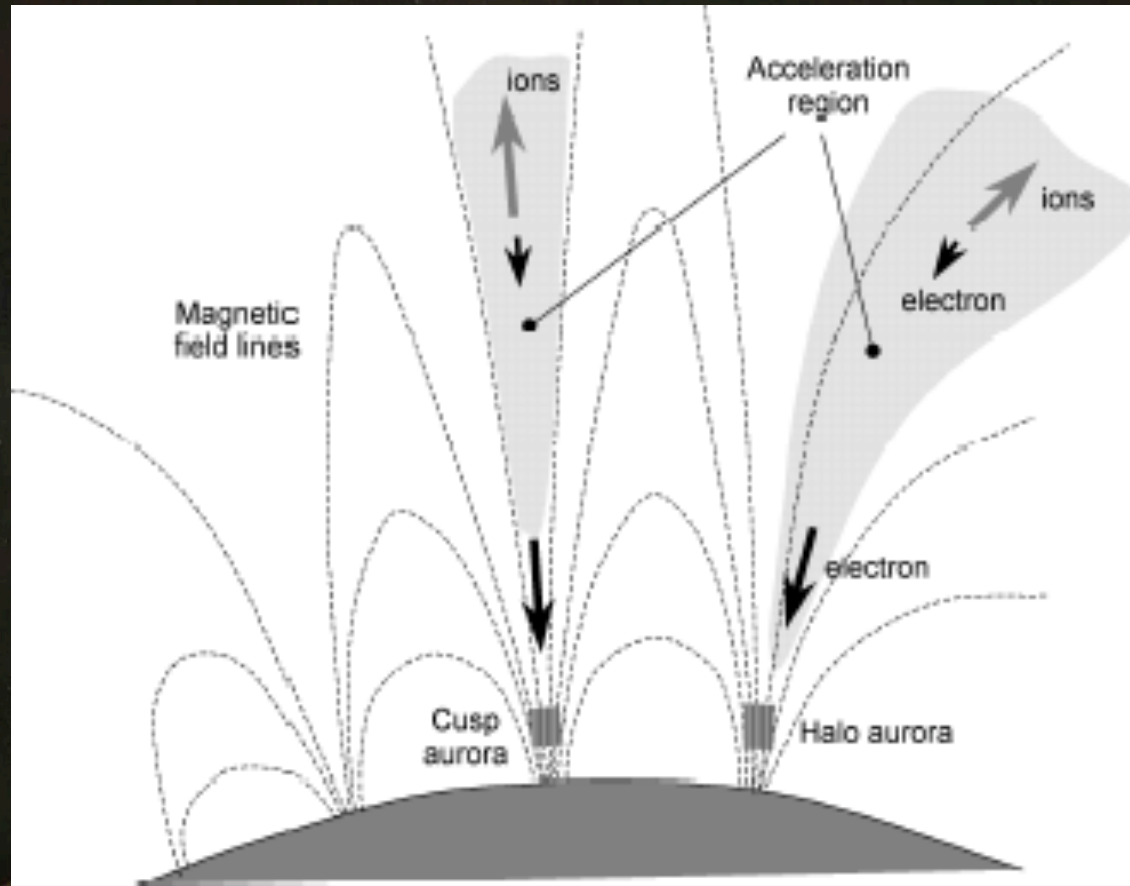
Crustal horizontal component at level 100 nT



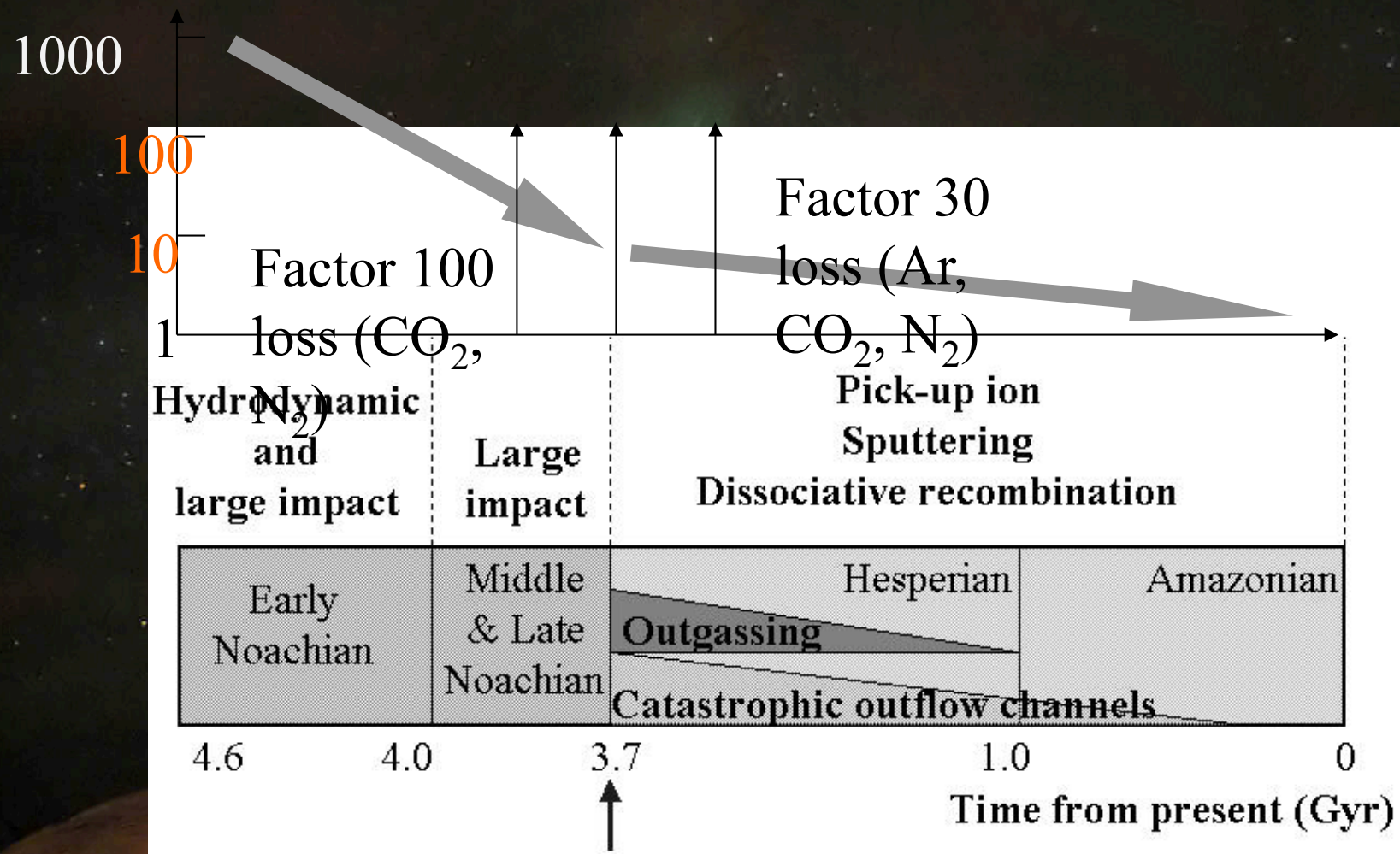
Aurora emission corresponds to an open field line region

From Krinsky et al. (2002)

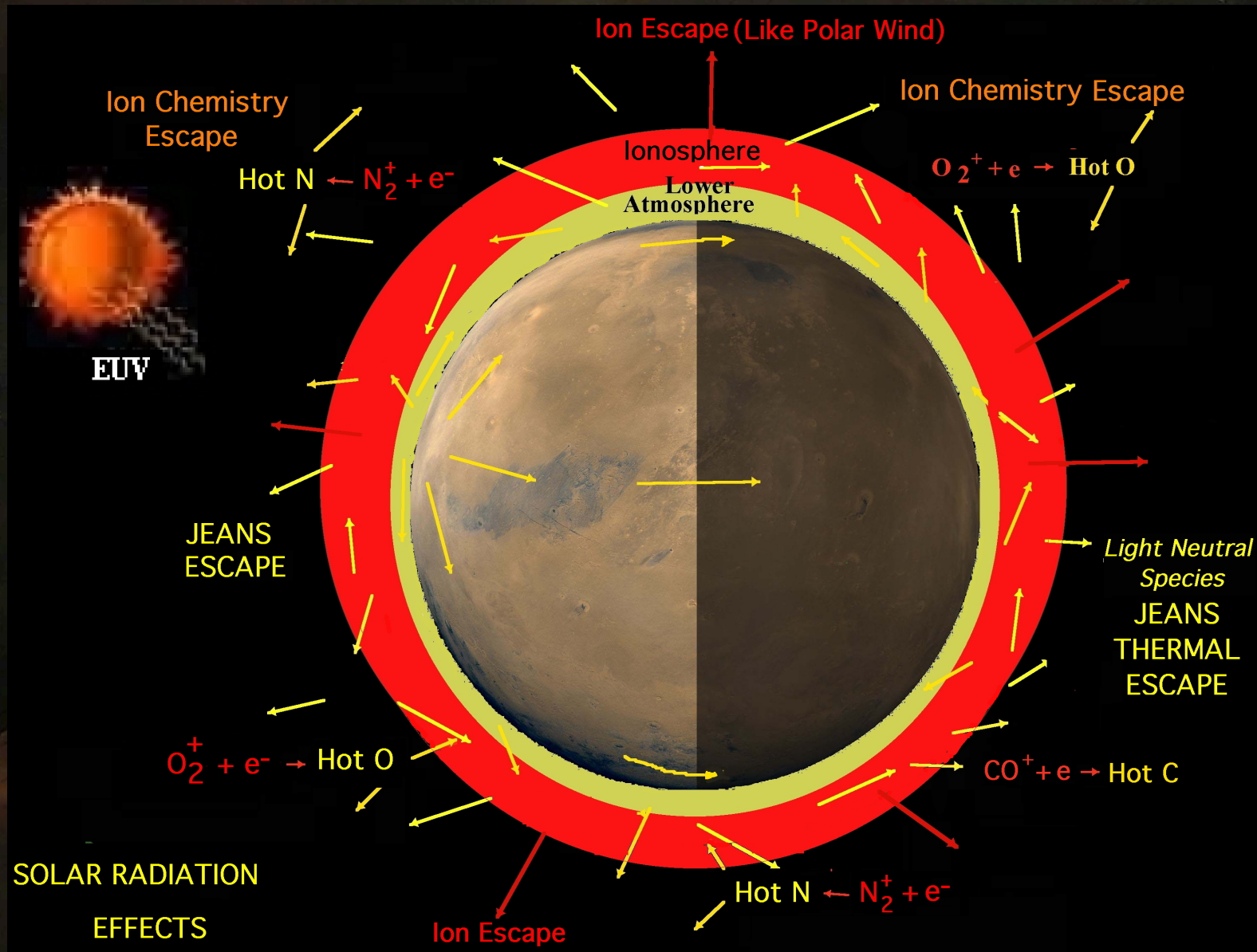




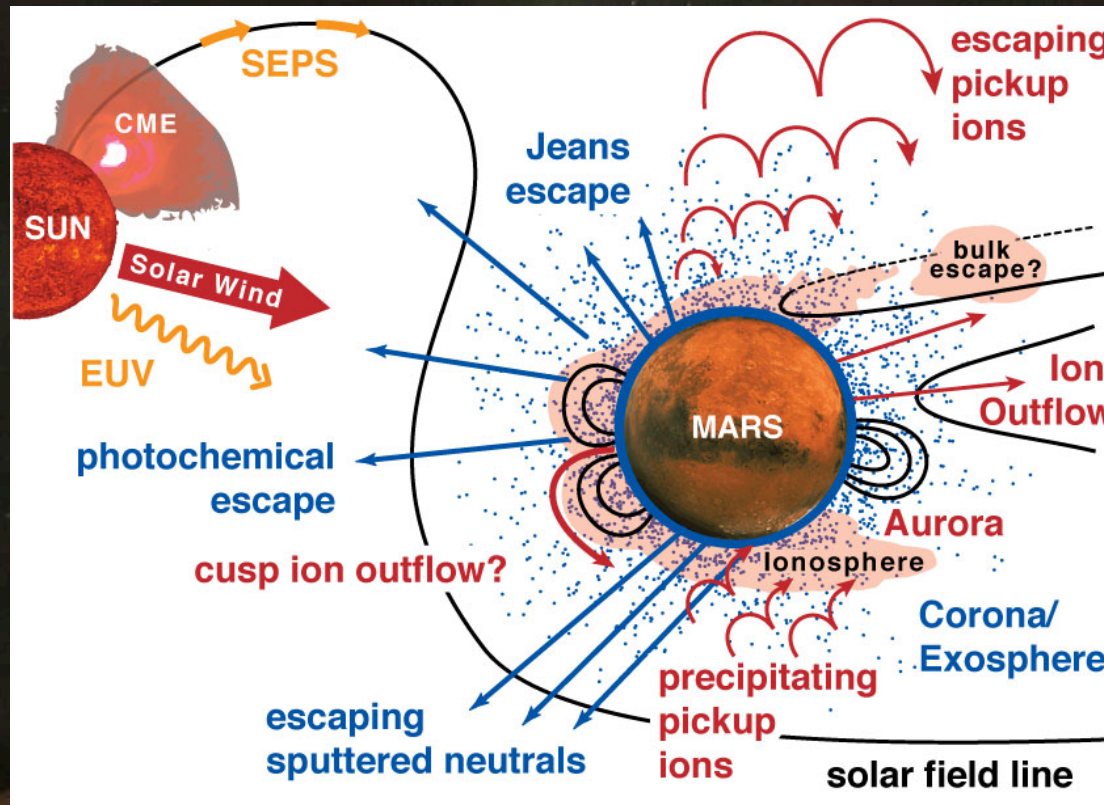
Possible chronological scheme



Solar EUV Driven Escape Without Solar Wind and Magnetic Fields



Solar Wind and Magnetic Fields Expands the Escape Scenarios



- Absence of intrinsic magnetic field exposes parts of atmosphere to solar wind/IMF - driven escape



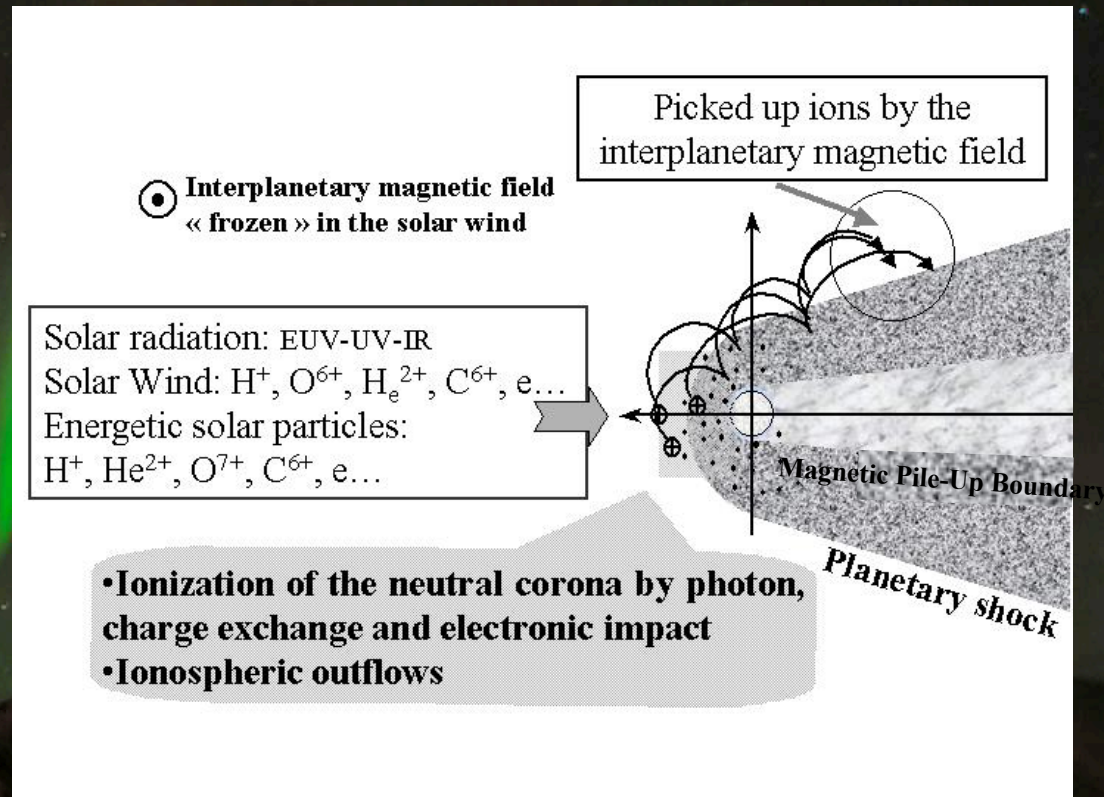
- Permanent magnetic field regions with aurora may have wave-driven loss processes

Escape to space by sputtering

Sputtering is possible only in the absence of a global magnetic field.

Sputtering is strongly non-linear with solar EUV flux :

8

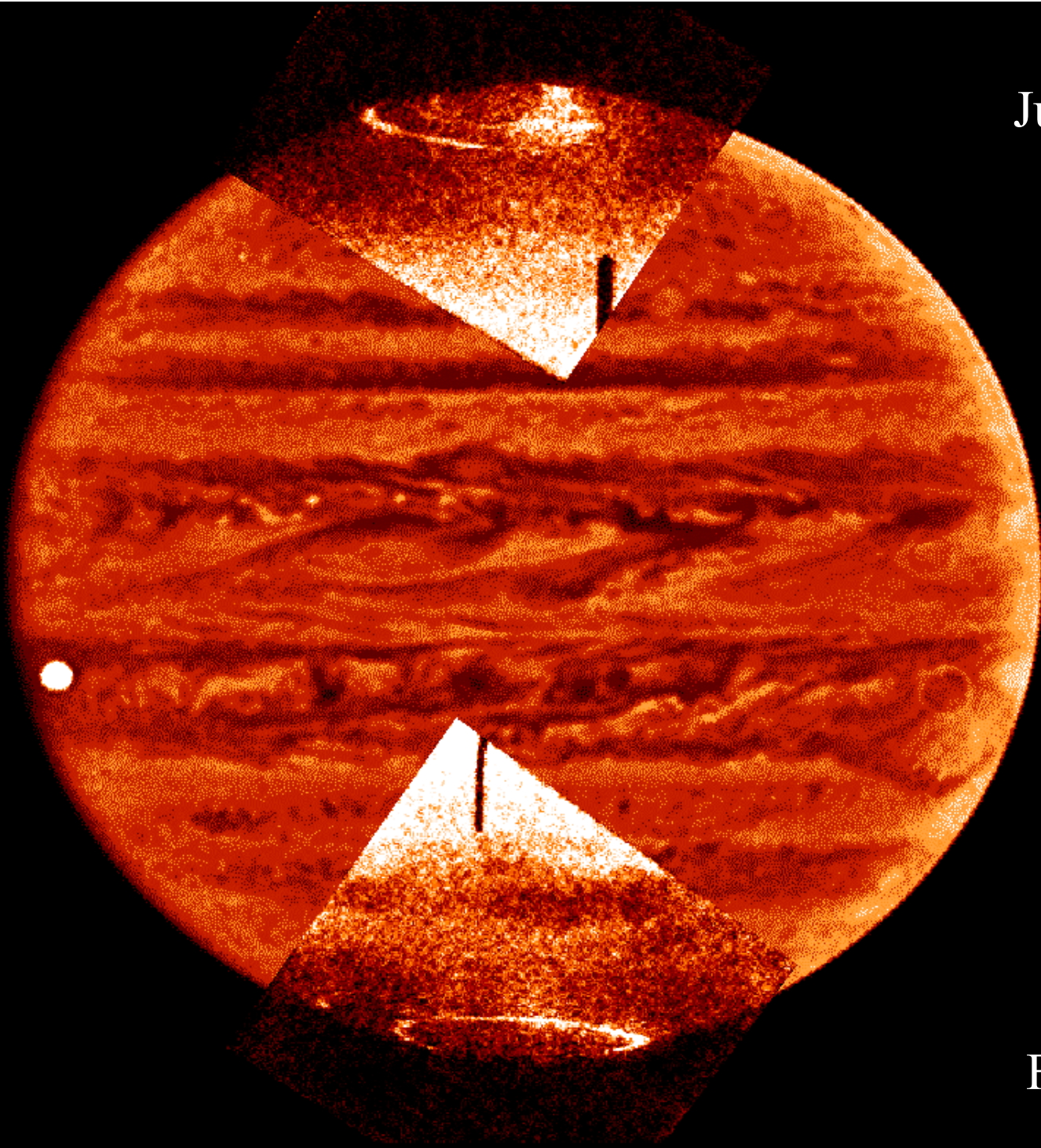


Present	-2.5 Gyr	-3.5 Gyr	reference
$5 \cdot 10^{23}$	$1.4 \cdot 10^{26}$	$1.8 \cdot 10^{27}$	Leblanc and Johnson (2002)
$3 \cdot 10^{24}$	$7 \cdot 10^{26}$	$7 \cdot 10^{27}$	Kass and Yung (1995, 1996)
$7 \cdot 10^{23}$	$1.6 \cdot 10^{26}$	$4.2 \cdot 10^{27}$	Luhmann et al. (1992)

Values given in O atoms s^{-1}

Magnetized planets : the gaseous planets...

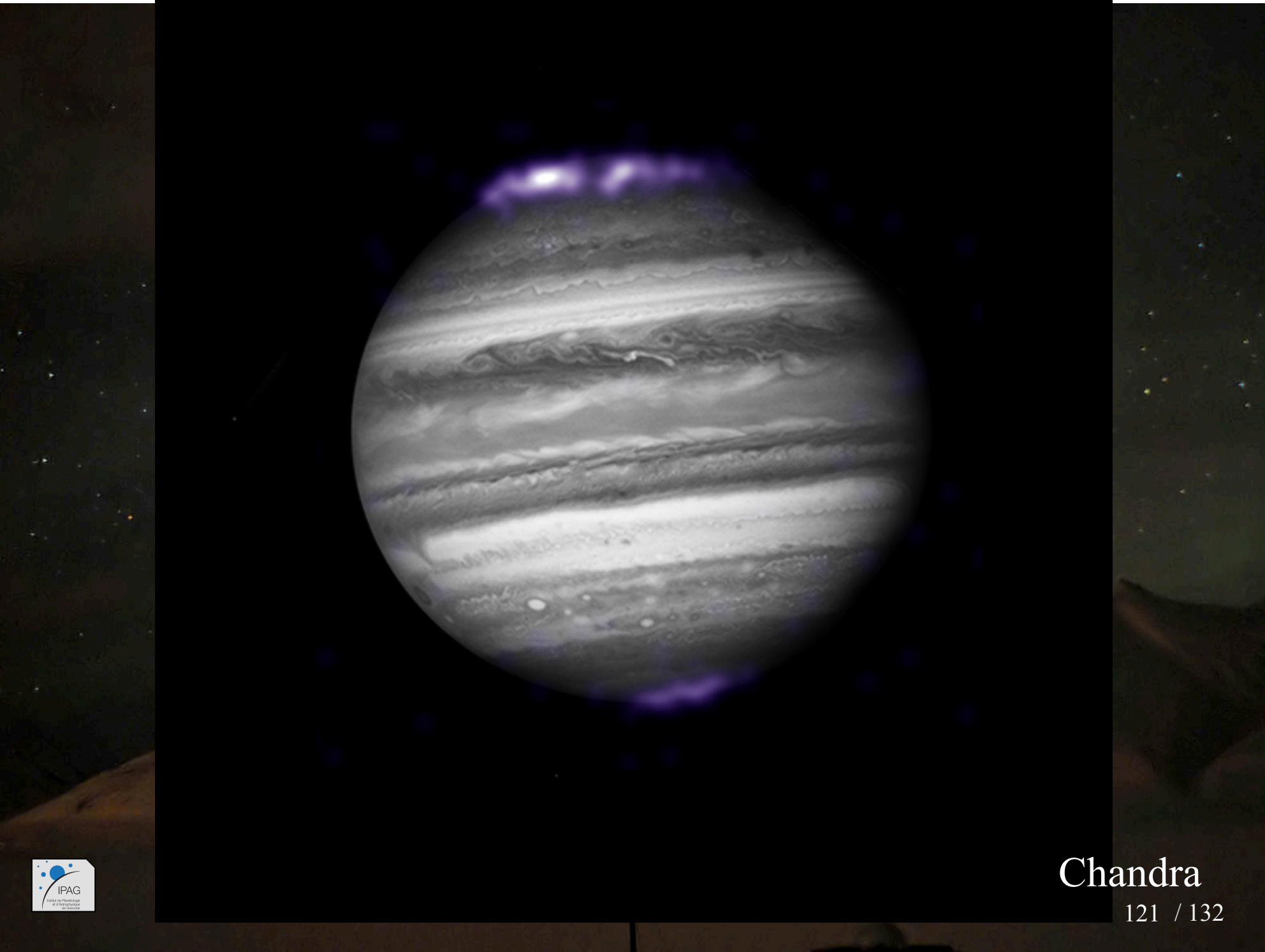
Jupiter

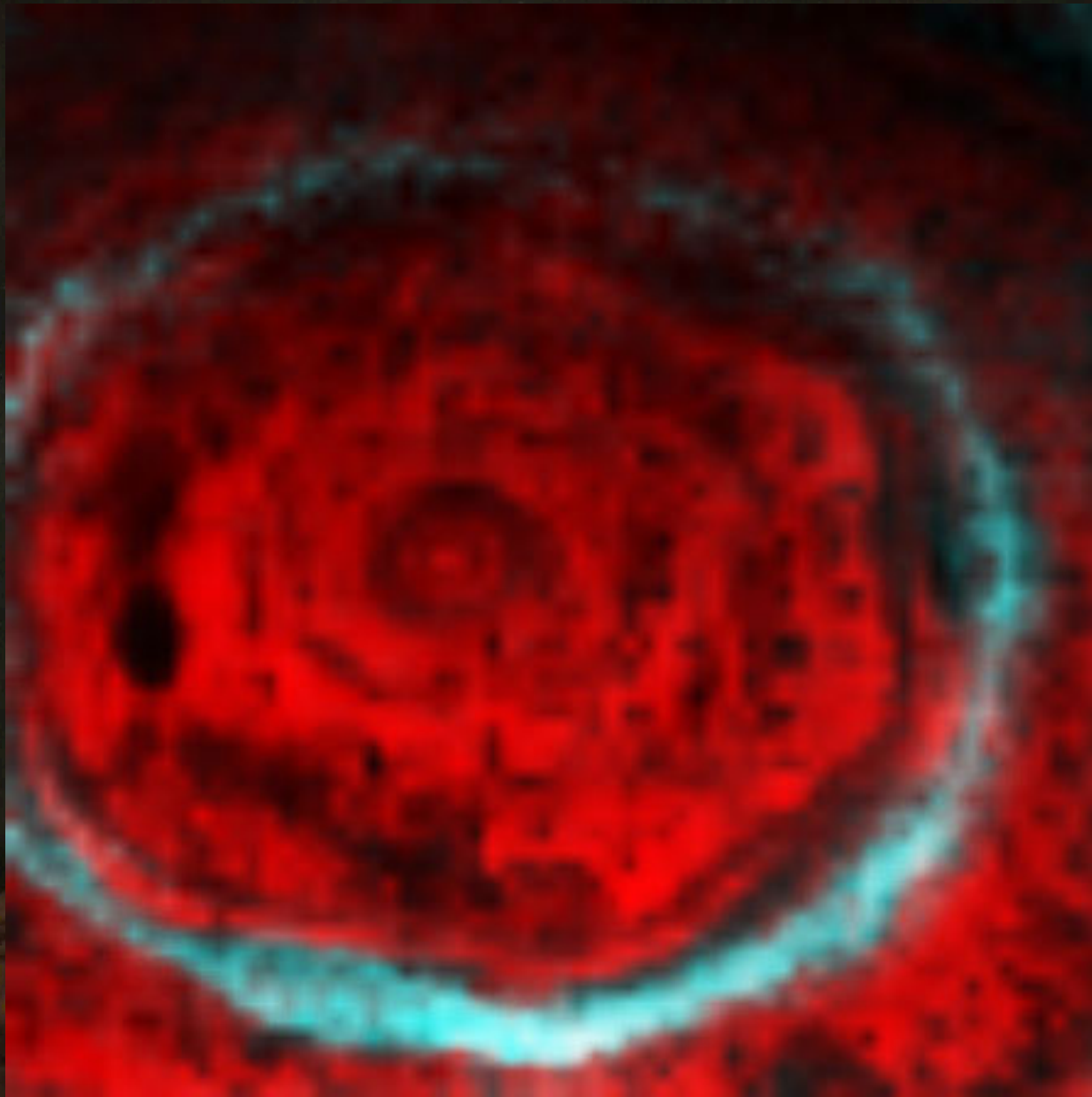


FOC

120 / 132







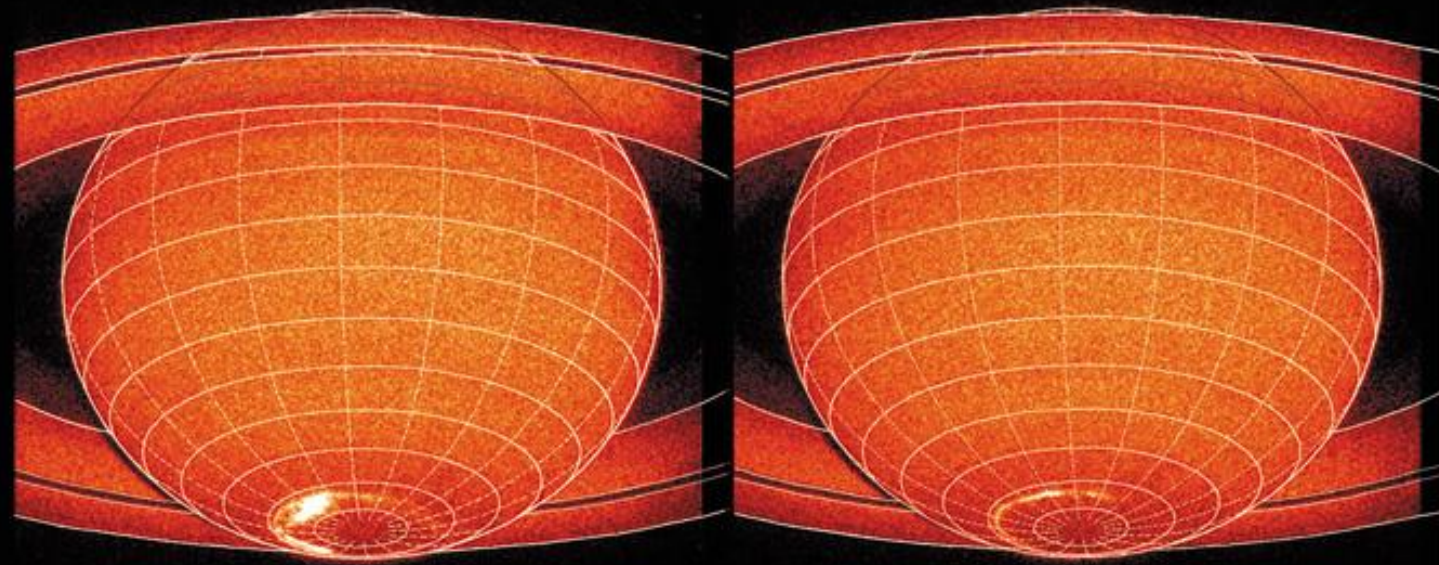
Saturn



SATURN

HST-STIS + f25srf2

~1400 - 1900 Å (H2 Werner & Lyman bands)

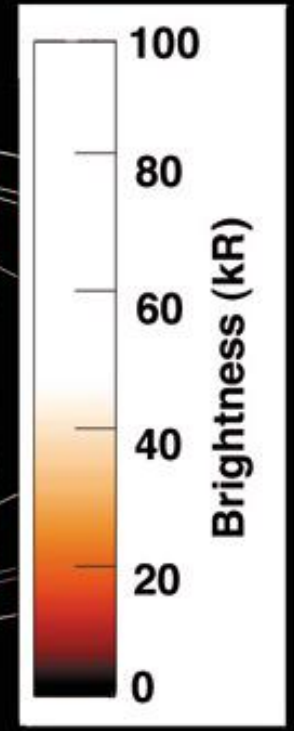


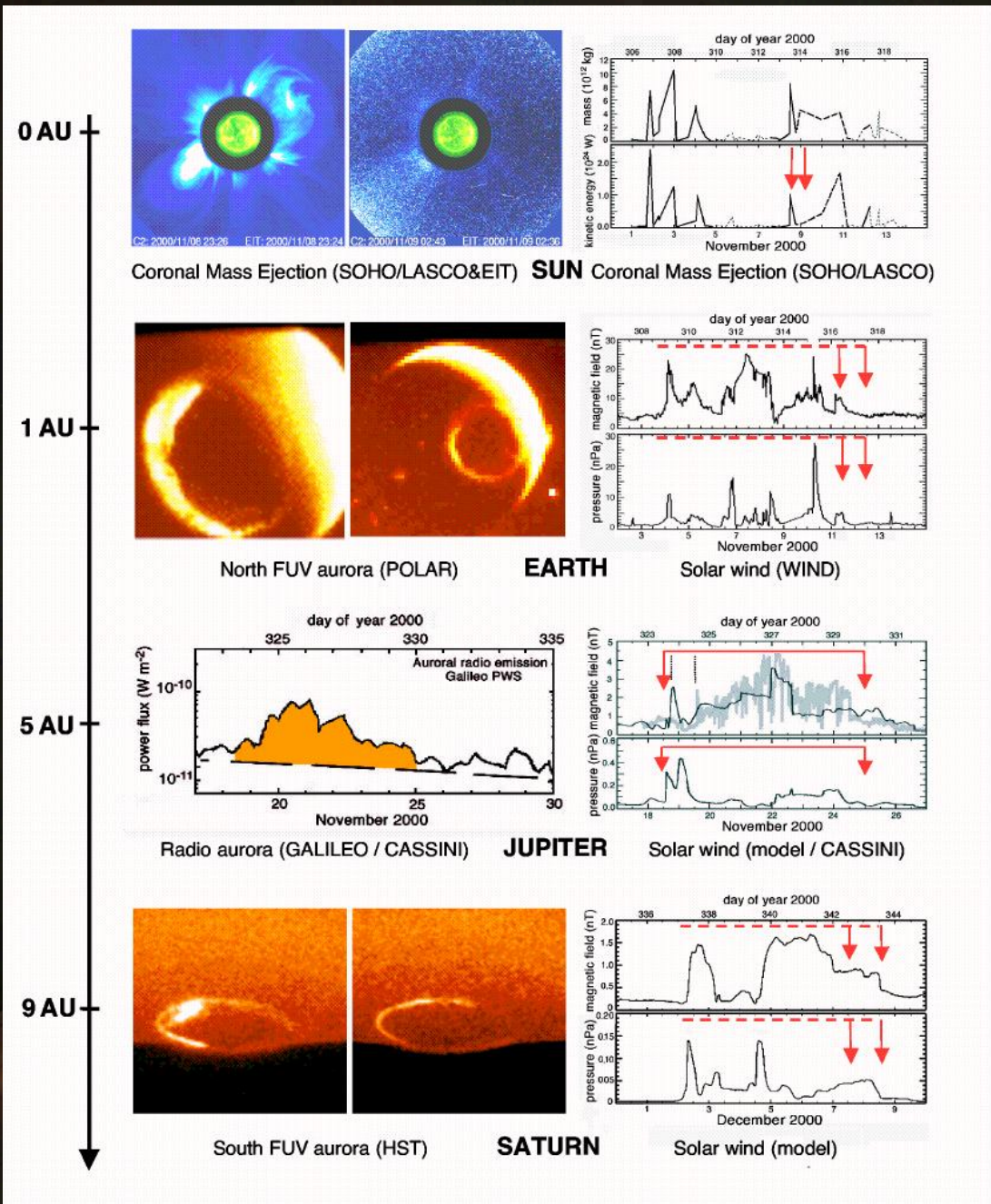
7 December 2000

CML = 243

8 December 2000

CML = 283



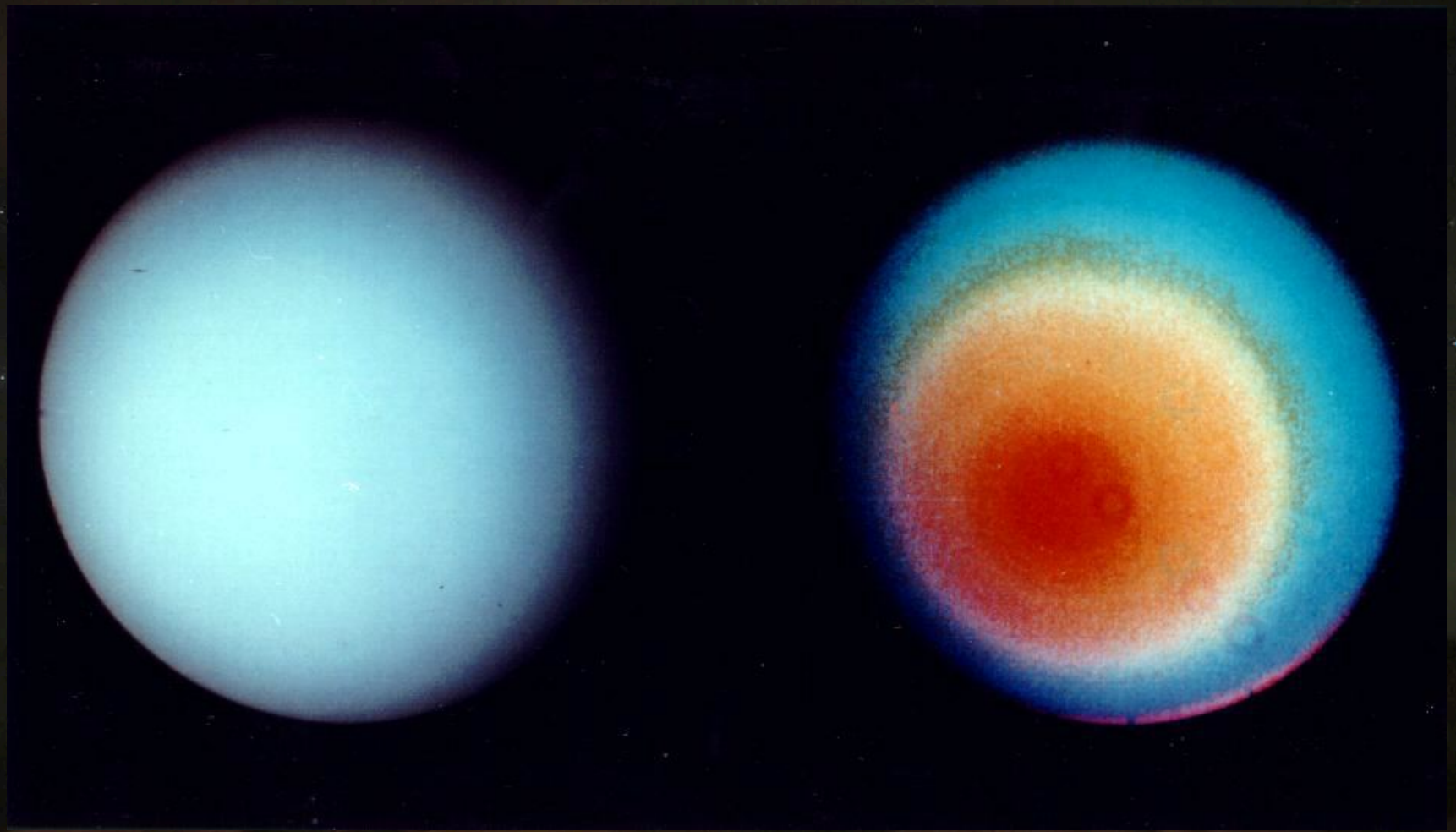


Prangé et al., nature, 2001



Uranus





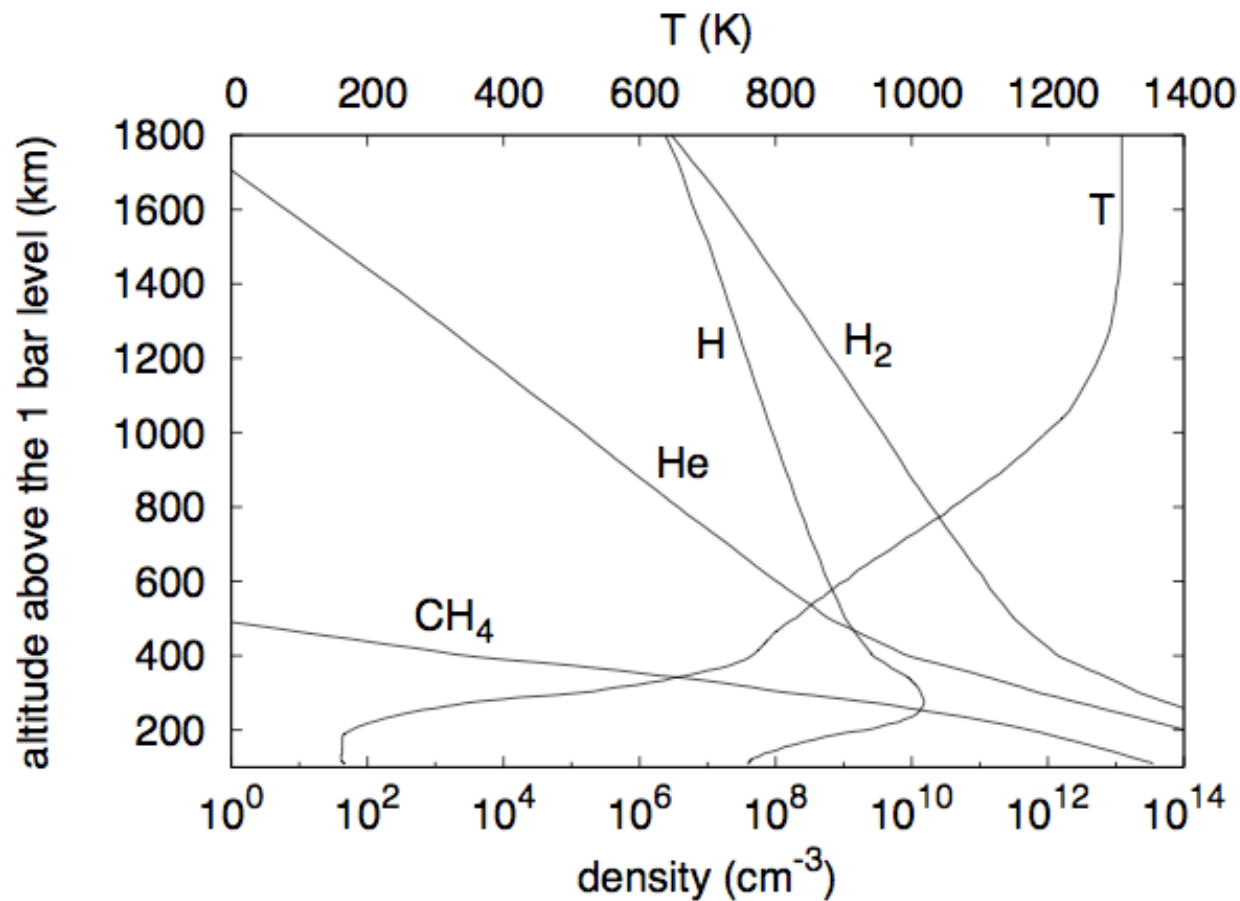


Fig. 1: Composition and temperature profiles in the atmosphere of a discrete aurora, after Grodent & Gérard (2001).

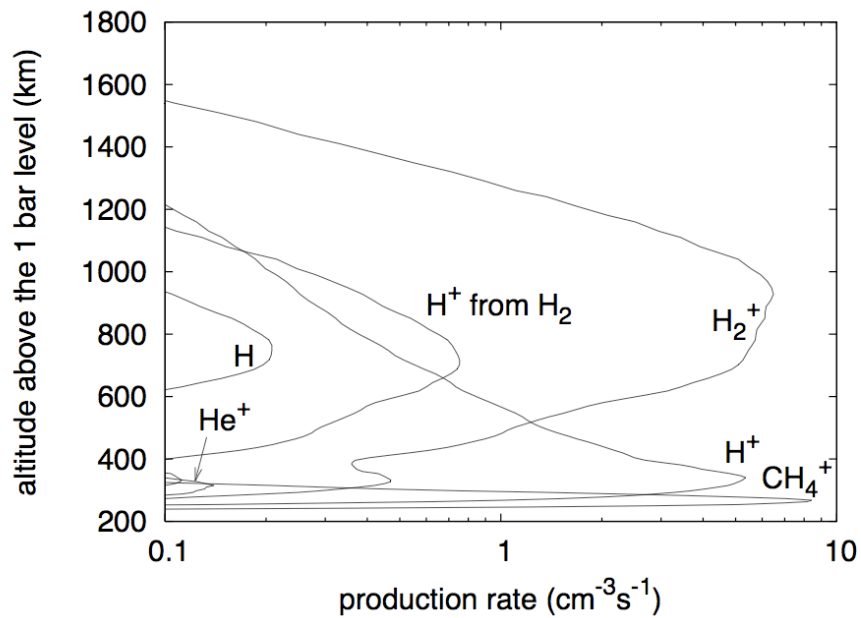


Fig. 2: Photoionization rates for a solar zenith angle of 70° and F10.7= 100.

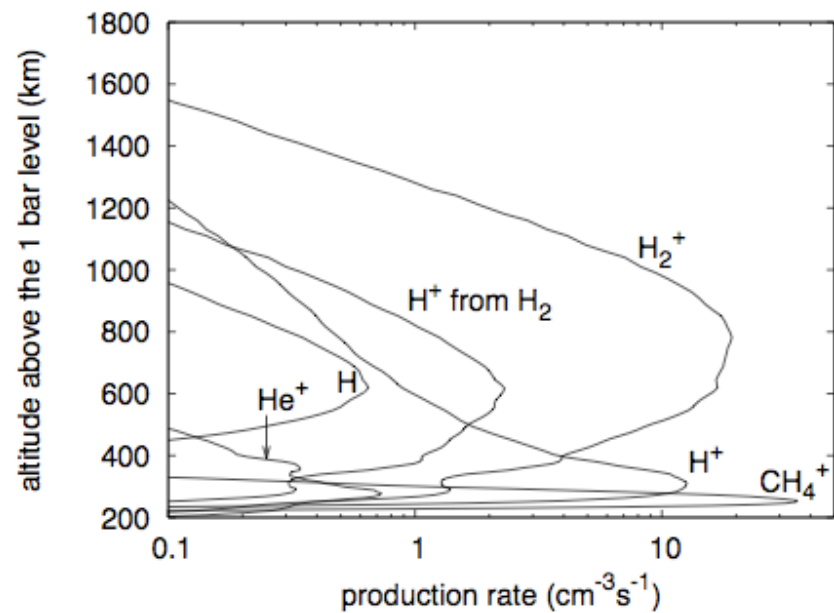


Fig. 4: Photoionization rates for a solar zenith angle of 0° and F10.7=100.

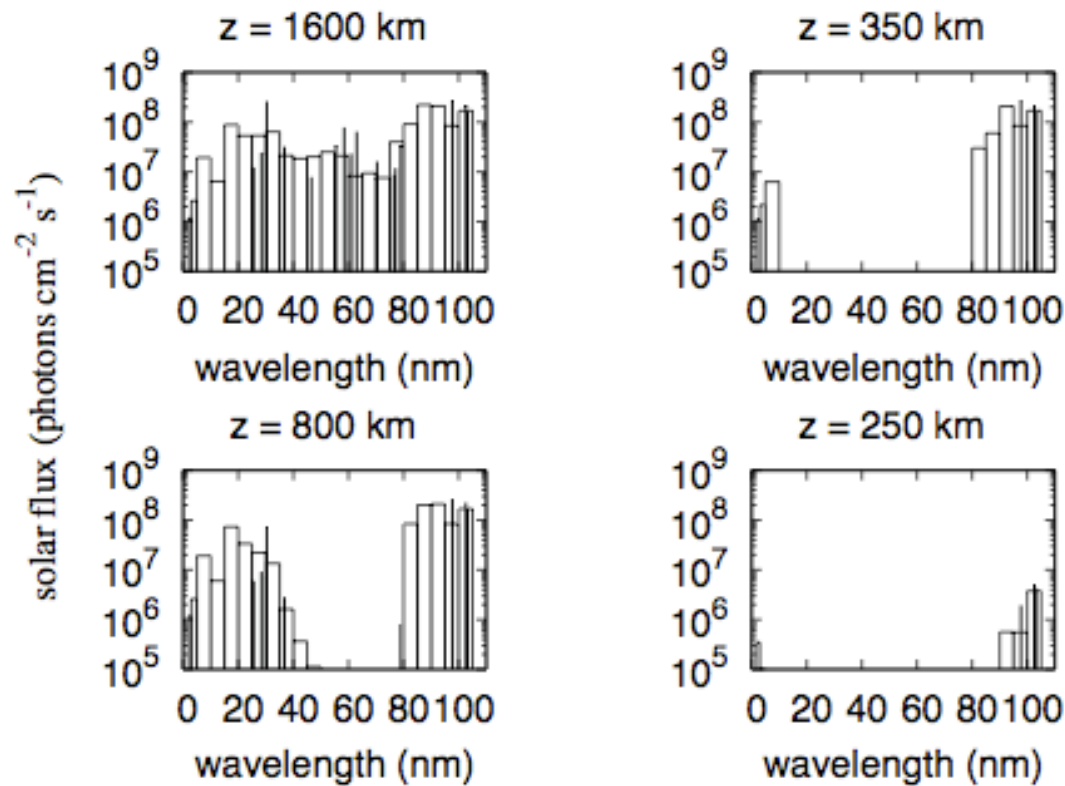


Fig. 3: Penetration of the solar UV flux in the atmosphere of Jupiter for a solar activity of F10.7=100 and a solar zenith angle of 70° .

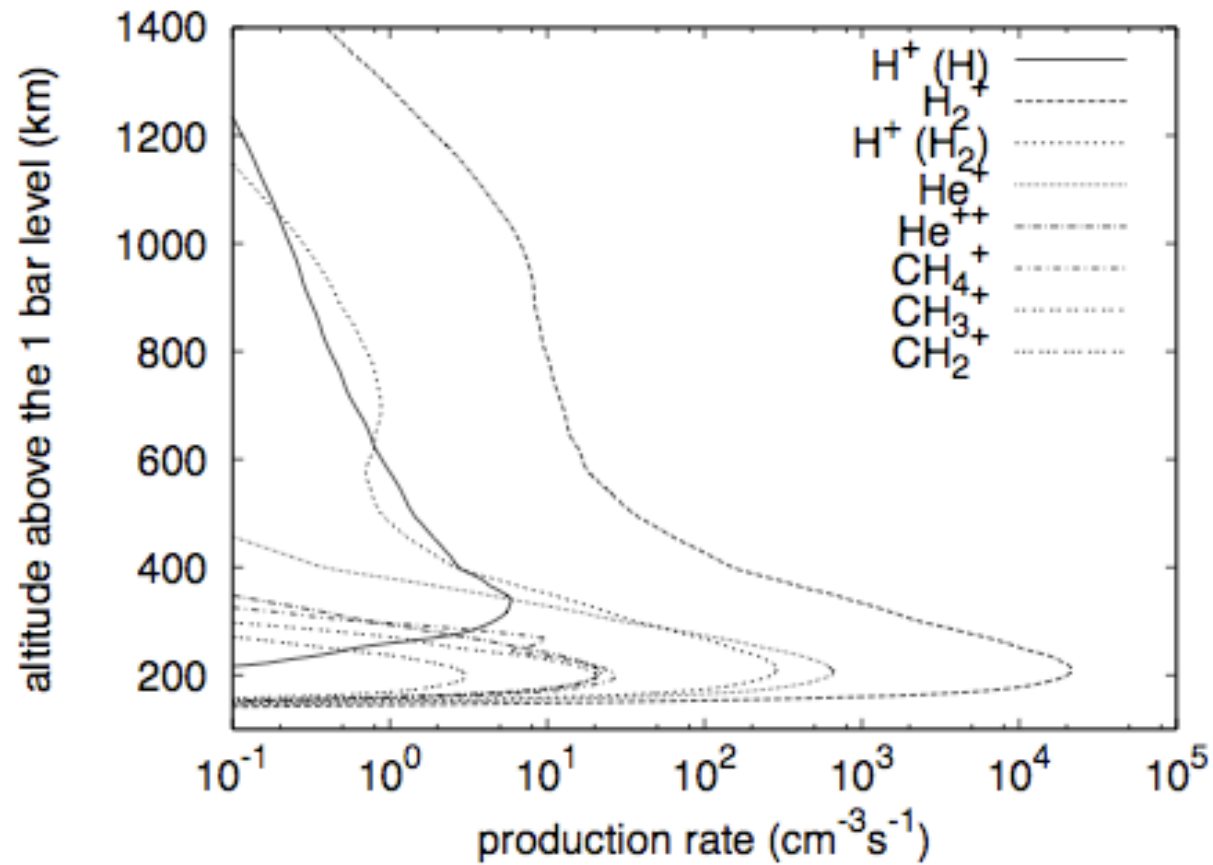


Fig.5: Ionization rates for maxwellian precipitations of 50 keV

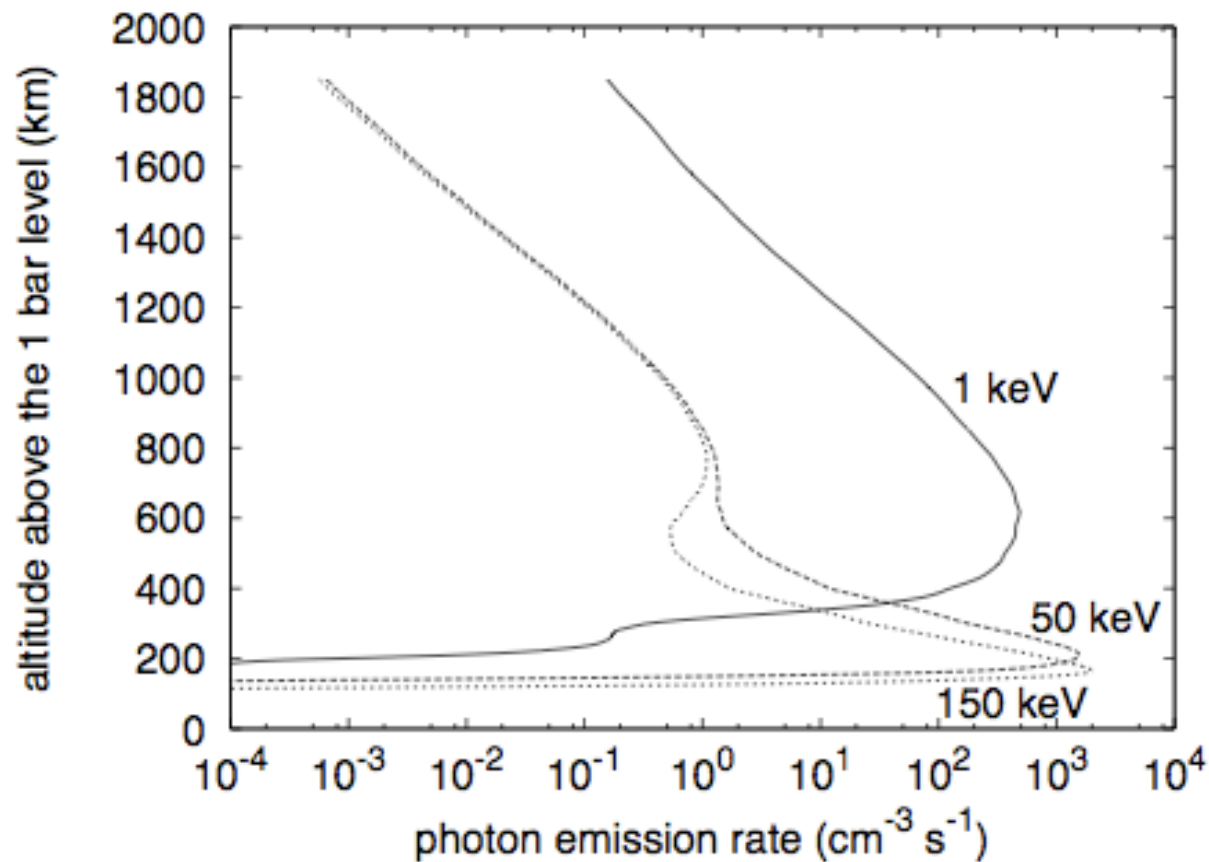


Fig. 9: Emission rate of Lyman Alpha photons, a low solar illuminance ($F_{10.7} = 100$, solar zenith angle of 70°) and maxwellian precipitations of 1 keV, 50 keV and 150 keV